LRP 552/96 July 1996

D324-1 ITER DESIGN TASK ON PLASMA CONTROL 1995 - 1996

J.B. Lister, D.J. Ward, X. Llobet, Y. Martin,
P. Bosshard

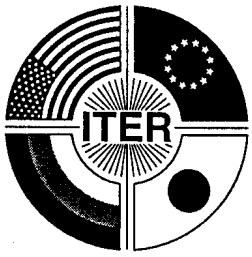

D324-1 ITER Design Task

on Plasma Control

1995-1996

J.B. Lister, D.J. Ward, X. Llobet, Y. Martin, P. Bosshard

Work carried out as part of ITER Task N 47 TD2-(EC),

partly funded by NET Contract ERB 5000 CT95 0116 NET

July 1996

Contents

- Work Carried out under Phase I and Proposition for work which could be carried out under Phase II
- Linearity of the Plasma Response of the TSC Code
- Shape Control Considering Voltage and Current Saturation
- Non-Linear Simulations without Feedback
- Model of Errors on the Estimators of the Control Parameters
- Protective and Corrective Strategy Control Modes

Acknowledgements: The interest of Prof. F. Engelmann in overseeing this work is warmly acknowledged, as is the support of Prof. F. Troyon. The interest of the Naka ITER JCT is essential in driving these studies. The work was partly supported by the Fonds national suisse de la recherche scientifique

This is a progress report on work which is not yet completed, intended for internal use by the ITER team. It should not be quoted other than as a "private communication". It may contain some preliminary and unconfirmed results.

EIDGENÖSSISCHE TECHNISCHE HOCHSCHULE LAUSANNE
POLITECNICO FEDERALE DI LOSANNA
SWISS FEDERAL INSTITUTE OF TECHNOLOGY LAUSANNE

CENTRE DE RECHERCHES EN PHYSIQUE DES PLASMAS
Association EURATOM - Confédération Suisse

ÉCOLE POLYTECHNIQUE
FÉDÉRALE DE LAUSANNE

Final Report

ITER Design Task D324-1 Phase I

Work Envelope V

Work Carried out under Phase I and

Proposition for work which could be carried out under Phase II

Compiled by

J.B. LISTER et al.
(CRPP-EPFL)

15 July, 1996

Introduction

This report contains a summary of the work carried out by the EUHT during the Phase I of Design Task D324-1, together with a proposition for work which the EUHT feels it is competent to carry out during the Phase II of contract D324-1. As such, it is a required part of the Phase I of the D324-1 contract. The workload is large, in excess of the allocated pmy.

The list of work envelopes is based on the existing EUHT work breakdown of D324-1, expanded where necessary for Phase II. Some reorganisation of this list has been necessary.

Work carried out for Phase I during 1995-96 is printed as Italics. Work more or less agreed and/or forseen for 1996-97 is printed as normal font.

A second list corresponds to the JCT wish for a summary of the work to be delivered, including an indication of the dates.

Actions on the JCT are listed in a 3rd section of this report.

A. MODEL OF ERRORS ON THE ESTIMATORS OF THE CONTROLLED PARAMETERS

A1. Quantification of the likely errors

- *Statement of the problem*
- *Questionnaire sent to different experimental groups*

- Summarise the results from current experiments
- Finalise the noise model
- Finalise the error model
- Finalise the delay and filtering models
- Distribute the results for the simulators
- Iterate with the diagnostics group of ITER
-

Collaborators : J.B. Lister and experimentalists [A-UG, JET, TCV, Compass, TS]
{ Strong interaction with Garching JCT on the results }
Deliverables : Formal model and its defense

A2. Effect of these errors on the plasma shape estimators

- *Statement of the problem*
- *Definition of the approaches available for modelling the errors in the loop*

- (This work is executed as part of the D18 Design Task, not the D324-1 Task, but its results are directly incorporated into the D324-1 Task)
- Incorporate the quantified errors into the error propagation mapping
- Attempt to provide a statistical representation of the deterministic error propagation
- Investigate and compare approximated mappings, ANN and FP
- Investigate inverse equilibrium code error-gap mapping, maybe by random pollution runs ?
- { There should be a strong interaction with Garching JCT on the results }

Collaborators : G. Ambrosino
Deliverables : Deterministic and statistical models of the gaps and gap velocities to be used for plasma shape control.

B. ADJUSTMENT OF THE 2-D PASSIVE STRUCTURE MODEL FOR 3-D STRUCTURES

- *Effects of the segmentation of the first wall on the electromagnetic model used for plasma control*

- Effects of ports and other non-axisymmetric structural elements
- Continued evolution as the ITER design is modified
- Estimation of the effects of the 3-D structures on field and flux diagnostics
- Recommendations to the Diagnostics Group on the requirements due to this effect

Collaborators : CREATE for the first 2 points.
None for the 3rd and 4th points. This data should be provided by the Diagnostics Tasks as soon as possible
Deliverables : Recipe for inclusion into the 2-D modelling of control
Recipe for inclusion into the 0-D modelling of breakdown
Quantification of the model modification - indication of the uncertainties
The requirements for this envelope should be agreed directly between B. Lloyd and CREATE.

C. CHOICE of CONTROLLED VARIABLES and CONTROLLER STRUCTURE

- *Analysis of the optimal point gap choice for minimising the wall interaction*
- *Proposition for alternative gap choices*

- Continued conceptual analysis of the choice of control variables, gaps, arcs
- Alternative control structures, embedded vertical stabilisation, embedded flux control...
- Simplified and operationally robust plasma control structures for commissioning
- Include the discrete-time controller delays, embedded loops?
- Simulate the power supply delays, sample-hold
- Continue work on decoupling controllers, MIMO PIDs, LQG, H-inf

- Develop a concept for full discharge control, including all transitions
- Controllers for :
    - Breakdown
    - Startup
    - Limited (especial attention to the short poloidal length)
    - Diverted
    - Limited
    - Shutdown

Collaborators : G. Ambrosino, D. Ciscato, J. Lister, D. Limebeer, JET
Deliverables : Justification of an overall control concept for limited and diverted regimes
Transition methods between different control variables
Proposed controller structures

D. CONTROL LAWS FOR IP, POSITION and SHAPE

- *Model of the ITER TAC-8 magnetics*
- *LQG, PID and H-inf controllers designed*
- *AC losses computed during feedback actions*
- *Minimum optimal excursions following the defined list of disturbances*
- *Control Laws including voltage and current saturation compensation*
- *Testing of the effect of time-delays on the loop*
- *Power surge suppression using the CS*
- *Plasma Current control incorporated*

D1 Saturation problems
- Further development of compensation for Current and Voltage supply limits
- Simulation in linear models
- Simulation in non-linear models

D2 AC losses
- Strategy for reducing AC losses
- Simulation in linear models
- Simulation in non-linear models

D3 Power envelope
- Strategy for reducing the total power envelope
- Simulation in linear models
- Simulation in non-linear models

D4 Modelling
- Develop a linearised PROTEUS model of limited plasmas for controller design and simulation
- Specify the method chosen

D5 Complete Controller

- Complete consistent control architecture and controllers able to perform current and shape control from XPF to EOC

D6 Miscellaneous

- Evaluation of a Performance Indicator Set for comparing different linear and non-linear controllers and models
- Summary of the experience gained

Collaborators : G. Ambrosino, D. Ciscato D. Limebeer, J. Lister, A.W. Morris
Deliverables : Algorithm specifications and coefficients for simulations

E/F. LINEAR and NON-LINEAR SIMULATIONS WITHOUT FEEDBACK

- *Import and set up the TAC8 ITER Model from PROTEUS linearisation*
- *Calculations with the simple model of the AC losses*
- *Model the detailed perturbation list for different operating points*
- *Model the results with square pulse injection*
- *Calculation of the optimal response to disturbances for each gap*
- *Import and set up the TAC-8 ITER Model in TSC at Manno*
- *Test the "hyper-resistivity" version of TSC*
- *Square pulse injection in open-loop*
- *Disturbances modelled for comparison with linearised model*

- Continued validation of the linear model by comparing the open-loop step response of the separatrix contour with non-linear evolutions of the same
- Continued validation of the linear evolution following the defined set of disturbances, until understanding of the comparison with non-linear evolutions
- Store the required data for post-calculation of the simple model of AC losses
- Test the square wave responses with MAXFEA
- Continued work on the square pulse and disturbance until understanding the differences with the linear models
- If necessary, heuristic modification of the linear model

Collaborators : R. Albanese, D.J. Ward, G. Marchiori
Deliverables : Time evolution of all waveforms : coil currents/volts, separatrix, shell currents
Detailed comparison between linear and non-linear models
Validation or modification of the linear models

G. LINEAR SIMULATIONS WITH FEEDBACK

- *Linear evolution following a given set of disturbances*

- *Control Law studies in other envelopes*

- Modelling of the frequency response of the contours with weak feedback
- Modelling the effect of plasma disturbances
- Export the data for calculating AC losses
- Evaluation of the Performance Indicator Set
- Evaluation of the effects of 3D structures
- General control law studies in other envelopes

Collaborators : G. Ambrosino, D. Ciscato
Deliverables : Evolution of all relevant waveforms and AC loss calculations
Modelled frequency responses
PIS results
Summary of the closed loop tolerance to the 3D modelling

H. NON-LINEAR SIMULATIONS WITH FEEDBACK

- *Linearity studies*

- Modelling of the complex frequency response of the separatrix displacement with weak feedback
- General control law verification
- Export the data for calculating AC losses
- Import proposed general discrete-time controller law structures into TSC
- Continued work on the TSC gap frequency response
- Runs with the reference controller for typical disturbances in TSC
- Test the disturbances, square wave injection and gap frequency response on MAXFEA
- Test the reference controller for typical disturbances in MAXFEA

Collaborators : D.J. Ward, G. Marchiori
Deliverables : Evolution of all relevant waveforms
Modelled frequency responses

J. POWER SUPPLY LIMIT + AC LOSSES REVIEW

- *AC losses calculation performed, inadequate comparison as yet*
- *No definitive result either way*

- Review the disturbance AC losses in open-loop
- Review the success of different controllers for reducing the voltage and power requirements
- Review the AC losses of the different disturbances and establish a pulse inventory
- Compare the simple model of AC losses with the JCT detailed model
- Establish a qualitative success measurement for the different controllers

- Submit an M-file to Naka for distribution to home teams

Collaborators : CREATE with Group conclusions and Naka reactions
Deliverables : Assessment of margins of present design
Recommendation concerning different models/controllers

K. APPRECIATION OF EXPERIMENTAL RESULTS

- *Ongoing, part of the EUHT R&D*

- Assessment of the confirmation or otherwise of the assumptions made in the ITER plasma control tasks, following new experimental results
- Present results on current/voltage saturation in experiments

Collaborators : J.B. Lister, D. Ciscato, D.J. Campbell, O. Gruber, W. Morris
Deliverables : Relevant experimental results, evaluated from the point of view of ITER control

L. 3-D EFFECTS MODELLED IN 2-D FOR PLASMA INITIATION

- *Pending*

- Statement of the problem
- Use the 2-D modelling of the 3-D structures, Envelope B, with the startup scenario to evaluate the stray field levels due to the 3-D modifications, both first wall and structure/ports
- Determine whether these are important or not
- Information from the 3-D stray field calculations giving typical toroidal connection lengths
- Establish whether these effects need to be modelled in more than 0-D
- Establish how to incorporate them on 0-D
- { JCT : PF Current waveforms during startup, for calculating the 3-D image currents

Collaborators : R. Albanese, B. Lloyd
Deliverables : Stray field maps due to 3-D effects
Evaluation of the effect of this level of stray field on the breakdown
Statement of the problem

M. WAVEFORMS OF PLASMA CURRENT DURING BREAKDOWN

- *Establish the range of conditions for this study*
- *Model the effects of impurity level, confinement time of energy and impurities, ECRH power, plasma size and major radius*

- *Incorporate time-dependent electric fields and evaluate their importance*
- *Establish the likely current ramp-up rates*

- Examine further the effects of time-dependent electric fields during start-up
- Include the study of the transition to a lower plasma current ramp rate by cutting back the applied electric field at some point during the ramp up
- Investigate the problems/possibilities of start-up at reduced major radius
- Establish up to what current this model should be used
- Establish a recipe for the necessary conditions for startup to succeed
- Establish a recipe for the sufficient conditions for startup to fail
- Establish the effect of early cutback in applied electric field
- Establish a simple model for predicting current ramp-up rate given the input variables, for use as an interface to the Leuer code

Collaborators : B. Lloyd
Deliverables : Evolution of the plasma waveforms for all of the modelling assumptions
Statement of the minimum time before cutting the electric field
Effect of different connection lengths

N. SOURCES of POLOIDAL ERROR FIELDS

- *Establish the sources of error to be studied*
- *Work on the "Acceptable" invasion of correction coils outside the vessel*
- *Import the JCT definition of the X,Y,Z coordinates of the correction coil bars*
- *Definition of the problem to be solved*
- *Iteration of this definition*
- *Calculation of the compensating fields from the different designs*
- *Concept and estimate of N*Imax and its time derivative for the 3 primary error sources*
- *Analyse the effect of a single ferromagnetic blanket module*

- More of the same using Naka revised correction coil designs
- "Analysis of the Fourier spectrum at the q=1,2,3 surfaces for error field correction coil designs supplied by the Naka JCT will be undertaken. As the design becomes closer to finalised more detailed design features such a multi-turns in the correction coils and their current feeds will be included in the modelling."
- Appreciation of the present magnetics for detecting and correcting locked-modes
- Appreciation of the implementation of the error compensation system
- Optimisation of the amount of superconducting material for different designs

Collaborators : T. Hender
Deliverables : Map of the errors for the different sources
Coupling coefficients from the correction coils to the errors
Conception/design of a global poloidal error correction system
Statement on the adequacy of the proposed magnetic diagnostics

Commissioning proposal
Currents required in the final design

O. ABNORMAL PF COIL OPERATION

- *Pending*

- Sources of abnormality to be studied
  - Pre-disruption
  - Loss of current/voltage range on one or more coils
  - Overheating of plasma-facing components and AC losses
  - Loss of feedback control
- Analyse the coil current evolution produced by each source
- Analyse the present methodology in current experiments
- Propose a set of corrective actions and overall strategy
- Test corrective actions in a simulation
- {JCT : Detailed definition to be discussed }

Collaborators : J.B. Lister, D. Ciscato, [O. Gruber, D.J. Campbell, W. Morris]
Deliverables : Coil currents and AC Losses evolution with/without corrective action
Strategy of corrective actions
Proposal for and test of corrective action for all cases
Tolerance for number of events (inventory of AC losses etc.)

P. PF SYSTEM PROTECTION ANALYSIS and QA

- *Pending*

- Define a strategy for the PF coil protective actions
- Evaluation of proposed protective actions in worst case events
- Define a set of maximum tolerances for the PF system, compatible with the correct operation of the PF and Plasma Control Systems
- {JCT : Detailed definition to be discussed}

Collaborators : J.B. Lister, D. Ciscato, [O. Gruber, D.J. Campbell, W. Morris]
Deliverables : Exhaustive list of PF and Plasma conditions requiring protective action
Protective actions proposed
Simulation, calculation of their effects
Maximum tolerances for the PF and Plasma Control Systems

Q. PF SYSTEM and PLASMA COMMISSIONING

- *Pending*

- Proposal of a full plasma-less commissioning planning for :
    - PF Coil instrumentation
    - PF Coil geometry
    - Magnetics instrumentation
    - PF-Magnetics consistency (TCV and DIII-D-like)
    - System linearity
    - Local control loops
    - Feedforward tests
    - Abnormal event simulation/creation
    - Diagnostic and Safety measurement integrity
    - Creation of an ITER electromagnetic model/comparison with prediction
    - Error fields
    - Plasma-less controller tests
    - Local/system trips
- Proposal of a full commissioning planning for first low performance plasmas:
    - Simple and robust control loops
    - Feedforward tests
    - Plasma controller tests
    - Scenarios
    - Strategy for increasing performance

Collaborators : J.B. Lister, D. Ciscato, [O. Gruber, S. Puppin, P. Lomas, D. Campbell]
Deliverables : Proposal for a commissioning methodology and timescale

R. PF SYSTEM CONTROL HARDWARE and SOFTWARE

- *Pending*

- { JCT : Detailed definition of the scope }
- { JCT : CODAC compatibility requirements }
- Defintion of the PF Control states and interaction with CODAC
- Evaluation of current implementations of hardware and software
- Evaluation of required hardware and software

Collaborators : J.B. Lister , D. Ciscato [O. Gruber, S. Puppin, P. Lomas]
Deliverables : Appreciation of the current plasma control implementations
Scaling of the current Plasma Control implementations for ITER
Requirements of the man-machine interface for commissioning and operation
Proposition for the scale of the required hardware/software
Estimate of procurement cost/manpower

S. FULL PULSE SIMULATION USING A NON-LINEAR EVOLUTION CODE

- *Pending*

- Reference case and a small number of alternatives, to be agreed with the USHT
- Complete simulation with noise, disturbances, saturations etc, to demonstrate control
- Possibly executed as segments to be stitched together
- Incorporation of all necessary ideas to achieve the design goal

Collaborators : D.J. Ward + Controller architects
Deliverable : Final, Credible, All-encompassing ITER look-alike

T. NON-LINEAR SIMULATIONS TO ESTIMATE LINEARISED RESPONSE

- *Check on the linearisability of the contour response with TSC*
- *Check on the apparently conserved quantities with TSC*
- *Gap frequency response with TSC*
- *Develop and import System Identification analysis tools*

- Definition and test of a fixed stimulation on all codes, linear and non-linear
- Confirm the linearity out to 3 times lower frequency
- Continuation of the design of suitable stimulation of the ITER model in TSC
- Runs of TSC with these stimulations for 4 fiducial diverted plasmas, plus a limited plasma
- Analysis of these data to produce the effective linearised response
- Comparison of the results with currently favoured linear models
- Results for different equilibria

Collaborators : J. Lister, D. Limebeer, D. Ward
Deliverables : Frequency response in these different situations
TSC Linearised Plant Model

U. SYSTEMATIC MODEL REDUCTION STUDIES

- *Model reduction using the state significance criterion*

- Continued work on the state significance - physical significance of the retained states
- Model reduction from the System Identification data
- Eigenmode reduction of the CREATE model for all 4 fiducial states
- Method of reduction including the E,F matrices

Collaborators : D. Ciscato, D. Limebeer, J. Lister
Deliverables : Different recipes for the model reduction applicable to ITER

Implication on the diagnostic design
Reduced model properties

Z. PF SYSTEM FINAL DESIGN REPORT

- *Pending*
- Again !

Collaborators : J.B. Lister

Proposition for D324-1 Phase II sub-task definitions - EUHT

The following two lists provide a brief overview of the work to be delivered, the participating institutions and the timescale for delivery of intermediate results, where predictable

Task Definitions and deliverables

The work to be accomplished during this second Phase of the Design Task D324-1 shall include the following items, with the appropriate deliverables listed in {}.

Participating institutions and the dates for presentation of results are indicated in [] for the 3 meetings forseen :
(1=Garching,Nov 96, 2=San Diego,Feb 97, 3=Naka,June 97).

1. Quantify the likely experimental errors on the raw sensor signals and model the resulting errors on the control variables, using approximated mappings. The propagation of the errors through an inverse equilibrium code will be addressed, using USHT information on E-FIT sensitivity studies. This work will be carried out in close conjunction with JCT Garching {Frequency spectrum of the likely errors of both raw data and control variables} [CREATE, CRPP 1,3]

2. Model the effects of 3-D passive structures on an equivalent 2-D description of the passive structures, including the vessel structure and vessel ports. Crowns, TF coil cases, inter-coil structure and cryostat will be neglected. {Geometrical and electrical description of the equivalent 2-D structures, recipe for obtaining this result and a quantification of the effect of the 3-D structures on the A,B,C,D,E,F plant plus disturbance model, timescales and map of the residual 3-D fields} [CREATE 3]

3. Model the effect of 3-D passive structures on the flux and field diagnostics. Make a recommendation concerning the design of these diagnostics. The USHT has made a start on this and a report can be provided {Model of the diagnostic transfer function suitable for control studies and design recommendations} (Note that this work load should be taken from the results of a diagnostic development task, according to JCT Naka) [Not in the list]

4. Quantify the effect of 3-D passive structures and ports on the poloidal field structure at breakdown and the effect of the 3-D error field on the plasma initiation itself {Map of the modified axisymmetric stray field, description of the effect on the breakdown process, evaluation of the effect on the plasma initiation} [CREATE 3, CULHAM 3]

5. Study concepts of different sets of control variables, different controller architectures and evaluate their potential advantages/disadvantages in terms of flexibility during transitions, robustness, performance. {Propositions for different configurations and

their defense with respect to a reference controller} [CREATE, PADOVA, CRPP 1,2,3]

6. Study different design algorithms for the standard A,B,C,D controller architecture, Decoupling, MIMO PID, LQG, H-inf {Design procedures, simulation results and a comparison} [CREATE, IC, PADOVA 1,2,3]

7. Study the use of suitable different control variables for the different phases of the ITER pulse : breakdown, startup, limited, diverted, burning, cooling, rampdown, with the full pulse simulation in mind {Control variables recommendations and simulation results} [CRPP, IC, CREATE 1,2,3]

8. Compare the performance of all the controllers tested on either linear or non-linear models against the ITER basic gap control requirements, in the presence of defined plasma disturbances and steps in the reference inputs {Controllers tested and simulation waveforms} [CREATE, IC, CRPP, PADOVA 2,3]

9. Compare the performance of all the controllers tested on either linear or non-linear models on the basis of a more complete Performance Indicator Set containing control constraints and control optimisation targets, the PIS definitions to be agreed with Naka {Definition of the PIS and their values for different controllers} [CREATE, CRPP, IC 2,3]

10. Study the explicit inclusion of the closed loop time-discretisation in the design of the controller and a simple model of the power supply transfer function {Proposition of a suitable method and evaluation of the benefits} [IC, CREATE, CRPP 1,3]

11. Derive a simplified PROTEUS based linearised plasma model for limiter and limiter-divertor configurations to be used for the controller design and massive simulations {Conceptual simplified model, final model in numerical form} [CREATE 1,2,3]

12. Design of a feedback controller to be used in abnormal regimes, such as excessive disturbances, reducing the number of active control variables and changing their identity, applicable to early ITER operation {Proposed controller and its defense} [CREATE 1]

13. Study methods of saturation compensation, both for voltage and current in the PF coils {Proposed methods and simulation results} [CRPP, IC 1,2]

14. Study the AC losses with different controller designs and, possibly, techniques for reducing these AC losses on the basis of a clear definition of the procedure to be used to estimate the AC losses be provided by the JCT. Provide an M-file for the calculation of AC losses with a finer grid. {Quantification of the AC losses, the relationship between controller behaviour and AC losses and perhaps a reduction strategy} [CRPP, CREATE 3]

15. Incorporate plasma current control into a general coupled PF control, avoiding the present SISO-MIMO superposition {Proposed method and simulation results} [CRPP, CREATE 1]

16. Compare the admissible power envelope and the simulation requirements, developing a full Power Management Strategy {Power Management Strategy and the waveforms obtained during simulations} [CREATE 2]

17. Perform open loop simulations using linear and non-linear models, to evaluate their differences in the presence of coil voltage pulses and plasma disturbances as a measure of model agreement/disagreement {Results and the comparison between different models} [CREATE, CRPP, IC, PADOVA 1]

18. Perform closed loop simulations using linear and non-linear models, to compare the frequency responses of the separatrix to coil voltage modulation. Execute the resulting optimised method on data provided by the USHT to increase the range of models in this comparison {Results and their comparison, with explanations and propositions for improving the agreement, if necessary} [CRPP, CREATE 1,2]

19. Perform closed loop simulations using linear models, taking into account the 3D effects and their quantification in the closed loop {New linearised model, controllers tested, simulation waveforms and quantification of the 3D effects on the Performance Indicator Set} [CREATE 3]

20. Perform closed loop simulations using TSC, to evaluate a suitable plant model for controller design, using system identification, for different reference equilibria {Results, methods and the identified models} [CRPP, IC 1]

21. Perform closed loop simulations using linear models for controller development and evaluation {Controllers and the simulation waveforms} [CREATE, IC 1,2,3]

22. Perform closed loop simulations using non-linear models for general controller validation {Controllers and waveforms} [CRPP 1,2,3]

23. Appreciate ongoing experimental results which are relevant to the ITER controller design {Communication, appreciation and conclusions} [CRPP, IPP, JET 1,2,3]

24. Predict the waveforms of the plasma current and temperature evolution during plasma startup, using a 0-D code, including different waveforms of the loop-voltage leading to a reduction of the current ramp rate. Waveforms of the applied electric field in the breakdown region are to be supplied by Naka. Discuss the range of validity of this phase of plasma initiation {Evolutions for different assumed parameters, validity of the model in terms of kA} [CULHAM 1,2,3]

25. Evaluate the Fourier spectra of different geometries of the poloidal error field correction coils proposed by Naka JCT, including inter-turn connections and

winding geometry once the design has converged {Fourier spectrum at the agreed q-surfaces for error field correction coil designs} [CULHAM]

26. Develop plausible calibration, detection and commissioning procedures for the error field compensation system {Suggested procedures} [CRPP, JET, IPP, CULHAM]

27. Define of a set of abnormal PF coil or plasma conditions which will have to be addressed explicitly during plasma operation {Set of conditions} [CRPP, JET, IPP]

28. Define the corrective actions which can/must be undertaken for these abnormal conditions {Description of the actions, including PF control actions} [CRPP, JET, IPP]

29. Define the protective actions which must be undertaken for these abnormal conditions {Description of the actions, including PF control actions} [CRPP, IPP, JET]

30. Evaluate any significant machine effects of the proposed corrective and protective actions {Estimates of the problems which the proposed actions might create/alleviate} [CRPP, IPP, JET]

31. Specify any minimal tolerances of the PF system which are essential for correct plasma operation {Discussion of the most important issues} [CRPP, IPP, JET, CULHAM]

32. Outline a proposition for plasma-less PF commissioning up to first plasma tests {Credible and complete schedule with estimated effort required} [CRPP, IPP, JET]

33. Outline a proposition for plasma commissioning up to the lowest formal scenario with a diverted plasma {Schedule with estimated effort required, target minimal scenario} [CRPP, IPP, JET]

34. Describe the required Plasma Control System hardware and software functionality {Outline description, including the MMI and CODAC interface} [CRPP, IPP, JET]

35. Produce a full pulse simulation of the reference scenario, using a non-linear code, including noise, disturbances, plant uncertainties, saturations, energy management {Waveforms resulting from the simulation} [CRPP 3]

36. Produce a full pulse simulation of selected non-reference scenarios, as above, including the high fluence driven scenario {Waveforms resulting from the simulation} [CRPP 3]

37. Perform a model reduction on the CREATE 119 state model for simulations, using decomposition of the passive structure. Recipe for the E,F matrices. Typically less than order 35 model. Compare the effect of the reduction. {Model description, quality of the reduction using input-output transfer functions} [CRPP 1]

Information required from the JCT for the work to be started

In order that this work be carried out efficiently, the JCT will provide the following necessary information to the Home Team :

1. Definitions of the reference gap locations for the flat-top phase
2. A reference controller as a baseline for comparison with advanced controllers
3. Definition of the limiter geometry and the control targets for limited plasmas
4. Definition of the control targets during the X-Point Formation
5. Definition of the diverted plasma control targets and constraints in the form of a required Performance Indicator Set
6. The contour of the plasma facing wall surface
7. The current definitions of the vessel, 2-D passive structures, ports and PF coils
8. A simplified recipe for the calculation of the AC losses for verification
9. The waveforms for the reference scenario
10. Guidance concerning the plausible variations around this scenario
11. The waveforms for other scenarios for full-pulse simulations
12. Guidance on the likely timing and extent of the cutback in the applied electric field and the timescale over which the applied electric field will decrease in the plasma region
13. Data on the E-field magnitude as a function of time and possibly the stray field structure for inboard startup
14. Geometry of the proposed error-field correction coil system
15. The axisymmetric equivalent vessel structure to be used in the simulations
16. A definition of the global parameter variations during L-H and H-L transitions, and their timescales

17. A definition of the "sawtooth" type repetitive disturbances which bracket the plausible predictions during ITER operation

18. Guidance on a more constrained definition of the li-drop disturbance

19. Define the q- surfaces for the error field evaluation

20. Define the simplest model of the power supplies to be used in the simulations

21. Effects of 3-D structures on the diagnostic response

22. Provide the end of startup (500 kAmp plasma current) initial conditions and their derivatives for matching to the non-linear codes

EIDGENÖSSISCHE TECHNISCHE HOCHSCHULE LAUSANNE
POLITECNICO FEDERALE DI LOSANNA
SWISS FEDERAL INSTITUTE OF TECHNOLOGY LAUSANNE

CENTRE DE RECHERCHES EN PHYSIQUE DES PLASMAS
Association EURATOM - Confédération Suisse

ÉCOLE POLYTECHNIQUE
FÉDÉRALE DE LAUSANNE

ITER Design Task D324-1 Phase I

Final Report

Work Envelope T

Linearity of the Plasma Response of the TSC code

J.B. LISTER, D.J. WARD, Y. MARTIN, P. BOSSHARD
(CRPP-EPFL)

18 July, 1996

E_T_TC_2.DOC

1. INTRODUCTION

Demonstrating that the plasma response to changes in the Poloidal Field Coil voltages is linearisable is a prerequisite for subsequently quantifying the linearised response, another part of this work envelope.

We have used the TSC code to test the linearity of the response of the separatrix gaps and various global plasma parameters (li, Ip, βp, Rmag, Zmag) to voltage perturbations injected into the different poloidal field coils.

In this report, we show that the response is linearisable to within the accuracy of the code.

We have used the results obtained to investigate the presence of conserved quantities linking the variations of different plasma parameters.

2. METHOD

We have injected a voltage signal which is a composite of 8 sinusoidal signals at angular frequencies and phases given by the following Table. The frequencies are integral numbers of the inverse period of a stimulation cycle, the integral multiplier being shown as n in the table and a cycle being 10 seconds long.

	ω	ϕ	n
1	2.5133	1.7345	4
2	3.1416	2.3348	5
3	4.3982	2.9893	7
4	5.6549	0.7337	9
5	6.9115	4.1948	11
6	8.1681	5.2334	13
7	9.4248	0.0301	15
8	10.6814	4.5552	17

The integral frequencies were chosen so that their harmonics do not coincide with other fundamental frequencies or with harmonic frequencies of other sinusoids. The phases were chosen so that the sum of the 8 sinusoidal voltage signals has a minimum maximum amplitude.

The full excitation lasted for 8 cycles, each of 10 seconds duration, from 520 to 600 seconds. The results in this report were obtained for the EOB (End Of Burn) Equilibrium.

In order to maintain the plasma centred during this exercise, in the presence of the vertical instability, we retained weak feedback of the radial and vertical positions of the current centroid. This feedback action was only applied to two

coils, PF3 and PF5. In order to maintain the plasma current fairly constant, we applied a small fixed voltage to the PF1 (Central Solenoid) coil.

The amplitude of the applied voltage for each sinusoid was chosen to be 10 Volts, 1 Volt and 0.05 Volts. Only results from the largest amplitude of the excitation voltage are shown, for which the summed signal was up to 50 Volts, well in excess of the nominal coil saturation voltages.

3. LINEARITY TEST RESULTS

The raw results with the largest excitation amplitude, 10V, are shown in Figure 1 a)-d) for the case of PF2 excitation, illustrating the modulation of a) the coil voltages, b) the coil currents, c) the gaps and d) various plasma parameters. Alongside each time trace shown in the left hand column of the figure, we show the FFT of the signal in the right hand column, from 0-4 Hz. The FFT was obtained from the code response during only the last 6 cycles of the stimulation, corresponding to the time interval 540 - 600 seconds. The first two cycles were rejected for the slow response to the stimulation to settle down. In order to remove the effects of drifts in the response, a linear offset background was removed from each trace before the FFT was applied.

The fundamental frequencies are clear in all traces, except for the unexcited coil voltage traces. The amplitude of the PF3 and PF5 feedback is clear in the voltage traces. The coupling between all of the PF coil currents is visible. The modulation of the global plasma parameters is clear in the time traces and the FFT. These results for the PF2 coil are representative of all PF coils.

There is no evidence of harmonic generation to the eye when looking at these FFT responses. Figure 2 shows an expanded plot of the Ip and li responses, both full scale and with the scale multiplied by 20. We assess the upper limit of the amplitude of the harmonics to be less than 0.3%. The lack of harmonics of the stimulation frequencies was verified during excitation by all the coils separately.

Further more detailed analysis could define the upper limit within the limits of noise and also determine a better indication of linearity.

The absence of harmonics in the TSC code response is a demonstration of the effective linearity of the plasma response to within the accuracy of the code itself. The cases shown in Figures 1 and 2 correspond to a much greater level of excitation than the available voltages applied to the PF coils.

4. SUMMARY OF THE DIFFERENT COIL RESULTS

Figure 3 shows a summary of the absolute amplitude of the responses to all eight of the PF coils, only indicating the response at the driving frequency. The PF1 current has been divided by 10 for clarity.

Further runs could be performed on other equilibria, if considered useful, during Phase II of the contract.

Figure 4 shows the complex response for 2 typical cases, stimulation of PF2 and PF4. The responses of Ip, li, βp, Rmag and Zmag are illustrated, with an arbitrary scale. The responses are multiplied by the frequency, corresponding to an injection of volt-seconds, flux, into the coils.

The responses of li and βp are roughly proportional, seen to be generally true for stimulation of all coils. Their modulation is almost always in anti-phase with respect to the Ip modulation.

More detailed analysis of these results is not useful, since this subject will be treated in full by the System Identification part of this Design Task. These results are illustrated for general interest only.

5. CONSERVED PLASMA QUANTITIES

Inspecting Figure 4, we find modulation of the internal inductance, li, plasma poloidal energy, βp, radial and vertical positions, Rmag and Zmag, and the plasma current, Ip. We have attempted to determine the presence of, as well as the properties of effectively conserved quantities when running the TSC code in these conditions. We have taken the individual responses of these different modulated plasma quantities, expressed as the fractional change of each parameter normalised to the normalised volt-seconds stimulation V/ω. We then looked for a multiplier which sets their sum as close to zero as possible for all of the eight frequency responses:

$$\text{li-responses} - A * \text{Ip-responses} = \text{Combined-responses} \sim 0$$

Since the responses themselves are complex, A is naturally complex. In order that the combined response should correspond to the effective conservation of a physical quantity, we fitted a real multiplier A.

Since the modulation of the major radius should also enter into physically reasonable conserved quantities, we extended the fit to include a second real multiplier B, such that:

$$\text{li-responses} - A * \text{Ip-responses} - B * \text{Ro-responses} = \text{Combined-responses} \sim 0$$

a) Internal inductance

We plot the results obtained for PF2 and PF4 stimulation in Fig. 5 a) and b). The negative and positive numbers indicate the normalised responses of li and Ip respectively, already seen in Figure 4. We overplot the quantity A * Ip-responses as asterisks (*) for complex A and square crosses for real A. The residue of the combined-responses as defined above is shown as circles close to the origin.

When extending the fit to include the B multiplier, the approximation to the li-response is shown as diagonal crosses in the Figures.

b) Plasma energy

We applied the same procedure to the modulation of the plasma beta-poloidal, illustrated in Fig. 5 c) and d).

c) Results

From Fig. 5 a) and b) we can conclude that there exists a combination of Ip and li with a real multiplier which shows less than 10% of the modulation of the individual responses. Including modulation of the major radius, we obtain an even better approximation.

The same conclusion holds, with apparently more noise on the signal content, for the modulation of the plasma energy.

However, this exercise cannot determine the physics contents of the A- or B-multipliers from this one operating point. On the other hand, we can test the values of A and B against a priori choices of conserved quantities.

The fitted values of A and B for the 2 cases are :

	li(Ip)	li(Ip,Rmag)	βp(Ip)	βp(Ip,Rmag)
PF2	-1.85	-1.95,12	-1.65	-1.65, 0.8
PF4	-1.52	-1.56, -2.3	-2.2	-2.4, -3.3
PF4 and PF2	-1.4	-1.5, -1.8	-2.4	-2.8, -6

Excitation by PF2 hardly moves the major radius, so the data contain little leverage on the Rmag multiplier. We have therefore forced a fit on the A and B multipliers using the data from both PF2 and PF4 stimulation.

We must note that the presence of radial feedback limits the Rmag excursion, which probably reduces the accuracy of the data obtained.

These results are not far from the conservation of the internal magnetic energy and the internal kinetic energy. These results will be refined during the Phase II of the D 324-1 Design Task in order to compare them with a priori linearised models.

6. CONCLUSION

The TSC simulations of ITER PF coils has demonstrated the linearisability of the response around a single working point, by virtue of the absence of harmonics of the driving frequencies in the response.

The results have indicated the presence of conserved quantities with real linearised coefficients. These conserved quantities are not far from the conservation of internal magnetic energy and internal kinetic energy.

7. FUTURE WORK

Some work will be performed to check the linearity for other scenario reference points.

More work will be required to refine this approach during the System Identification part of the D324-1 Design Task.

FIGURE CAPTIONS

Fig. 1 a) Coil voltage time traces and FFT. Excitation is onto the PF2 coil.

Fig. 1 b) Coil current time traces and FFT. Excitation is onto the PF2 coil.

Fig. 1 c) Separatrix-to-wall gap time traces and FFT. Excitation is onto the PF2 coil.

Fig. 1 d) Various global plasma parameter time traces and FFT. Excitation is onto the PF2 coil.

Fig. 2 Test of the linarity of the response of Ip and li, showing the FFT of these signals. The fundamental driven frequencies and their harmonics are indicated. Each response is shown with full scale and expanded by x20.

Fig. 3 a) Summarised responses for the excitation of the PF1 coil.

Fig. 3 b) Summarised responses for the excitation of the PF2 coil.

Fig. 3 c) Summarised responses for the excitation of the PF3 coil.

Fig. 3 d) Summarised responses for the excitation of the PF4 coil.

Fig. 3 e) Summarised responses for the excitation of the PF5 coil.

Fig. 3 f) Summarised responses for the excitation of the PF6 coil.

Fig. 3 g) Summarised responses for the excitation of the PF7 coil.

Fig. 3 h) Summarised responses for the excitation of the PF8 coil.

Fig. 4 a) Complex responses of Ip, li, βp, Rmag and Zmag to PF2 excitation. The scale is arbitrary for illustration.

Fig. 4 b) Complex responses of Ip, li, βp, Rmag and Zmag to PF4 excitation. The scale is arbitrary for illustration.

Fig. 5 a) Complex response of Ip and li and their linear combinations with PF2 excitation.

Fig. 5 b) Complex response of Ip and li and their linear combinations with PF4 excitation.

Fig. 5 c) Complex response of Ip and βp and their linear combinations with PF2 excitation.

Fig. 5 d) Complex response of Ip and βp and their linear combinations with PF4 excitation.

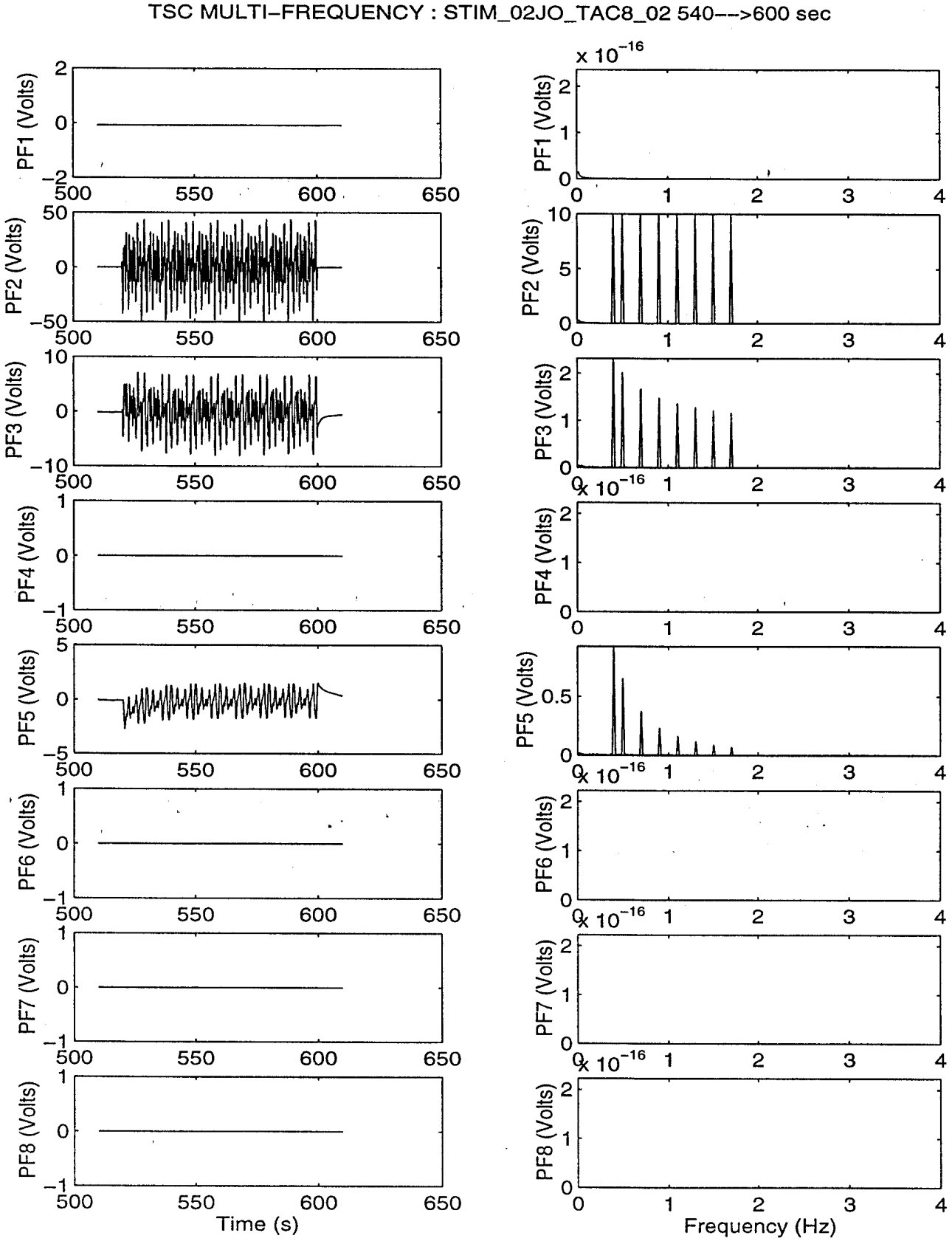

Fig. 1 a) Coil voltage time traces and FFT. Excitation is onto the PF2 coil.

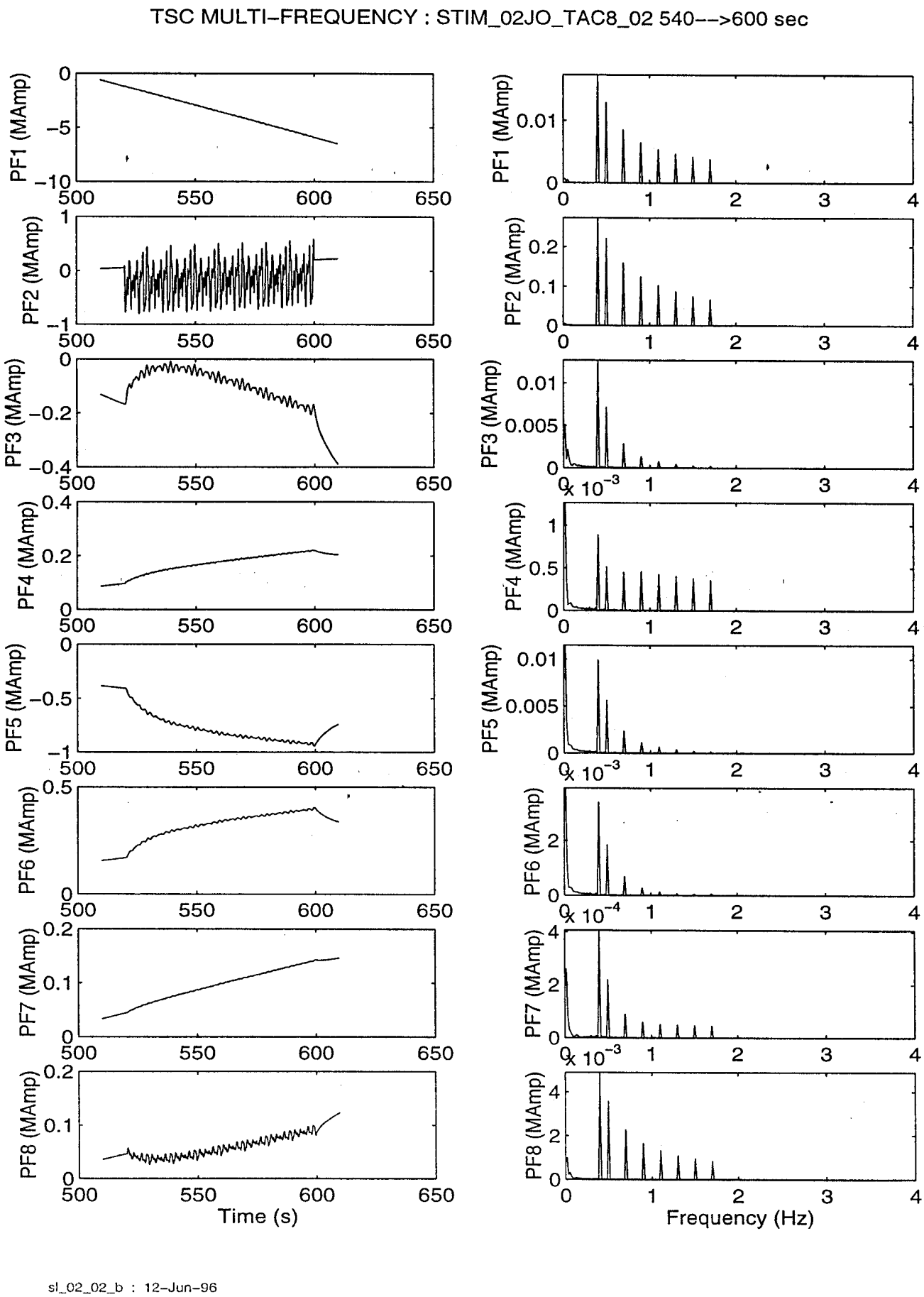

Fig. 1 b) Coil current time traces and FFT. Excitation is onto the PF2 coil.

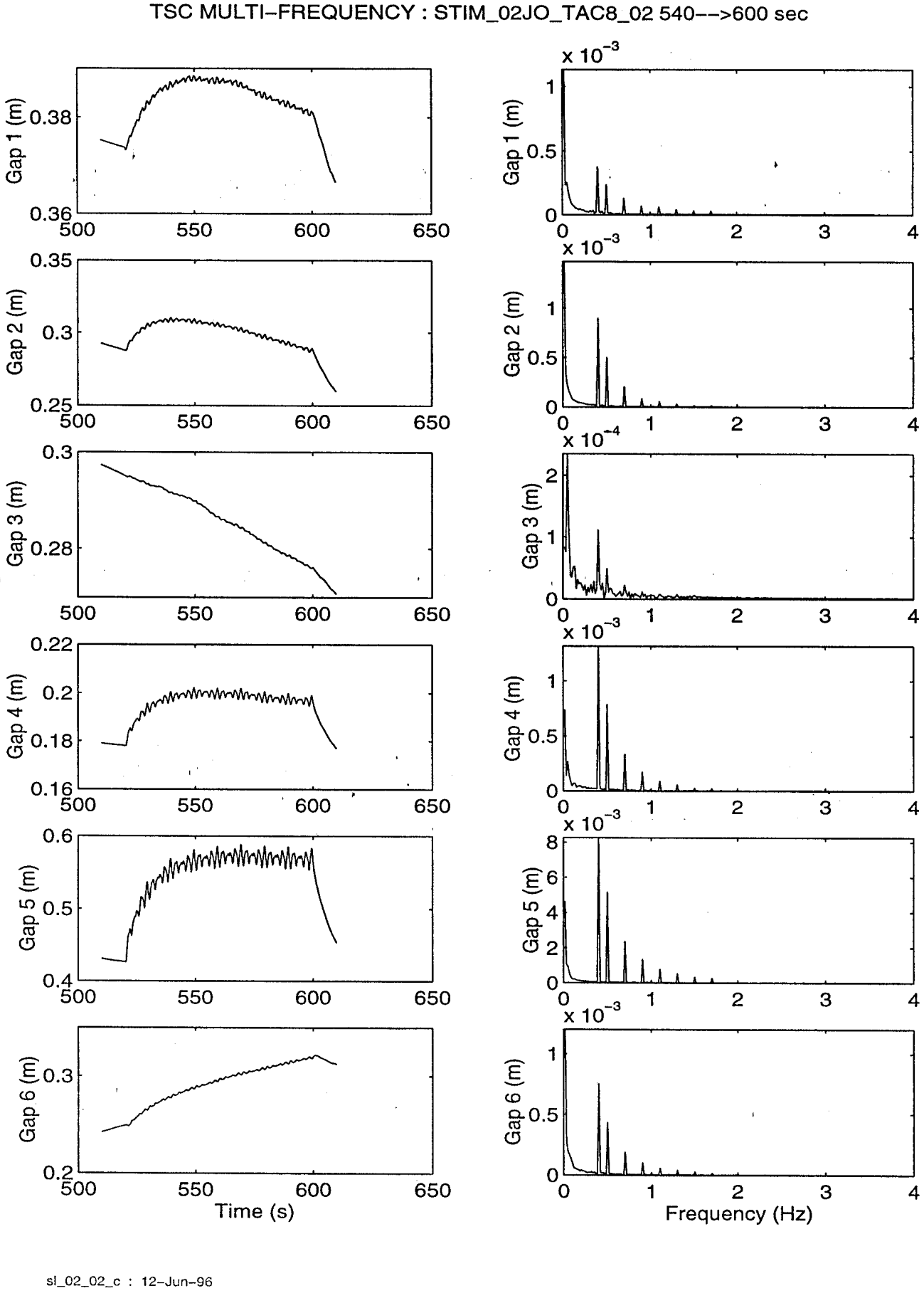

Fig. 1 c) Separatrix-to-wall gap time traces and FFT. Excitation is onto the PF2 coil.

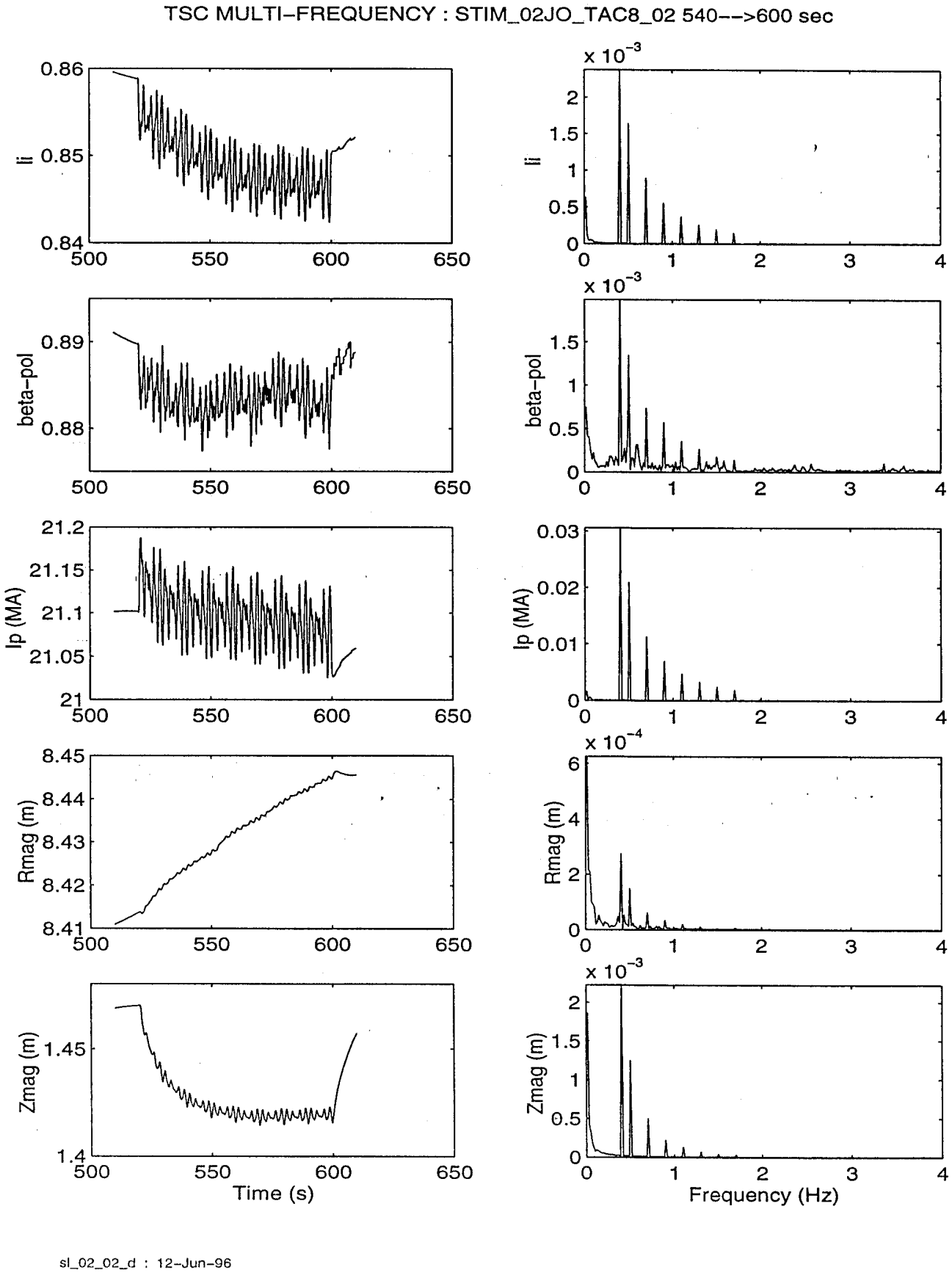

Fig. 1 d) Various global plasma parameter time traces and FFT. Excitation is onto the PF2 coil.

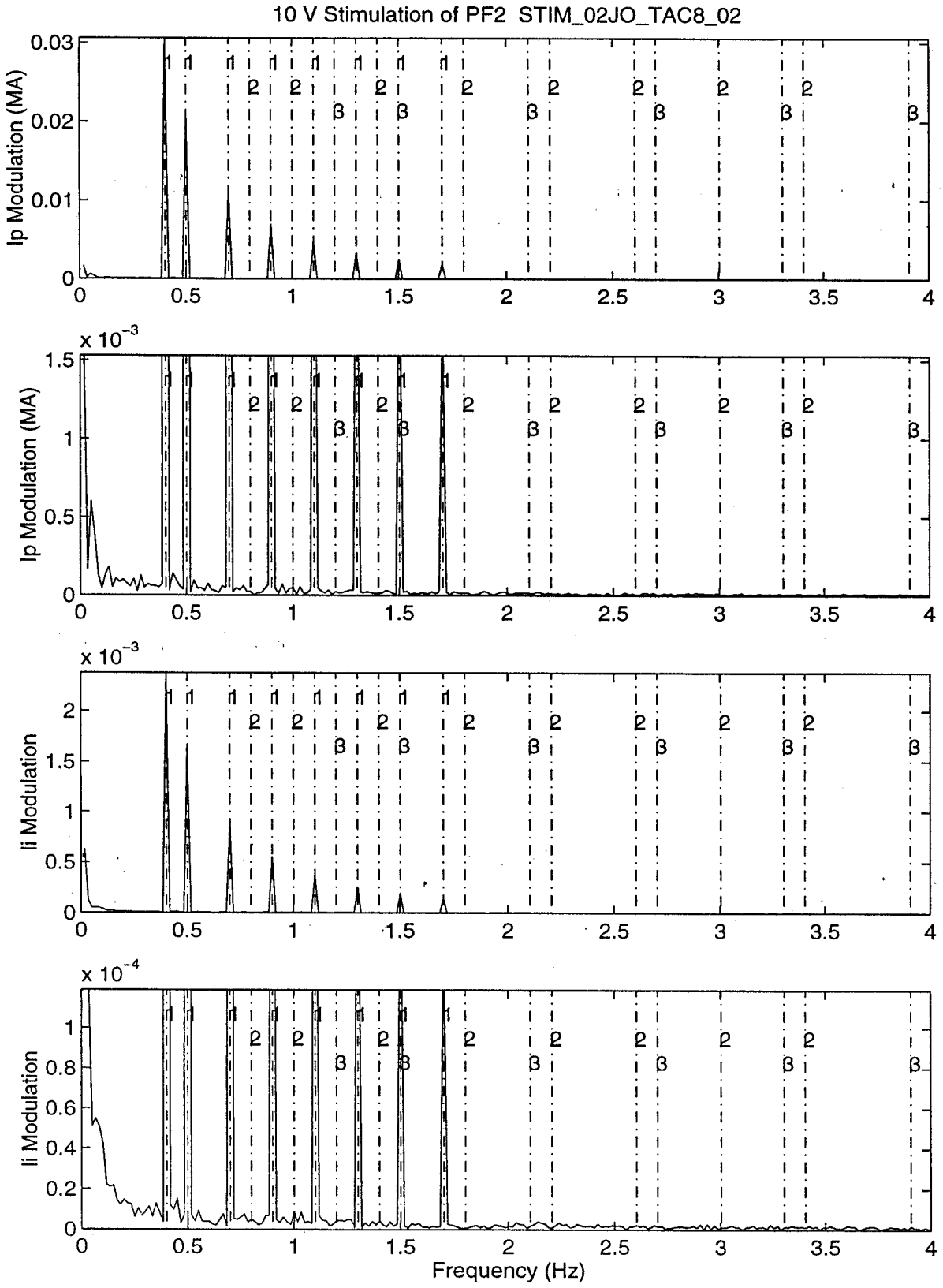

Fig. 2 Test of the linarity of the response of Ip and Ii, showing the FFT of these signals. The fundamental driven frequencies and their harmonics are indicated. Each response is shown with full scale and expanded by x20.

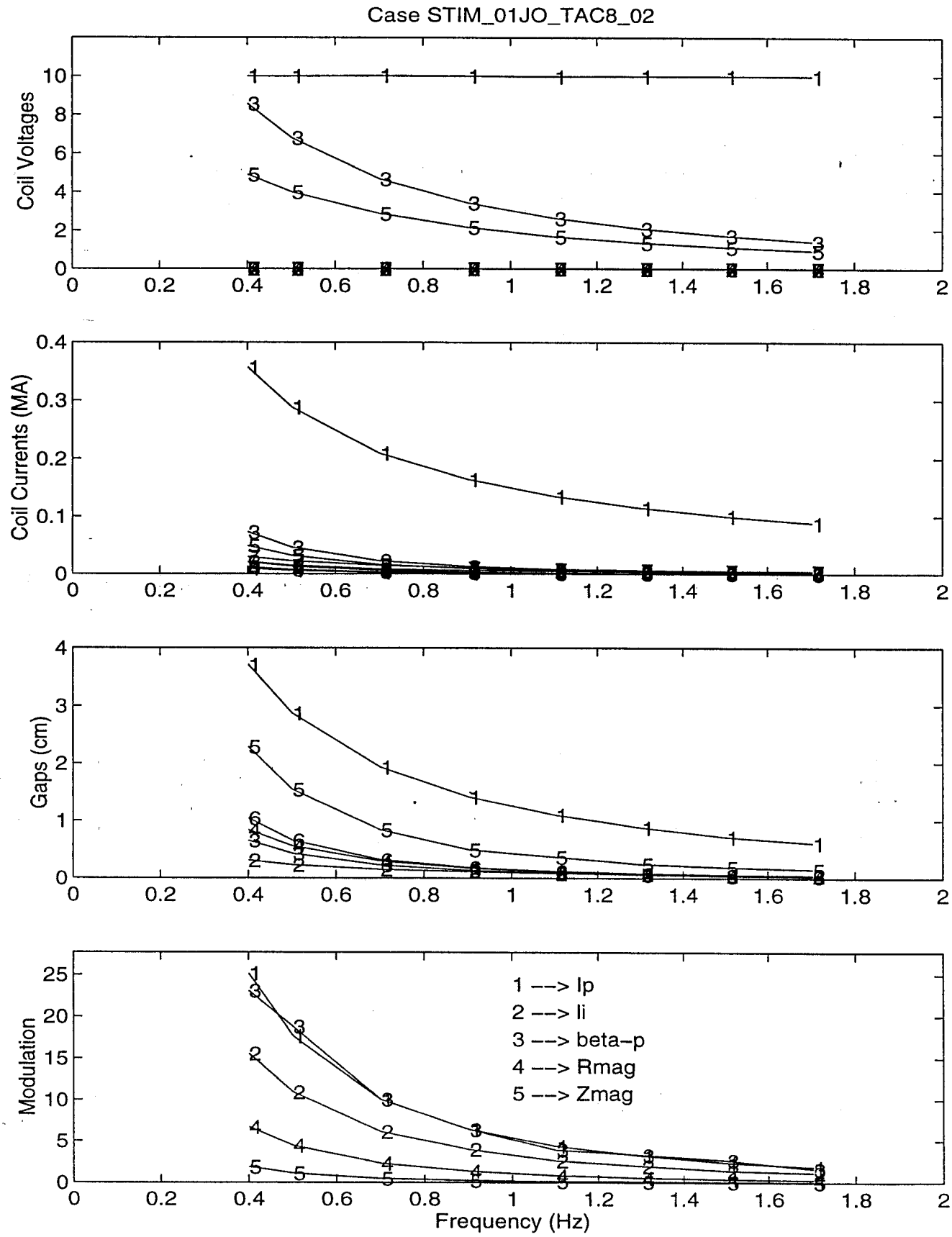

Fig. 3 a) Summarised responses for the excitation of the PF1 coil.

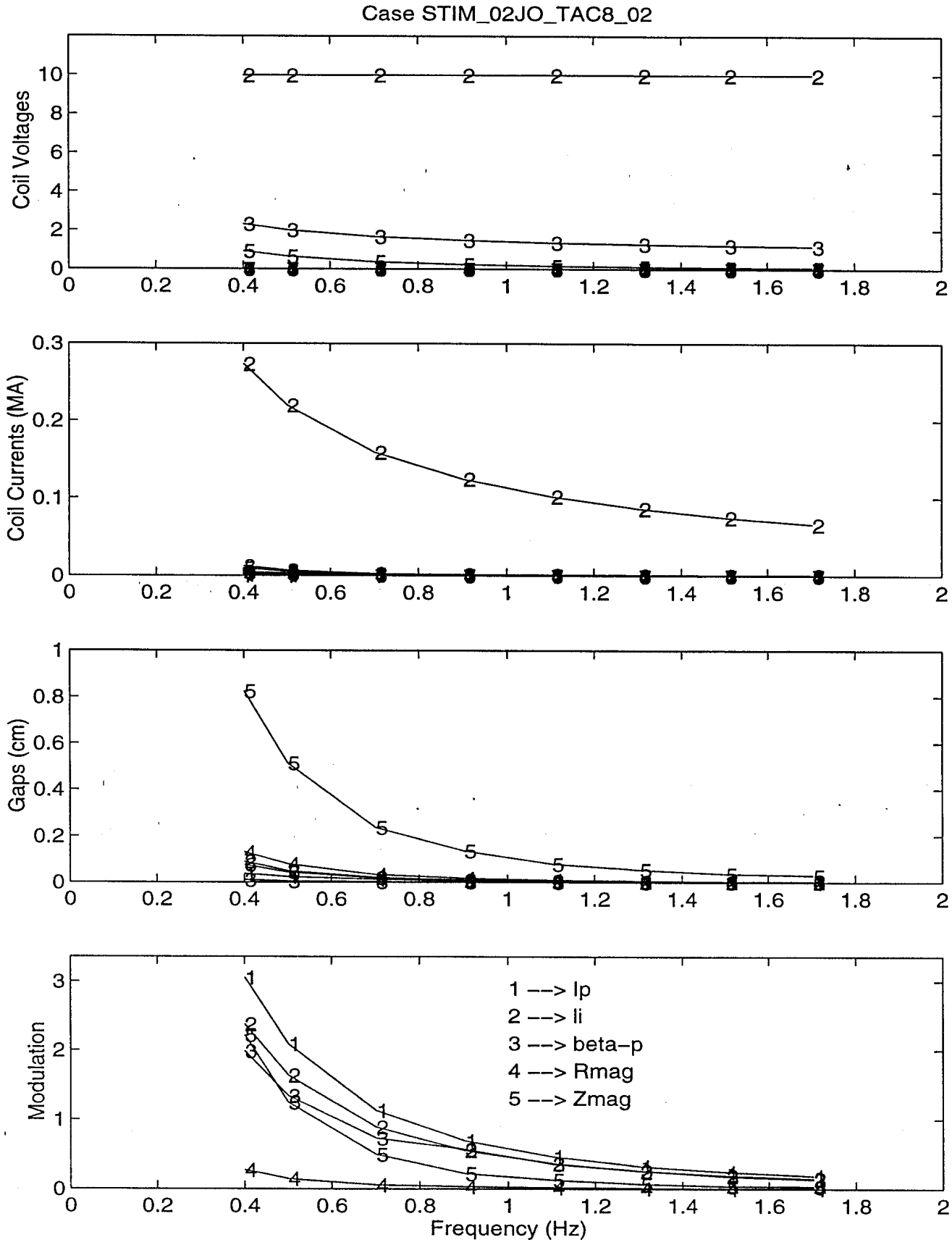

Fig. 3 b) Summarised responses for the excitation of the PF2 coil.

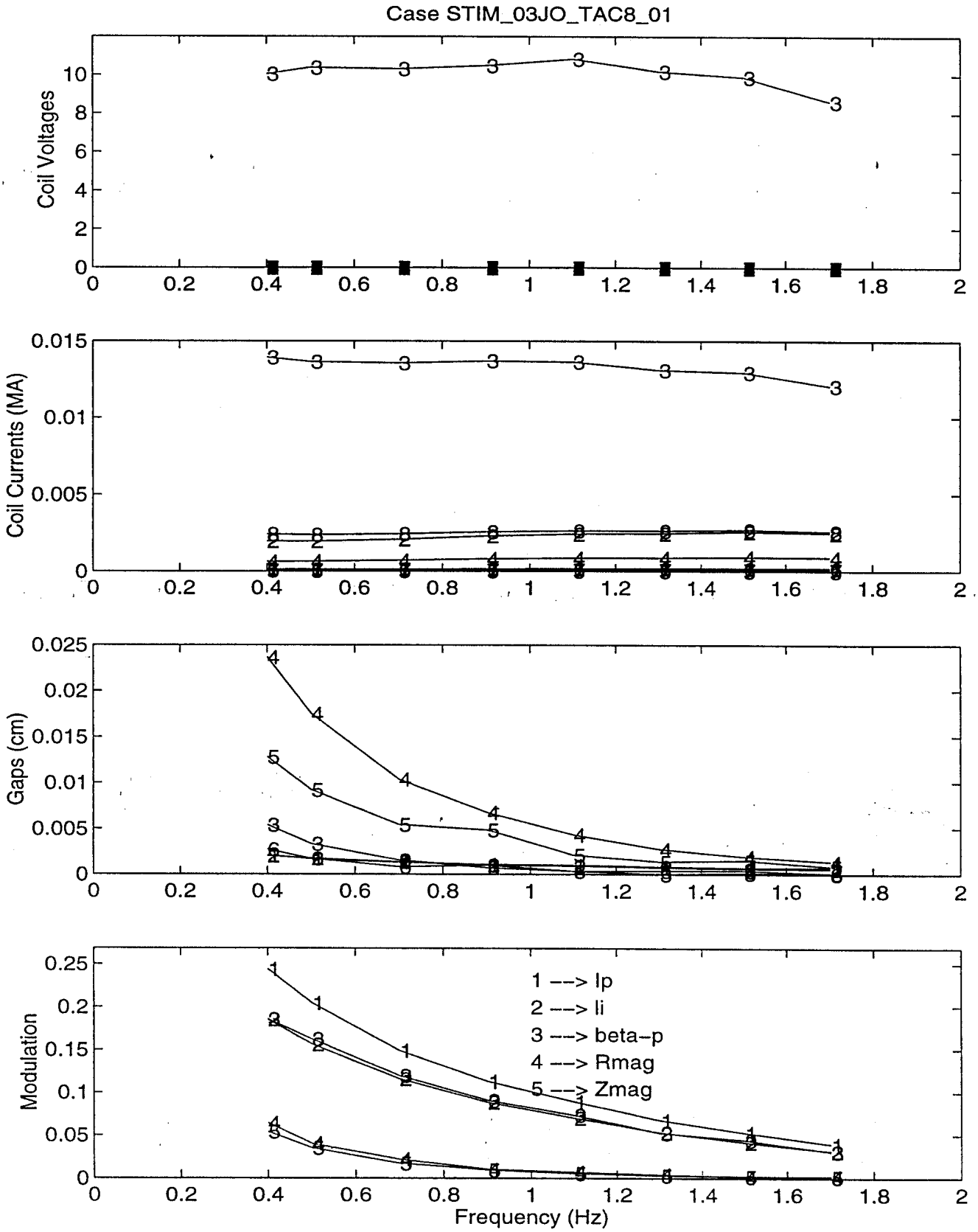

Fig. 3 c) Summarised responses for the excitation of the PF3 coil.

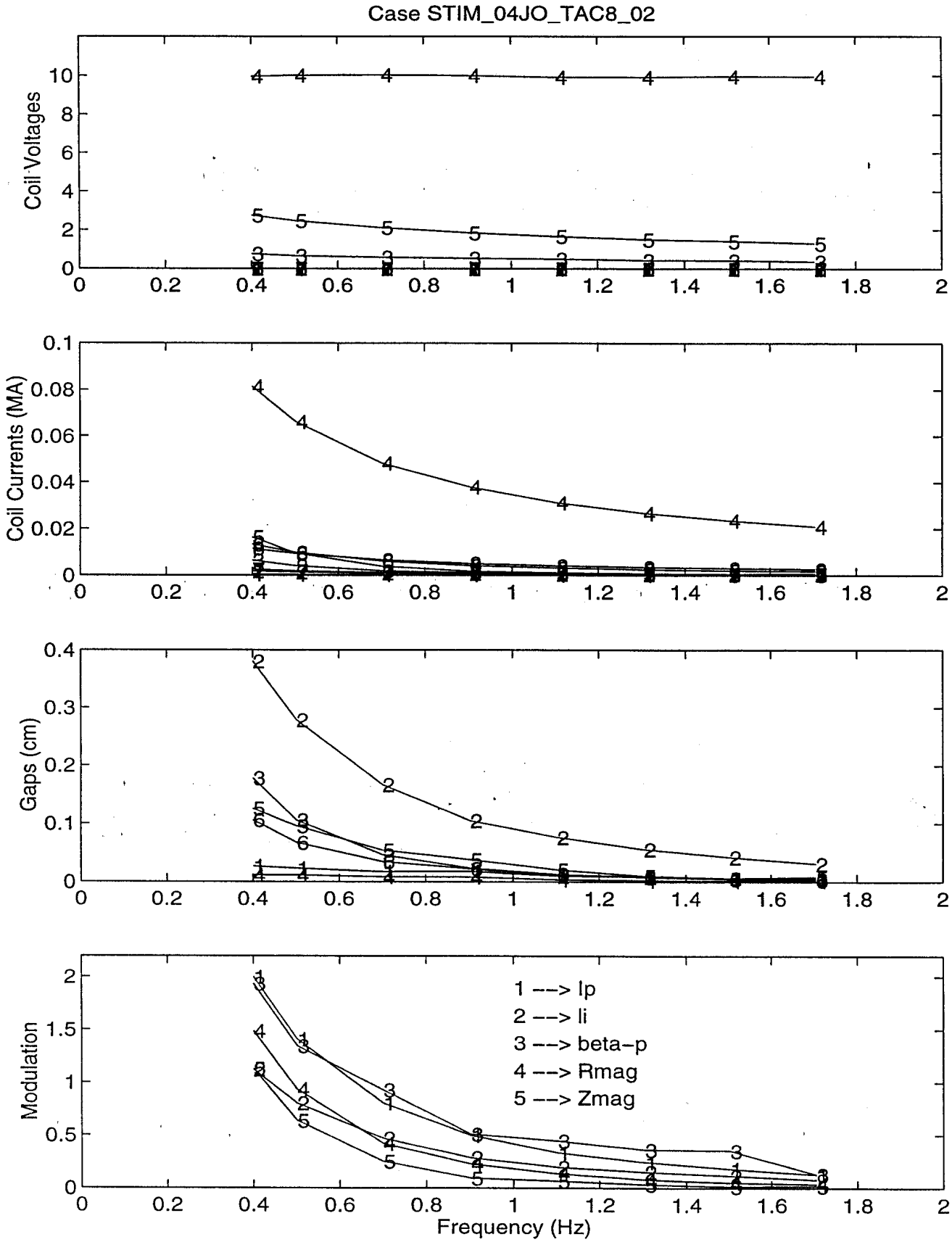

Fig. 3 d) Summarised responses for the excitation of the PF4 coil.

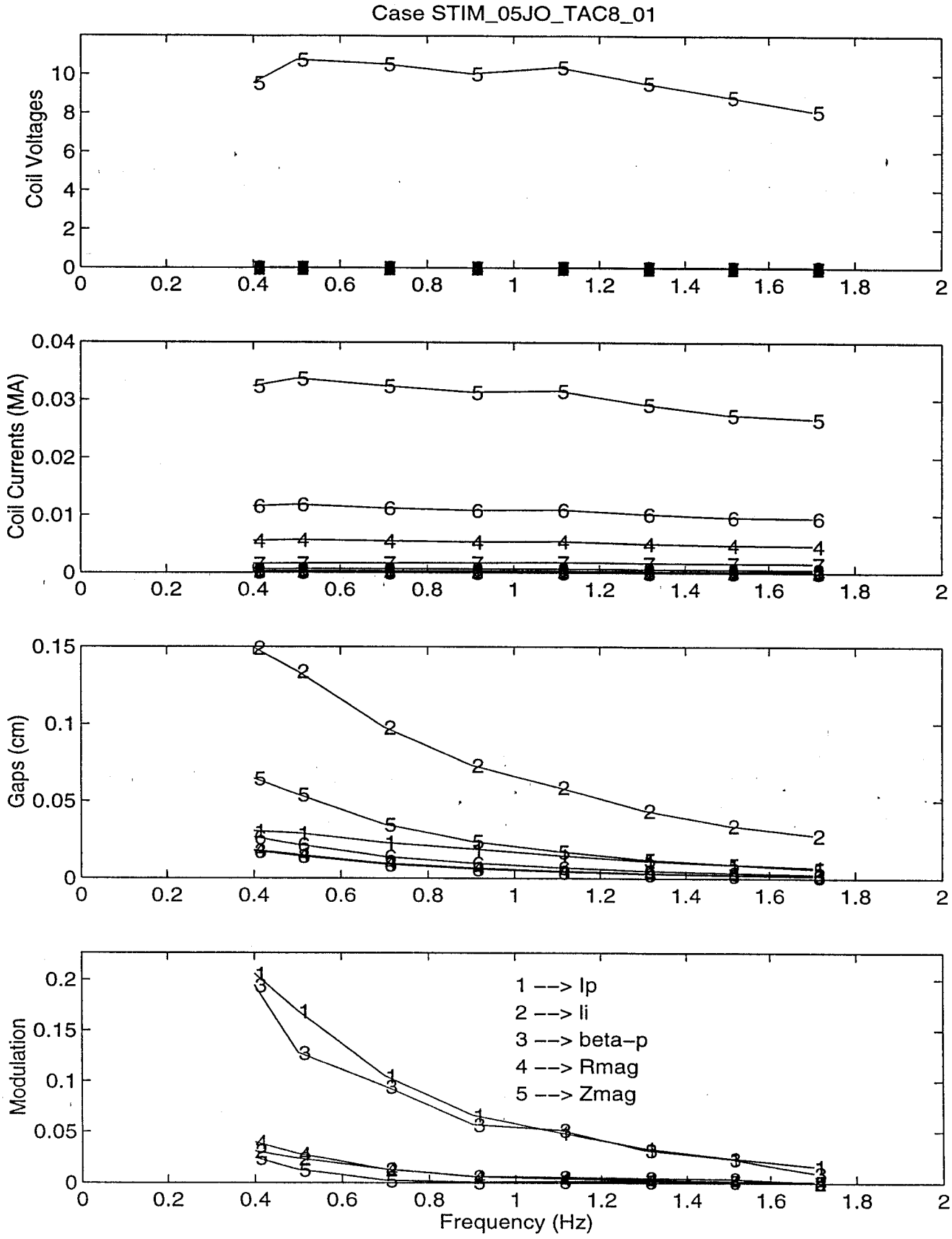

Fig. 3 e) Summarised responses for the excitation of the PF5 coil.

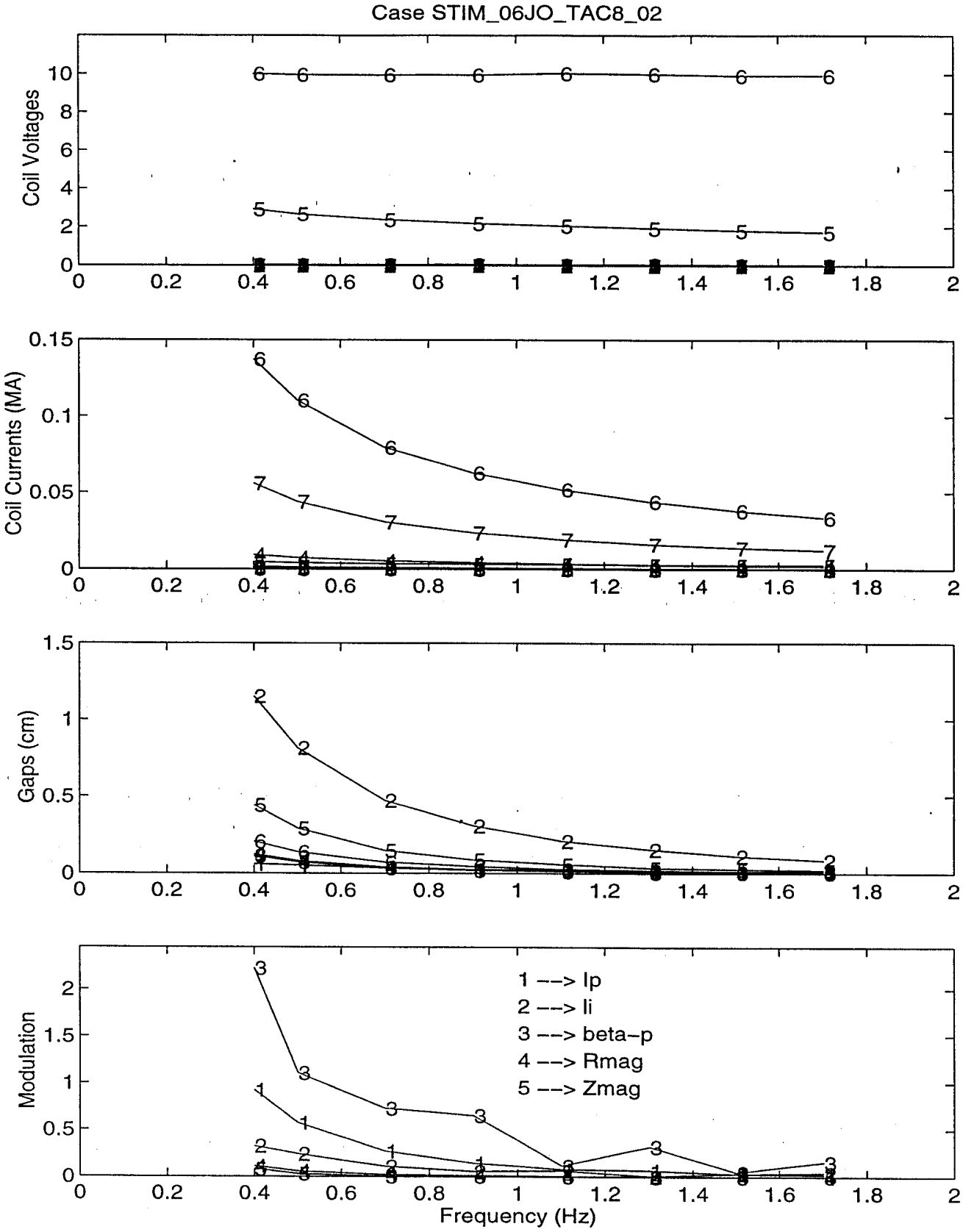

Fig. 3 f) Summarised responses for the excitation of the PF6 coil.

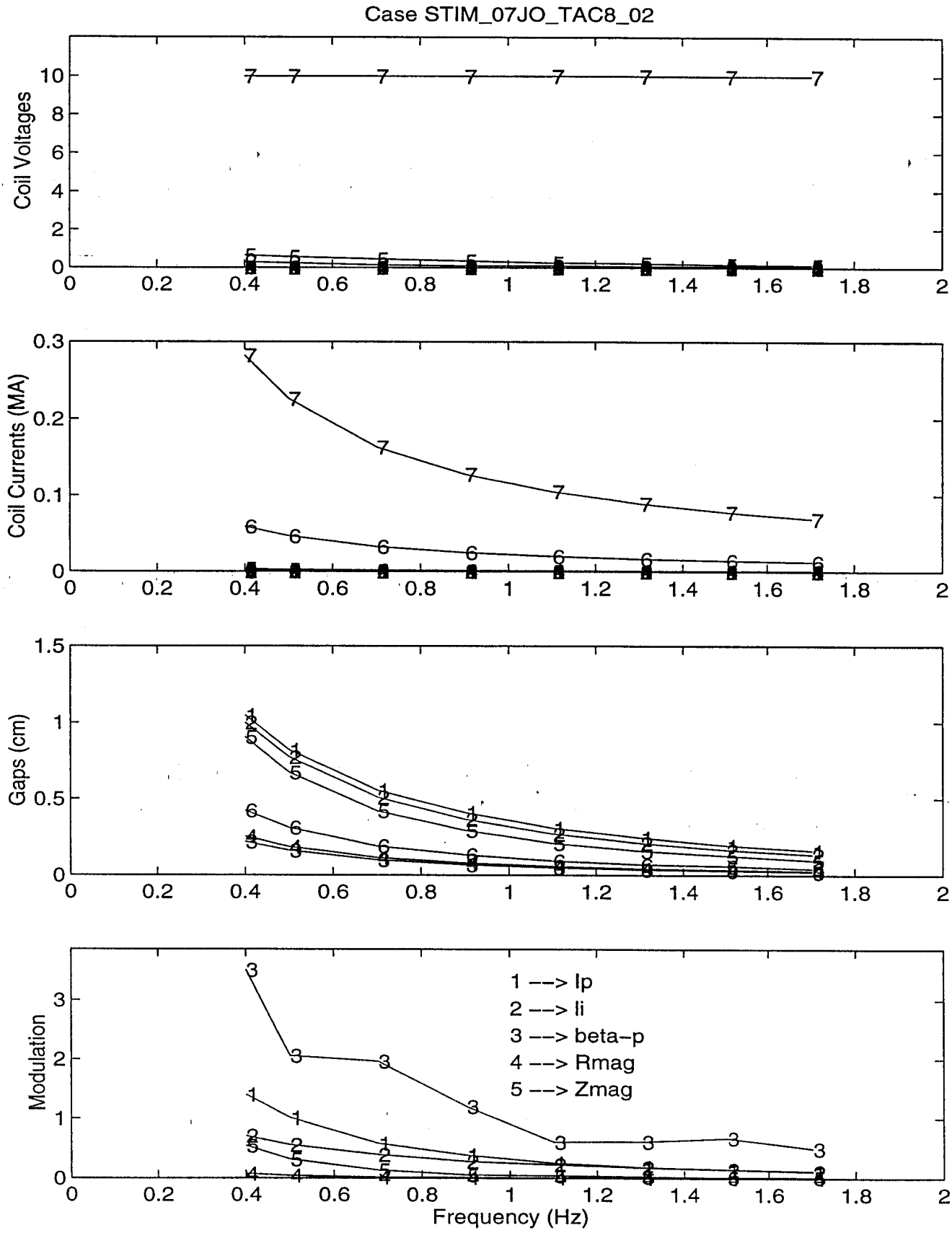

Fig. 3 g) Summarised responses for the excitation of the PF7 coil.

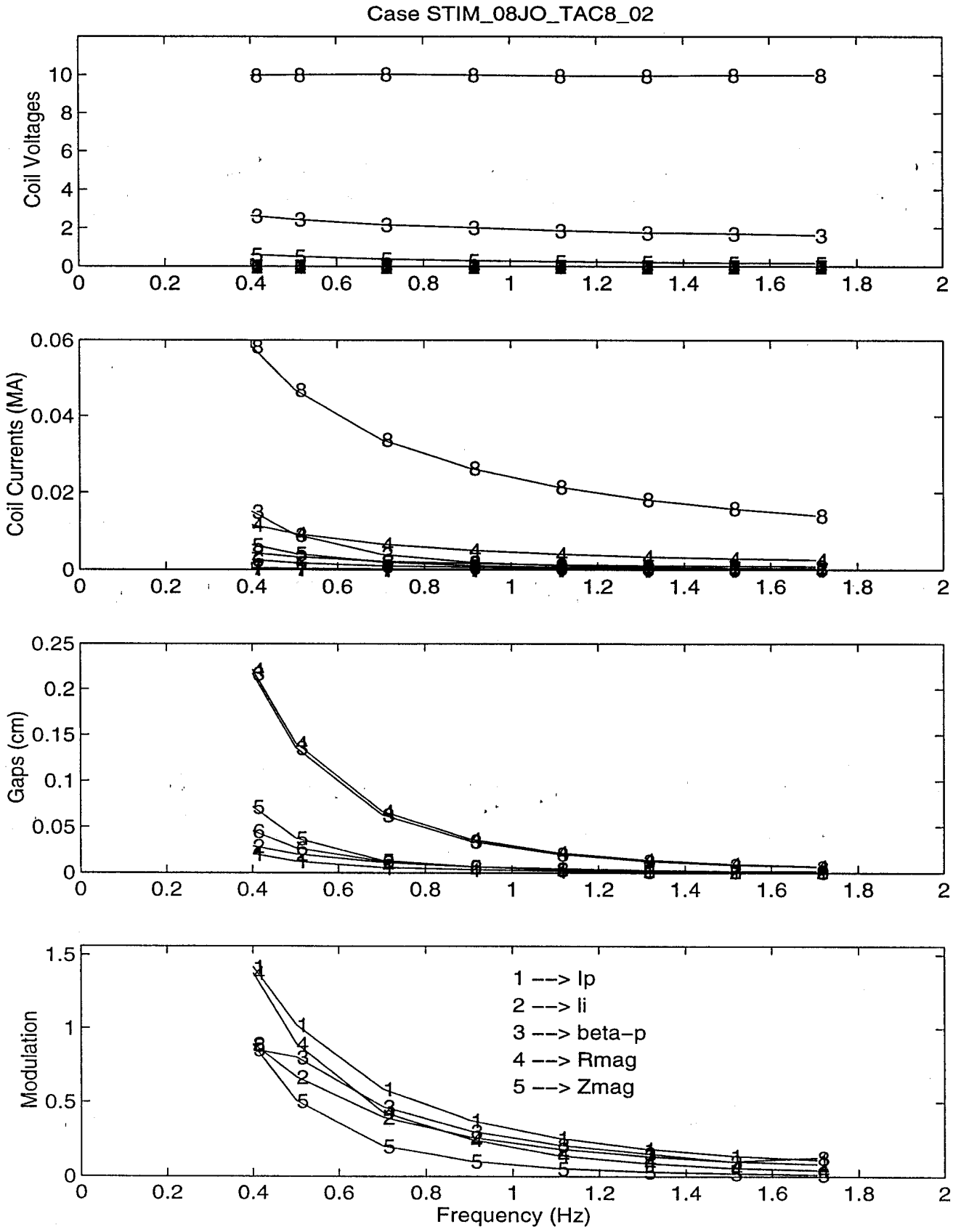

Fig. 3 h) Summarised responses for the excitation of the PF8 coil.

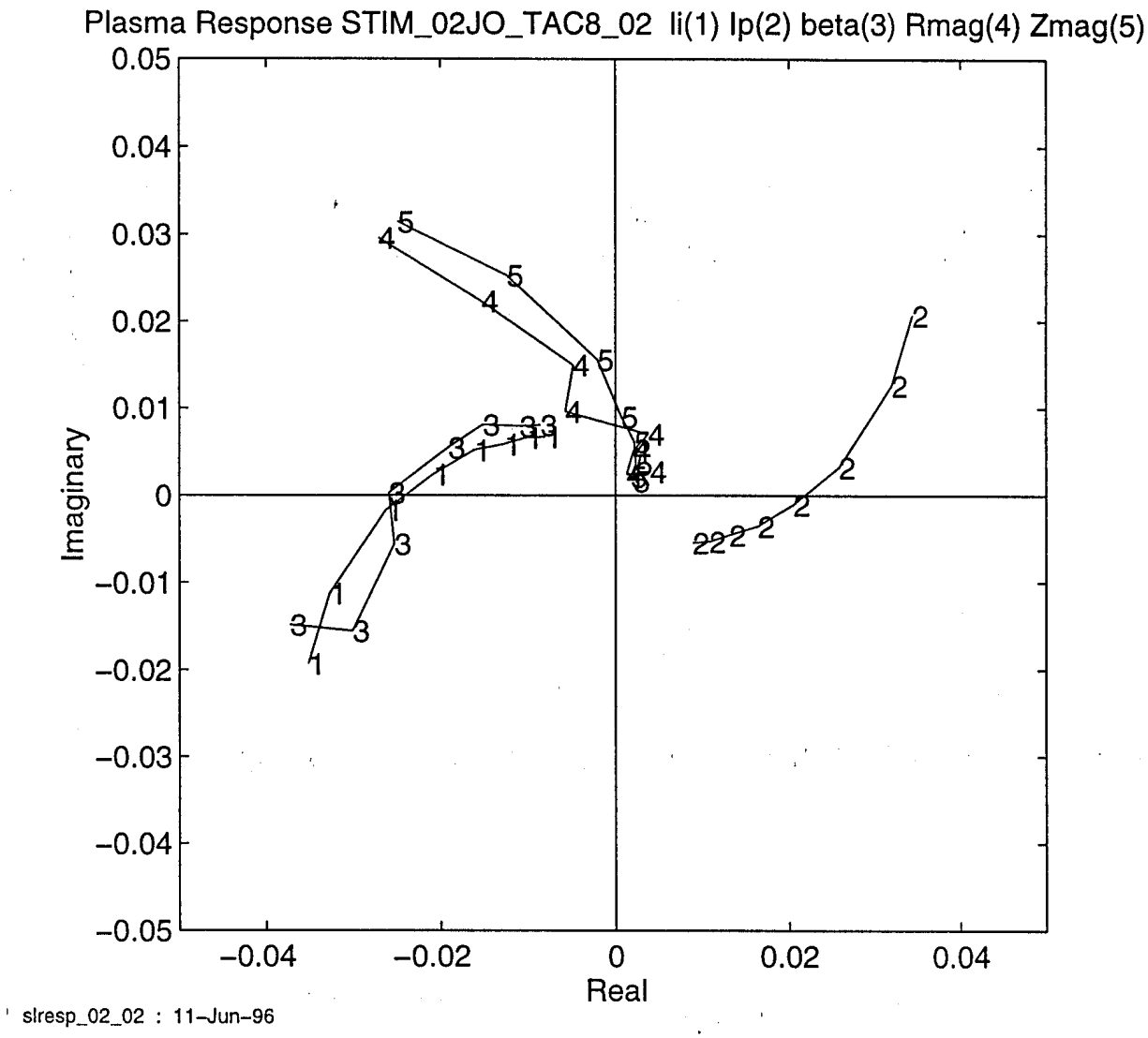

Fig. 4 a) Complex responses of Ip, li, βp, Rmag and Zmag to PF2 excitation. The scale is arbitrary for illustration.

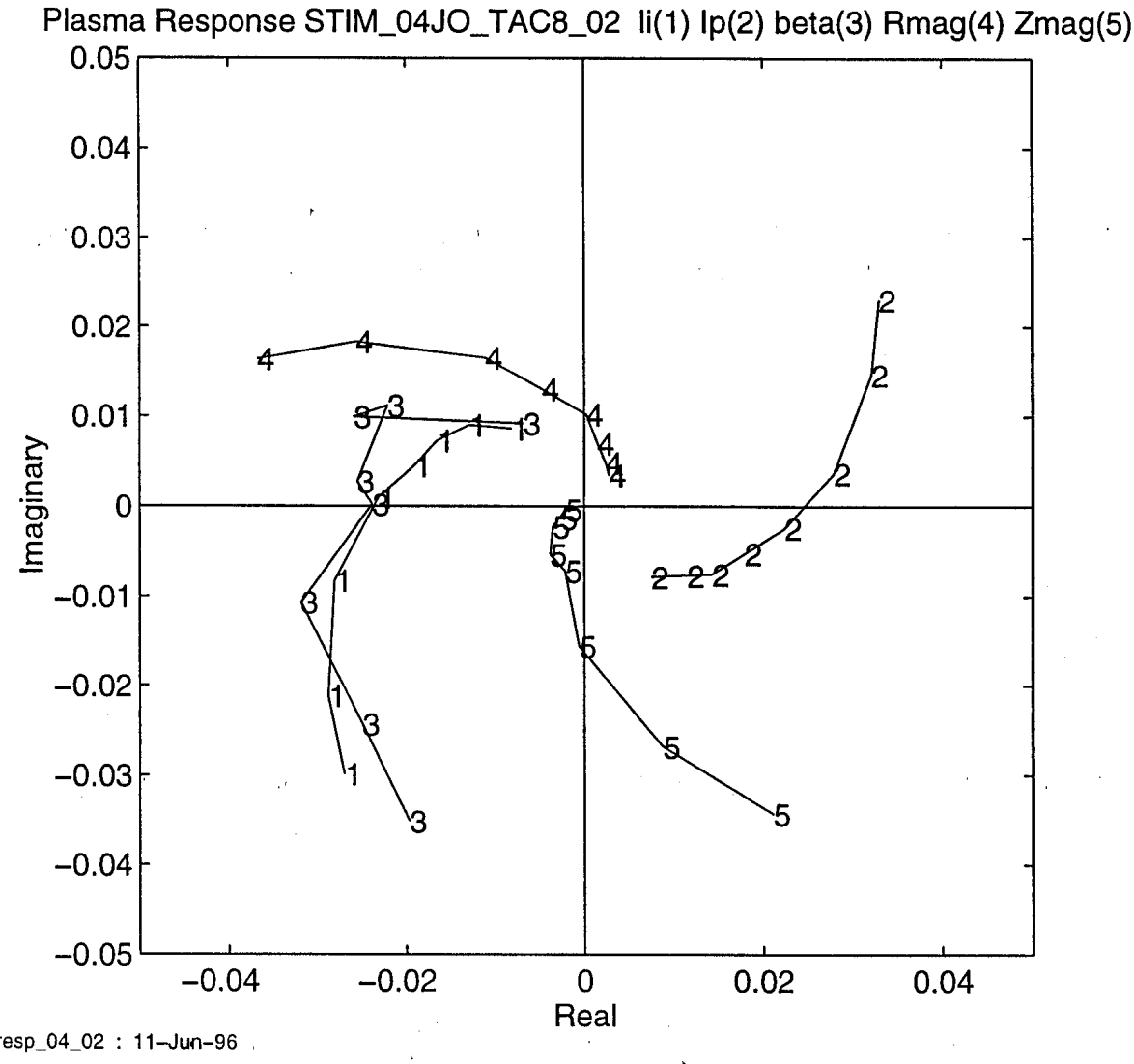

Fig. 4 b) Complex responses of Ip, li, βp, Rmag and Zmag to PF4 excitation. The scale is arbitrary for illustration.

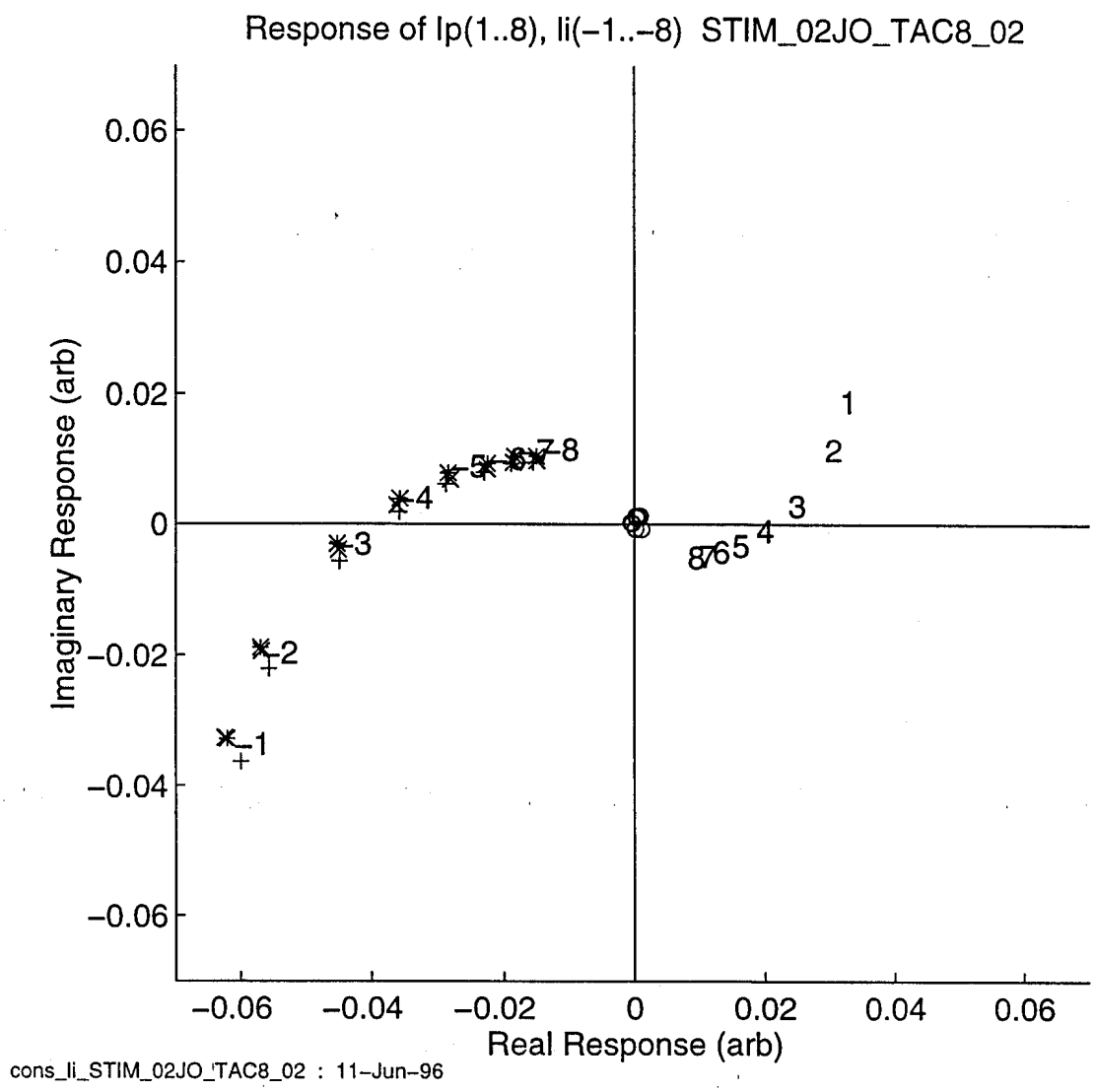

Fig. 5 a) Complex response of Ip and Ii and their linear combinations with PF2 excitation.

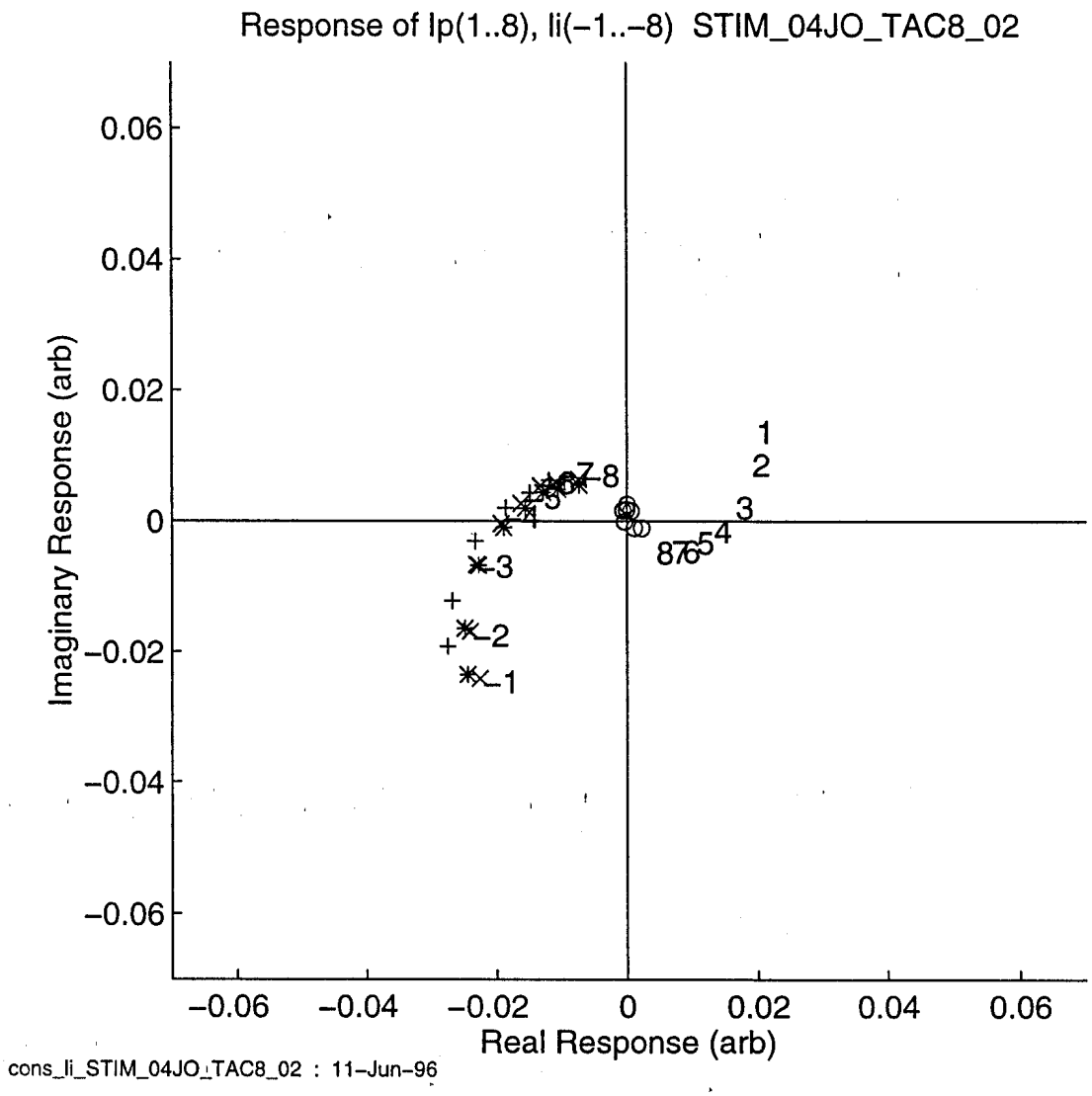

Fig. 5 b) Complex response of Ip and Ii and their linear combinations with PF4 excitation.

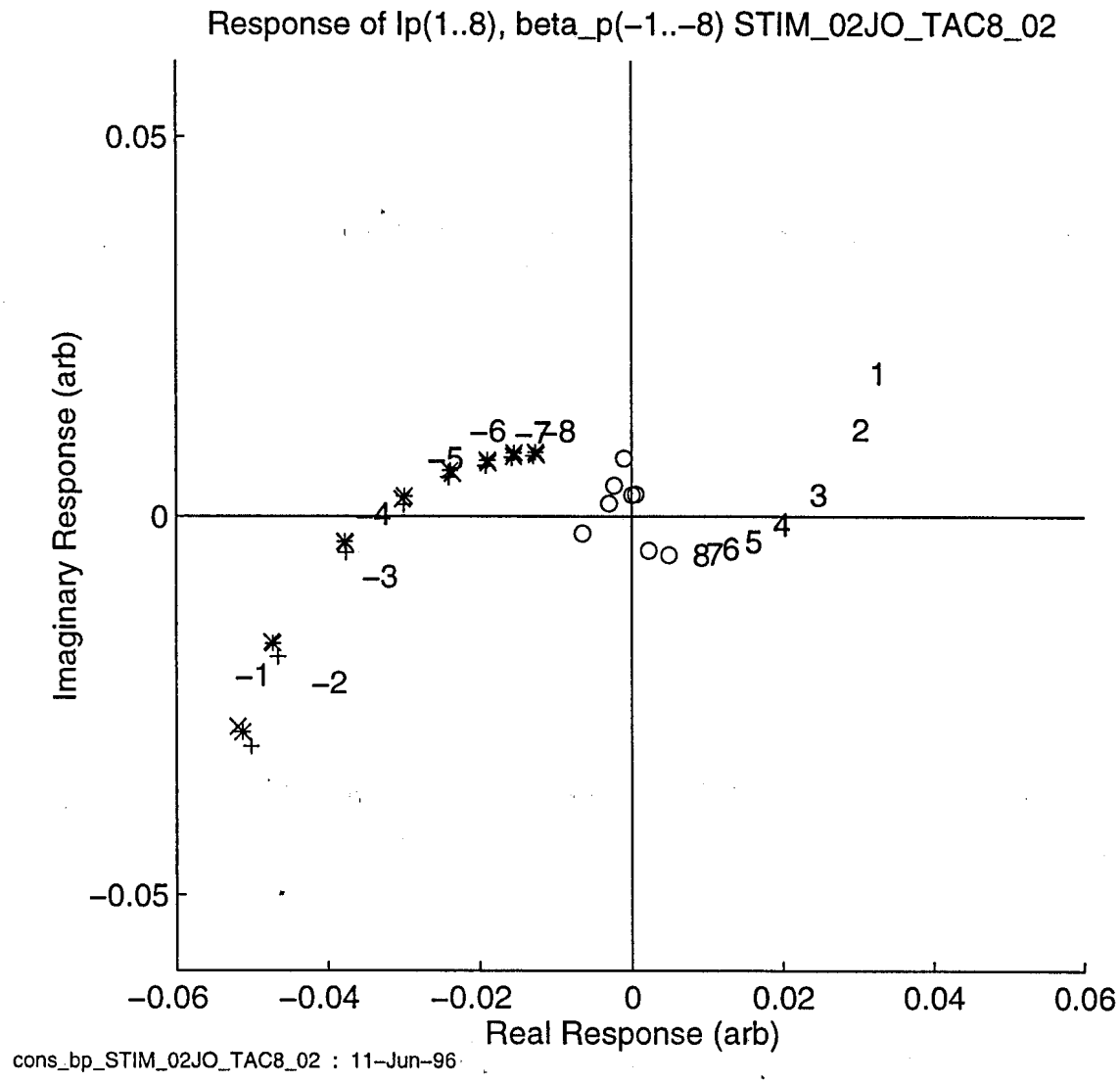

Fig. 5 c) Complex response of Ip and βp and their linear combinations with PF2 excitation.

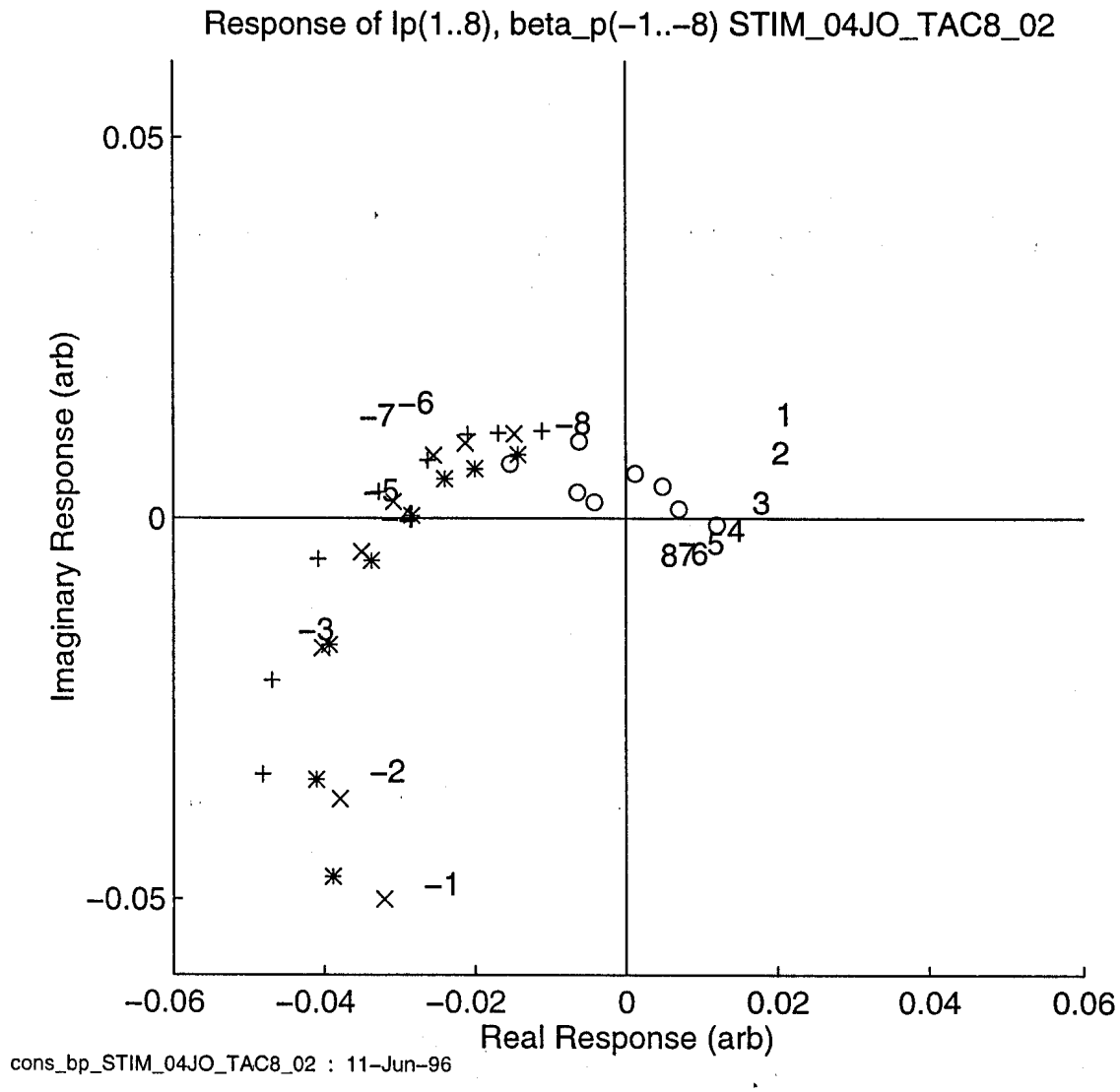

Fig. 5 d) Complex response of Ip and βp and their linear combinations with PF4 excitation.

EIDGENÖSSISCHE TECHNISCHE HOCHSCHULE LAUSANNE
POLITECNICO FEDERALE DI LOSANNA
SWISS FEDERAL INSTITUTE OF TECHNOLOGY LAUSANNE

CENTRE DE RECHERCHES EN PHYSIQUE DES PLASMAS
Association EURATOM - Confédération Suisse

ÉCOLE POLYTECHNIQUE
FÉDÉRALE DE LAUSANNE

Final Report

ITER Design Task D324-1 Phase I

Work Envelope D

Shape Control Considering Voltage and Current Saturation

J.B. LISTER and X. LLOBET
(CRPP-EPFL)

18 July, 1996

E_D_TC_3.DOC

1. PREAMBLE

This final report of ITER Design Task D324-1 Phase I contains preliminary information on the design of plasma shape and current controllers for ITER. The point of view taken is that the coil saturation presents a problem which is more serious than the differences between the different controllers with ideal power supplies. The results are sufficiently encouraging to be discussed but these results must not be considered to be the final word on this promising approach. Work in this direction should proceed during Phase II with collaboration with Imperial College, who have also shown interest.

2. INTRODUCTION

Considering a simplified view of the ITER Poloidal Field (PF) feedback control loop, Fig. 1, a set of reference inputs, plasma current and 6 gaps, is compared with the current values of these variables and the errors are transformed by a controller K to provide voltage demand signals to 7 PF coils. The power supplies for these coils have saturation limits, S, during normal operation and we consider them as clean saturations. These clipped voltages are then applied to the tokamak plant, P.

Habitually, the design of the controller, K, is based on a locally linearised model of the tokamak, using a variety of modern control engineering techniques which seek to optimise certain properties of the closed-loop system, such as its performance in the presence of disturbances or reference changes or its robustness to uncertainties in the parameters of the plant itself.

However, the saturation limits, S, are relatively low for ITER for two reasons, namely a) cost and b) AC heating of the superconductor magnets in the presence of large AC components of the applied control voltages. The behaviour of the closed loop then loses its ability to deliver its design goals and also loses its guarantee of closed loop stability. The applied voltages can become relatively unrelated to those expected as a result of the control variable errors.

As a result of these considerations, we are looking into the design of a controller which knows about the power supply voltage saturation levels and which itself decides upon a course of corrective action if saturation is about to

occur. The power supply voltage saturation no longer "takes the closed loop by surprise" and the designer can choose how his controller will react to the saturation limits.

Previously, A. Portone had dealt with voltage saturation in a SISO plant [1] by feeding back the voltage error due to the saturation, modifying the effective controlled variable error, in order to remove the saturation. These results, referred to as anti-windup, showed that the controller does not subsequently need to "unwind" an accumulated integral error due to the saturation once the saturation is removed.

Recently, the CREATE team [2] have drawn attention to the fact that in the presence of saturation, vertical stabilisation must be treated as most important and that we can do no better than apply the full saturation of all coils with the correct sign of the radial field time-derivative.

In what follows, we present results of a new MIMO approach which is linked to these two approaches. We choose to adapt the plant error so that the controller output is within the voltage saturation limits. We choose the modification to the plant errors to that some of them are better respected than others, giving rise to the apellation "Hierarchical Saturation Controller". We choose any controller which has been designed to be optimal in a small signal sense in order to preserve as much of its functionality as possible. We can consider the Hierarchical Saturation Controller as either respecting the most important controlled variables or polluting the least important controlled variables.

In the body of this report we present a description of the method, Section 3, together with the required algorithmic approach, Section 4, as yet incomplete due to the persistence of untreated cases. Section 5 presents the first results and Section 6 discusses our observations.

In all of this work we have used an available TAC-4 representation of the 6-coil, 6-gap PF system and an LQG controller designed for this ITER model. Both plant model and controller were provided by A. Portone of the ITER JCT at Naka.

3. METHOD

Considering, Fig. 1, a controller K, a saturation vector S and a controlled variable error vector E, we try to modify the error vector to a new vector E* such that:_

$$|Vref^*| = |K(E^*)| < S \tag{3.1}$$

so that the subsequent physical power supply saturation has no effect. A subsidiary condition is that the modified error vector E* be optimal in the sense of minimising

$$Q = (E^* - E)^T H (E^* - E) \tag{3.2}$$

where H is a design matrix which weights the modifications to E. The hierarchisation of the controlled variables is provided by a suitable choice of H.

In order to go further, we assume that the controller K(E) is a discrete-time generalised state-space controller defined by:

$$x_{n+1} = A_{kd}\ x_n + B_{kd}\ E_n \tag{3.3}$$

$$Vref_n = C_{kd}\ x_n + D_{kd}\ E_n$$

We assume $D_{kd} = 0$ in what follows and we have chosen $\Delta T = 30$ msec when implementing this discrete-time controller. The state variable x is the internal state variable of the controller itself.

Given 3.1 and 3.3 we see that the requirement of 3.1 is modified to

$$|V_{ref}^*| = |C_{kd}\ x^*_{n+1}| = |C_{kd}\ A_{kd}\ x_n + C_{kd}\ B_{kd}\ E^*| < S \tag{3.4}$$

for all the elements of Vref* separately. This condition ensures that the next voltage output be unsaturated, given a current state vector x_n and the values of C_{kd}, B_{kd}, A_{kd}. If x_n gave rise to an unsaturated voltage demand signal and if A_{kd} is stable, then there will always be a solution to Equation 3.4.

The problem is now clearly posed and we require an algorithm for choosing E* such that 3.4 and 3.2 be satisfied.

4. ALGORITHMIC APPROACHES

4.1. Simple Feedback Algorithm

The first, simplest and fastest method is to create an internal feedback loop on the saturation error (like the anti-windup scheme):

$$V_{err}^* = V_{ref}^* - \text{Clip}(V_{ref}^*, S) \qquad (4.1)$$

where the clip function restricts Vref* to the range ± S. V_{err}^* will be non-zero for those power supplies in voltage saturation. From (3.4) we see that

$$d\,V_{ref}^* = C_{kd}\,B_{kd}\,dE^* \qquad (4.2)$$

and so a correction

$$dE^* = K_H\,(C_{kd}\,B_{kd})^{-1}\,dV_{ref}^* \qquad (4.3)$$

should modify the controlled variable error in the correct sense. K_H can be usefully chosen to be $K_H = G \times H^{-1}$ where H is as previously defined by (3.2). The step gain G can be ~ 0.8 for numerical stability.

This simplistic approach is found to be inadequate for 2 reasons, namely a) the product $(C_{kd}B_{kd})$ is ill-conditioned, with a condition number ~ 1000 leading to excessive values of dE*, b) a considerable dynamic range of H leads to a large number of iterations for combinations of dV_{ref}^* which have low gain. As a result we have modified this method.

4.2. Adaptive and Conditioned Feedback Algorithm (H1)

In order to counteract the first problem cited above, we reconditioned the $(C_{kd}\,B_{kd})$ product before inversion. In fact, since the K_H matrix changes the conditioning again, we condition the product $(C_{kd}\,B_{kd}\,K_H^{-1})$ using SVD and eliminating singular values smaller than 1/200 of the maximum singular value.

To solve the second problem we continually adapted the K_H matrix inside the convergence loop for each time-step, such that

$$G\ K_{H(n+1)} = G\ (K_{H(n)})\ A \qquad (4.4)$$

with A typically 0.85 and $|H_{ij}| < 1$. This heuristic approach compresses K_H towards the unity matrix as the iterations proceed. The first few iterations modify E* on the basis of the low cost function weights in H, and progressively increase the modifications to the variables to be maintained close to their actual value. The chosen combinations of parameters in this algorithm gave excellent results with elimination of the saturation after a few (6 - 20) iterations - usually!

However, the remedy for the ill-conditioning of $C_{kd}\ B_{kd}\ H^{-1}$ has guaranteed a failure rate of this approach, since the combinations eliminated by reconditioning can and inevitably will appear. At this time no solution will be found and a fall-back solution is needed.

We also note that we have not formally minimised Q, but in fact we seem to get reasonably close to the E* corresponding to (3.4).

4.3 Formal Minimisation of a Modified Cost Function

We have checked that the algorithm described in 4.2 finds an E* close to the optimal one when convergence is obtained, i.e. when the saturation is removed. To check this we minimised a modified cost function:

$$Q' = (E^* - E)^T\ H\ (E^* - E) + J.\ Verr^{*T}\ Verr^*$$

To avoid saturation J must be large and since Verr* is a non-linear function (gradient discontinuity) of E* by (3.4), (4.1), the cost funtion Q' is not pleasant. Using a standard Simplex minimiser (MATLAB FMINS) gave extremely poor results. This approach was abandoned.

4.4 Robust Minimisation of a Simple Cost Function

The interest of the first results obtained using the iterative algorithm suggested that a new algorithm be found. The cost function defined in (3.2) corresponds to a linear transformation of the error space, such that

$$x^* = x * \text{diag}(\text{sqrt}(\text{Cost}))$$

Having made this transformation, the square of the Euclidian distance from the point E to E* has become the cost function. The problem posed earlier is now one of finding the closest point in the transformed space such that the condition of not exceeding the saturations is respected. The above transformation leaves the saturation conditions as planes, so the problem is reduced to finding a point on the hyper-plane surface of the saturation conditions, closest to the starting point.

This approach has been implemented. In 6-D, the algorithm is not pleasant, since the space is extremely ill-shaped due to the ill-conditioning of the transformations already discussed. However, we think that the new algorithm does in fact find the solution requested.

However, the results, discussed below, suggest that the control using this perfect solution is not as good as the control by the approximate solution. This suggests that the approximate solution had an implicit hidden benefit, possibly one of E* being close to E in the space of voltage as well as close in the space of errors. We have not had time to look into this yet.

4.5 Discussion

We can consider the algorithms discussed above as perfect controllers with no saturation, functioning normally, with a reference input equal to E-E*. Thus, provided E-E* remain bounded, i.e. provided the algorithm stabilises the plant, the behaviour of the closed loop is exactly that of the unsaturated loop. The behaviour of this set of algorithms is therefore exactly determined by the behaviour of the error modification. Problems found with the controller H4, see below, are certainly explicable in these terms.

5. RESULTS

5.1. Modelling

The algorithms in Section 4, together with the plant model, the references and disturbances were implemented in SIMULINK (lst version provided by A. Portone). Three controllers were implemented, namely :

a) Continuous time as supplied (C)
b) Discrete-time of supplied controller (D)
c) Hierarchical Saturation Controllers (2 versions H1, H3).

Figure 2 illustrates the SIMULINK layout. In order to examine the relative merits of the different approaches, the control loop will finally be closed using all three controllers for :

a) changes to the different reference inputs
b) different disturbances

Up to date, we have only run the case of a drop in beta-poloidal. For each case studied we show:

a) the evolution of 6 gaps
b) the evolution of 6 coil voltages
c) the evolution of 6 coil currents
d) the total power requirement $Vref^{*T} I_{PF}$

The coil voltage saturation levels were taken as:

S = [10, 16, 14, 15, 17, 10] Volts per turn

which are similar to the levels currently in the TAC-8 design.

Different values of the Hierarchisation weights were tested, but the results shown in this report correspond to values of 1.0, that is to say with no preferential weighting between the different gaps.

5.2 Nominal Beta-drop Disturbance

A sustained beta-drop of -0.1 - -0.3 was applied at t = 0 over 0.5 msec.

5.3 Preliminary results

Figure 3 shows a case with $\Delta\beta$ = -0.1 and with the discrete-time controller. The gap motion is small and the voltages required by the controller are small. The power requirement, shown as a solid line with circles, is small and smooth. Using a continuous time controller or using the modified controller gave almost identical results.

Figure 4a) shows a case with $\Delta\beta$ = -0.2 and with the discrete-time controller. The gap motion has increased and the voltages required by the controller have also increased. We observe voltage saturation on the coil marked 2 (PF3) and 3 (PF4). The power requirement has increased and shows a surge when the voltage saturation occurs. Physically, the energy required to correct a change in beta-poloidal is rather modest. However, if the correction is wrong, then the total energy injected during the correction is not small. Subsequently, the controller has to recover from this error, and the power demand is again excessive since this correction also suffers from a saturation.

Figures 5a) and 6a) show successive cases with $\Delta\beta$ = -0.25 and -0.3 respectively. The behaviour already seen becomes more pronounced. However, the loop remains stable.

Figure 4b) shows the same case as 4a), but with the saturation correcting controller. We see little difference in the gap waveforms, but most noticeably the power requirement has been reduced. Figure 5b) shows a similar conclusion for the case of 5a).

Figure 6b) shows the case of the largest drop in beta-poloidal treated. The power requirement using the saturation correcting controller is much less than in the case of the discrete-time controller, but towards the end of the simulation, it is not clear that the vertical motion has not become faster. It is possible that this case presents a loss of vertical stability.

6. CURRENT SATURATION

Saturation of the coil voltages presents a more serious problem to the control loop than the saturation of the coil currents, in the sense that the voltage saturation determines whether control is maintained and the current saturation determines whether the references can be respected. However, in the presence of

current saturation, loss of coil voltage may also occur, depending on how hard the current saturation limit is. A certain degree of voltage control can be retained by artificially imposing a soft current saturation just before the hard supply saturation. The problem of current saturation must therefore also be addressed.

We propose a similar approach, based on the propagation of the voltage control outputs through the tokamak model, to predict the next-step currents. If we assume that the coil currents are explicit elements of the state model of the tokamak, then we can feed the discrete-time tokamak model with the proposed voltage inputs, assess the next step coil currents, find the difference with respect to the current saturations and invert the full mapping from error inputs to coil current errors, feeding this back to the error inputs. This procedure is exactly analagous to the voltage saturation compensation.

Since the coils are almost perfect integrators, the increase in coil current is given roughly by:

$$L^* \, \delta I = U \, \delta t \qquad (6.1)$$

From Equation 6.1 we can see that the current saturation maps to a voltage limit, via:

$$| I_n + (L^*)^{-1} U \, dt | < I_{sat} \qquad (6.2)$$

from which:

$$L^* \, (-Isat - I_n) / dt < U < L^* \, (Isat - I_n) / dt \qquad (6.3)$$

The state-space model will simply represent this relationship.

The approach to be taken is therefore as follows. We assume a tokamak model P, demand signals V and current saturation Isat, and we therefore require that the current respects :

$$|Iref^*| = |P(V^*)| < Isat \qquad (6.4)$$

so that the subsequent physical power supply current saturation has no effect. Again, a subsidiary condition is that the modified current vector Iref* be optimal

in some sense to be chosen. This means that as well as not saturating a particular coil current, we choose to modify the currents in the other coils to respect some additional criterion, such as zero modification of the radial field on axis, a prerequisite for not interfering with the vertical positional control.

We assume that the plant P(V) is a discrete-time generalised state-space plant defined by:

$$x_{n+1} = A_d\ x_n + B_d\ V_n \qquad (6.5)$$

$$Iref_n = C_d\ x_n + D_d\ V_n$$

where x is now the state variable of the tokamak.

Given 6.4 and 6.5 we see that the requirement of 6.3 is modified to become

$$|I_{ref}^*| = |C_d\ x^*_{n+1} + D_d\ V_n\ | = |C_d\ A_d\ x_n + (C_d\ B_d + D_d\ )\ V_n\ | < Isat \qquad (6.6)$$

for all the elements of V_n separately. This condition ensures that the next current output be unsaturated, given a current state vector x_n and the values of C_d, B_d, A_d and D_d. If x_n gave rise to an unsaturated current demand signal and if A_d is stable, then there will always be a solution to Equation 3.4. However, in this case, A_d is not stable, due to the vertical positional instability. Physically, this corresponds to the coil currents increasing with no applied voltage, due to the undamped vertical motion. The existance of a solution is not therefore guaranteed. However, if we were to separate the control into a stabilising part and a shaping part, then the argument is simpler. The stabilising part has to provide crude stability in the presence of voltage saturation, as discussed by CREATE, and the A_d of the modified plant is now stable and a solution is guaranteed. This appears to be a motivation for explicit separation of the controller. This point is an important one and will continue to attract our attention.

The problem is now clearly posed. The form of the problem in Equation 6.5 is identical to that of Equation 3.4. Current saturation avoidance is therefore implemented by doubling the number of planes defining the admissible vector E*. This will be implemented during Phase II of this Design Task. This approach is a form of Predictive Control with constraints.

7. CONCLUSION and FUTURE WORK

These results show that the saturation correcting controller has a useful feature of reducing the power surge which is a feature of the uncorrected linear controller when the coil voltages saturate. In the last case studied, there is an indication that the compensation has caused loss of stability, not yet understood. The advantages of this approach seem clear and motivate continued work on this approach. We have shown that the handling of current saturation is clear in this implentation without a significant increase in complexity.

The future direction of this work during the Phase II of the D324-1 Deisgn Task will include :

- Setting up and testing a TAC-8 model and hopefully a better conditioned controller with TAC-8 defined gaps
- Inclusion of the proposed current saturation handling
- Verification of and improvements to the algorithm
- Verification of the conclusion that this approach is generally valid
- Testing of the algorithm applying reference input steps
- Supplying a robust general code module for use elsewhere

Imperial College have expressed interest in contributing to this study for Phase II, to be confirmed.

REFERENCES

[1] A. Portone, PhD Thesis

[2] CREATE, D255 Intermediate Report, March 1996

FIGURE CAPTIONS

Fig. 1 Simplified schematic of the ITER Poloidal Field feedback loop.

Fig. 2 SIMULINK schematic implemented for this study.

Fig. 3 Disturbance of $\Delta\beta$ = -0.1 with the discrete-time controller.

Fig. 4a Disturbance of $\Delta\beta$ = -0.2 with the discrete-time controller.

Fig. 4b Disturbance of $\Delta\beta$ = -0.2 with the saturation controller.

Fig. 5a Disturbance of $\Delta\beta$ = -0.25 with the discrete-time controller.

Fig. 5b Disturbance of $\Delta\beta$ = -0.25 with the saturation controller.

Fig. 6a Disturbance of $\Delta\beta$ = -0.3 with the discrete-time controller.

Fig. 6b Disturbance of $\Delta\beta$ = -0.3 with the saturation controller.

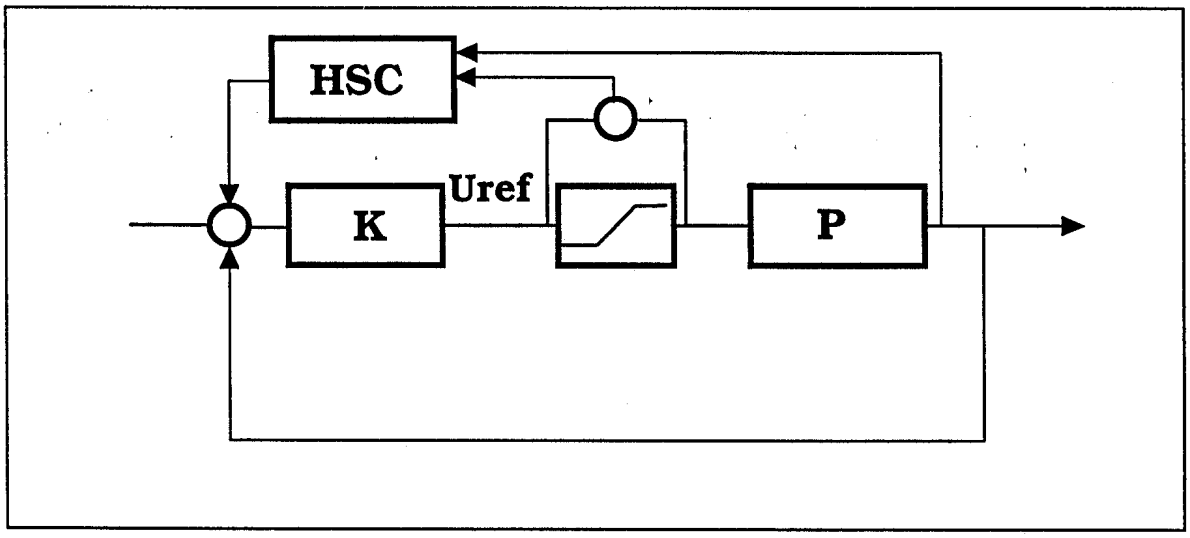

Fig. 1 Simplified schematic of the ITER Poloidal Field feedback loop.

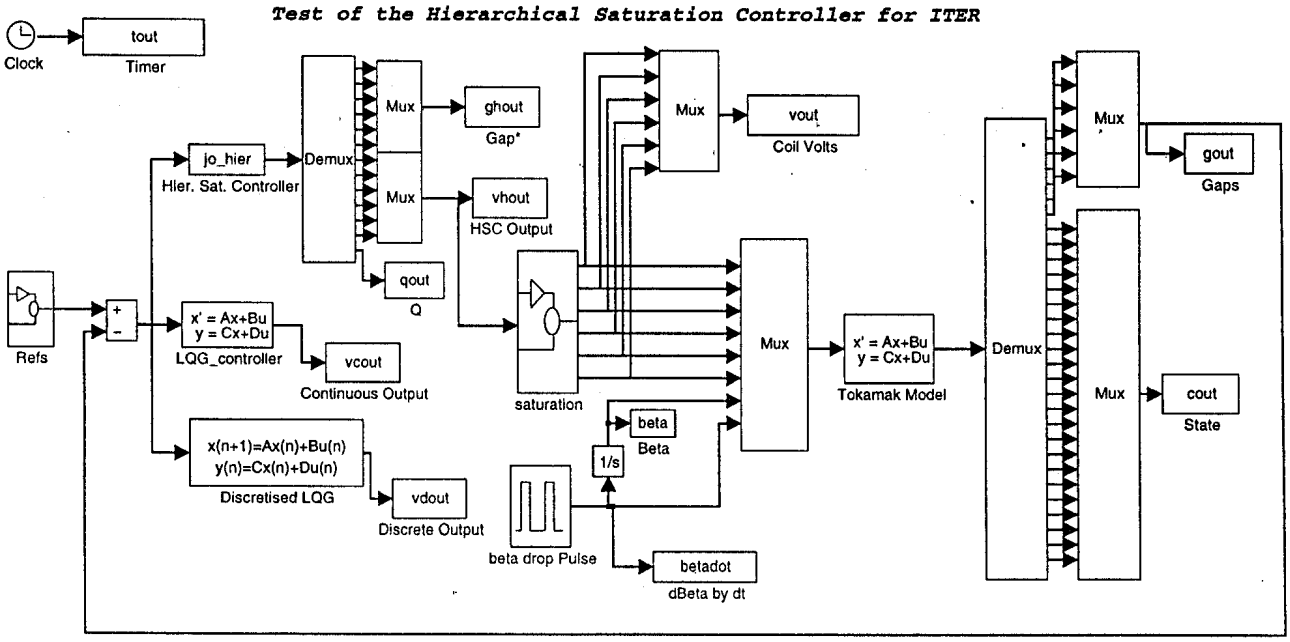

Fig. 2 SIMULINK schematic implemented for this study.

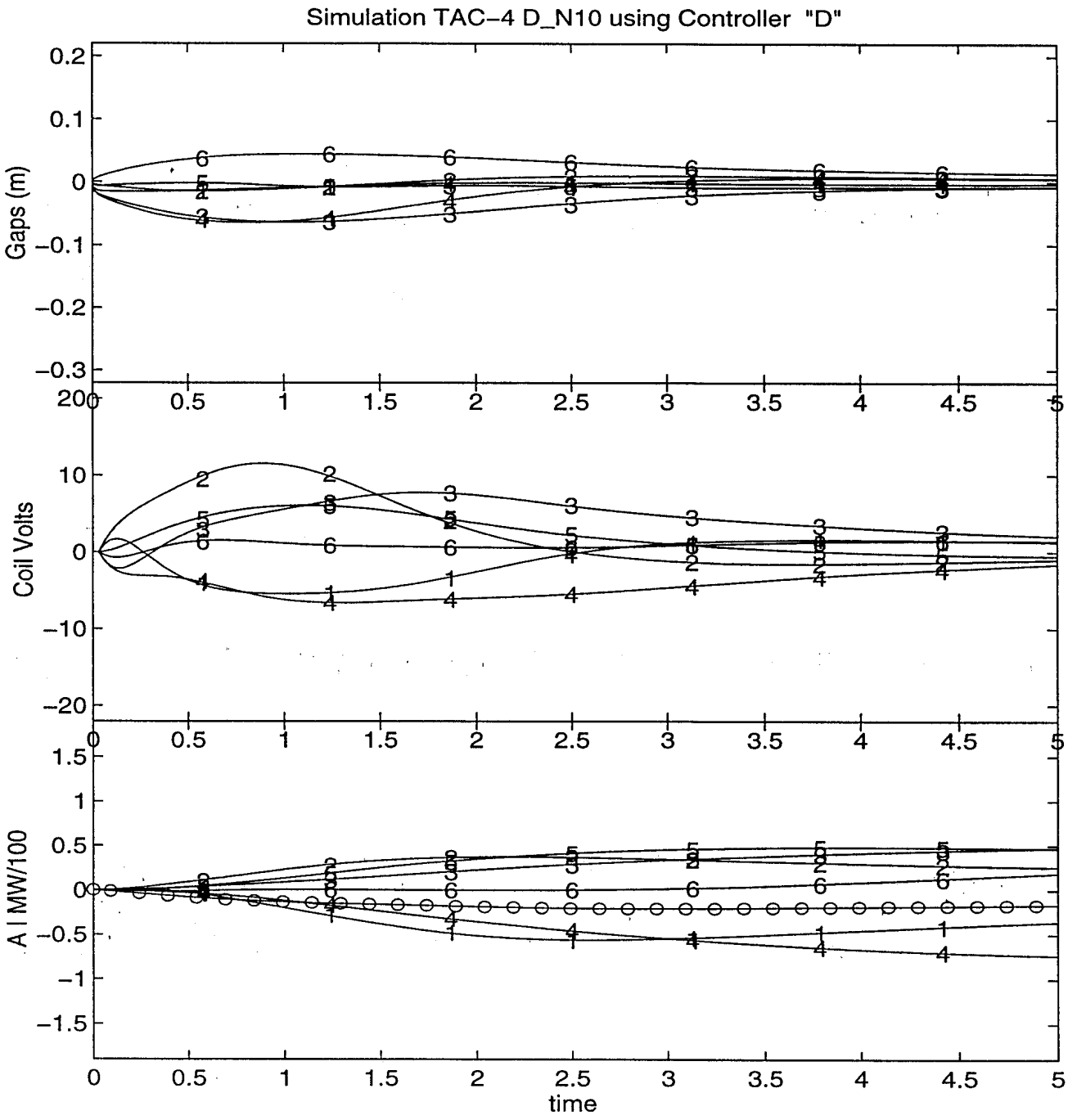

Maximum Gap = 0.02 0.01 0.06 0.06 0.01 0.04
Average Vsq = 7.9 27.9 23.7 20.7 10.1 1.1
Maximum Power for Each Coil = 60.8 87.7 103.1 46.2 37.5 9.2
Maximum Total Power = 20.62 MW
Currents in PF2,3 = –11 –7.8 MA
Currents in PF4,5 = –13.5 –6.8 MA
Currents in PF6,7 = 6 6 MA
Plasma Current = 24 MA

D_N10 : 15–Jun–96

Fig. 3 Disturbance of $\Delta\beta$ = -0.1 with the discrete-time controller.

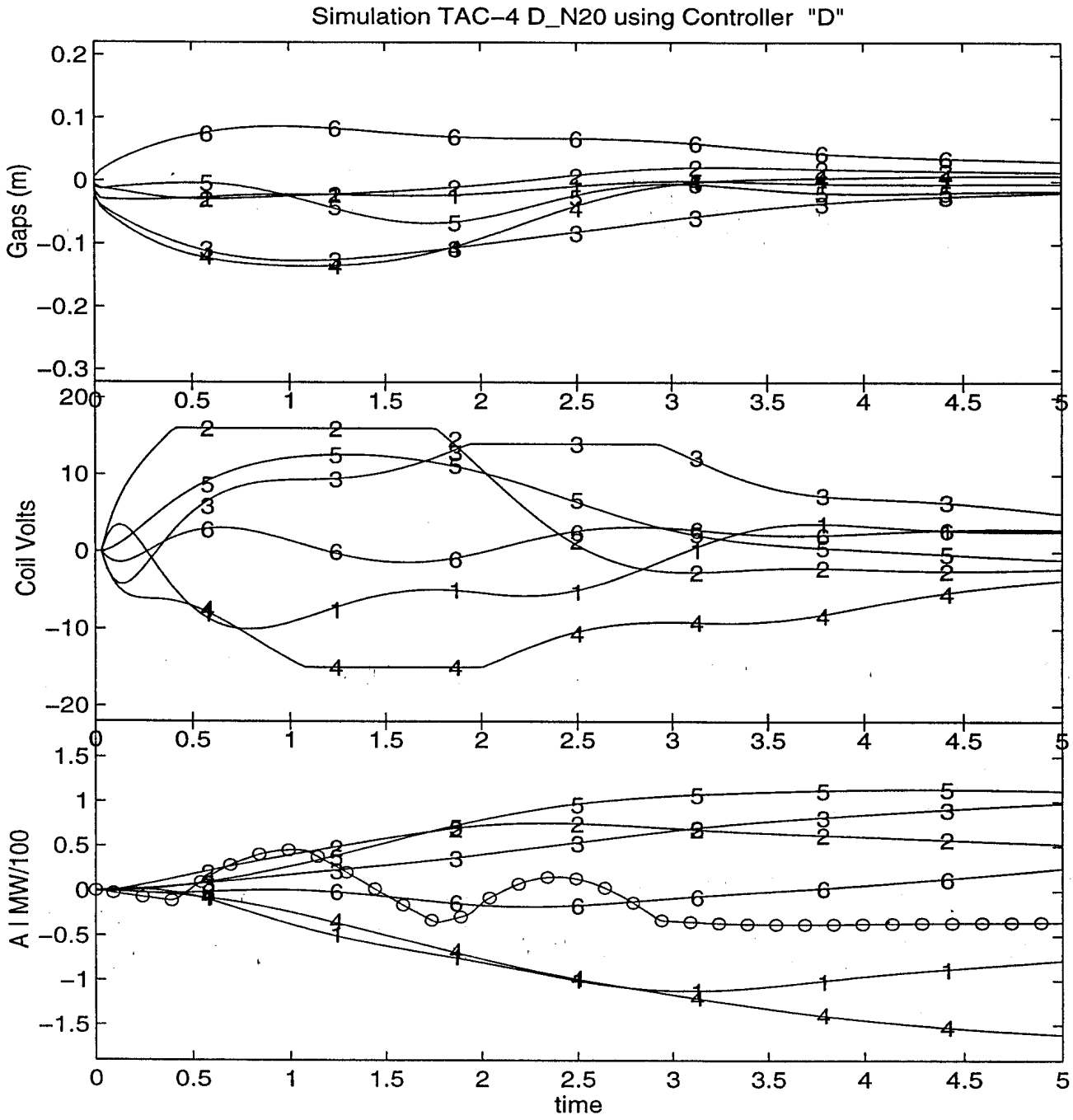

Maximum Gap = 0.03 0.03 0.13 0.14 0.07 0.09
Average Vsq = 24.9 91.4 93.7 102.4 51.0 4.9
Maximum Power for Each Coil = 112.5 122.5 183.5 113.2 81.2 18.8
Maximum Total Power = 45.52 MW
Currents in PF2,3 = –11 –7.8 MA
Currents in PF4,5 = –13.5 –6.8 MA
Currents in PF6,7 = 6 6 MA
Plasma Current = 24 MA

D_N20 : 15–Jun–96

Fig. 4a Disturbance of $\Delta\beta$ = -0.2 with the discrete-time controller.

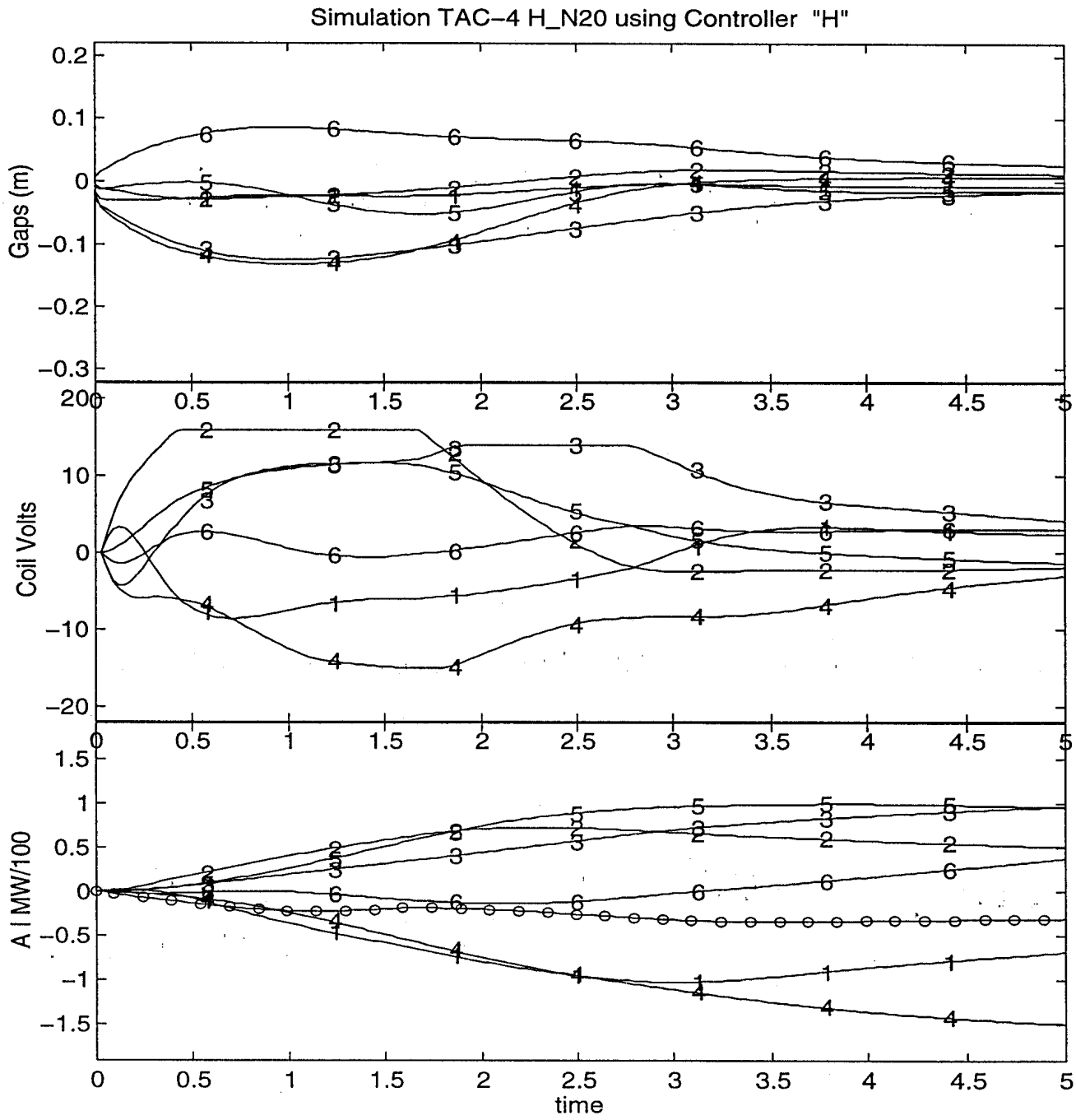

Maximum Gap = 0.03 0.03 0.12 0.13 0.05 0.09
Average Vsq = 20.8 87.9 95.0 86.9 42.3 5.6
Maximum Power for Each Coil = 96.1 122.1 183.1 111.7 75.9 20.8
Maximum Total Power = 34.31 MW
Currents in PF2,3 = –11 –7.8 MA
Currents in PF4,5 = –13.5 –6.8 MA
Currents in PF6,7 = 6 6 MA
Plasma Current = 24 MA

H_N20 : 15–Jun–96

Fig. 4b *Disturbance of $\Delta\beta$ = -0.2 with the saturation controller.*

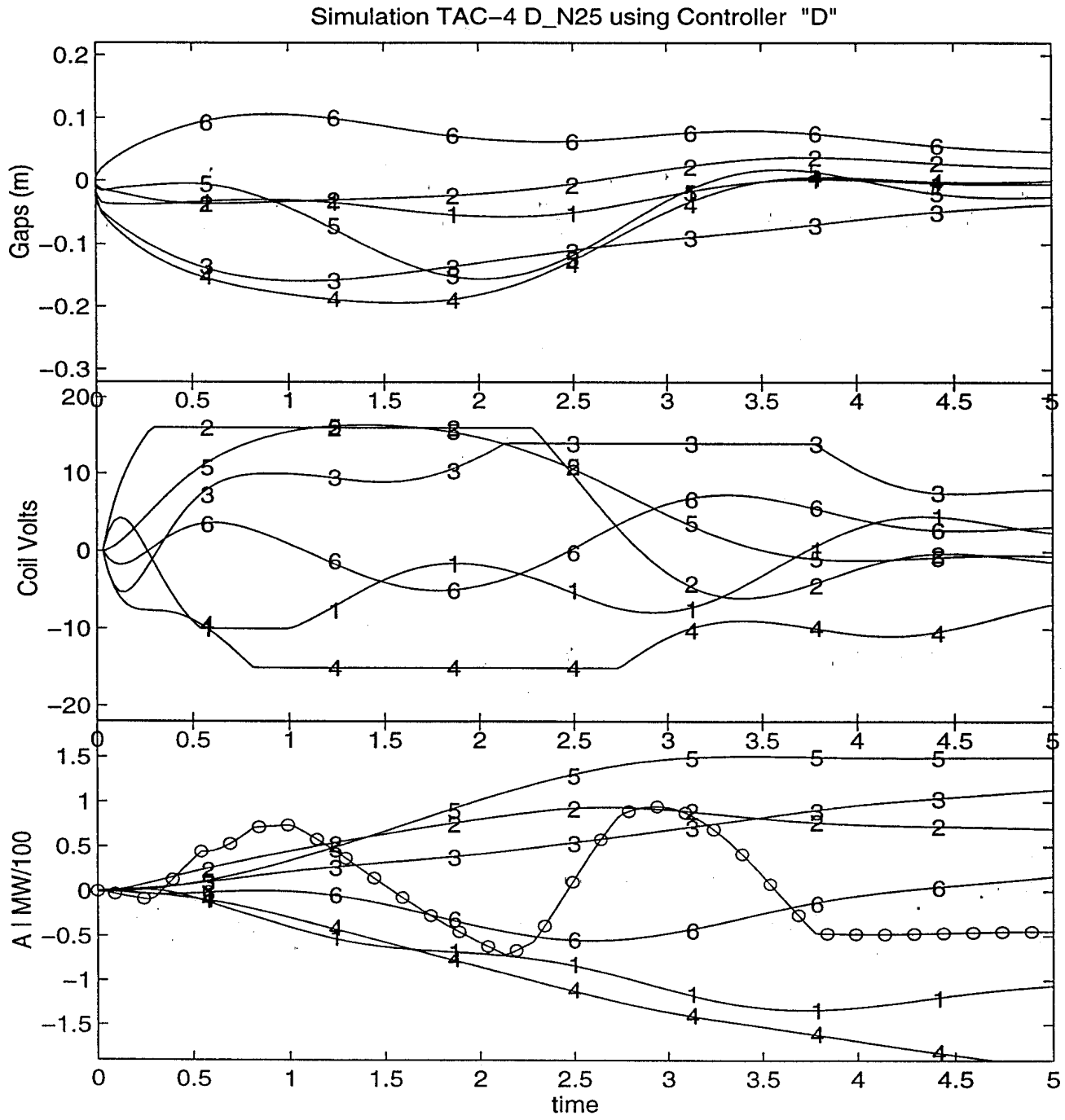

Maximum Gap = 0.06 0.04 0.16 0.19 0.16 0.11
Average Vsq = 30.1 120.2 116.1 143.4 93.8 16.2
Maximum Power for Each Coil = 113.9 123.0 182.6 120.6 109.2 41.6
Maximum Total Power = 95 MW
Currents in PF2,3 = –11 –7.8 MA
Currents in PF4,5 = –13.5 –6.8 MA
Currents in PF6,7 = 6 6 MA
Plasma Current = 24 MA

D_N25 : 15–Jun–96

Fig. 5a *Disturbance of $\Delta\beta$ = -0.25 with the discrete-time controller.*

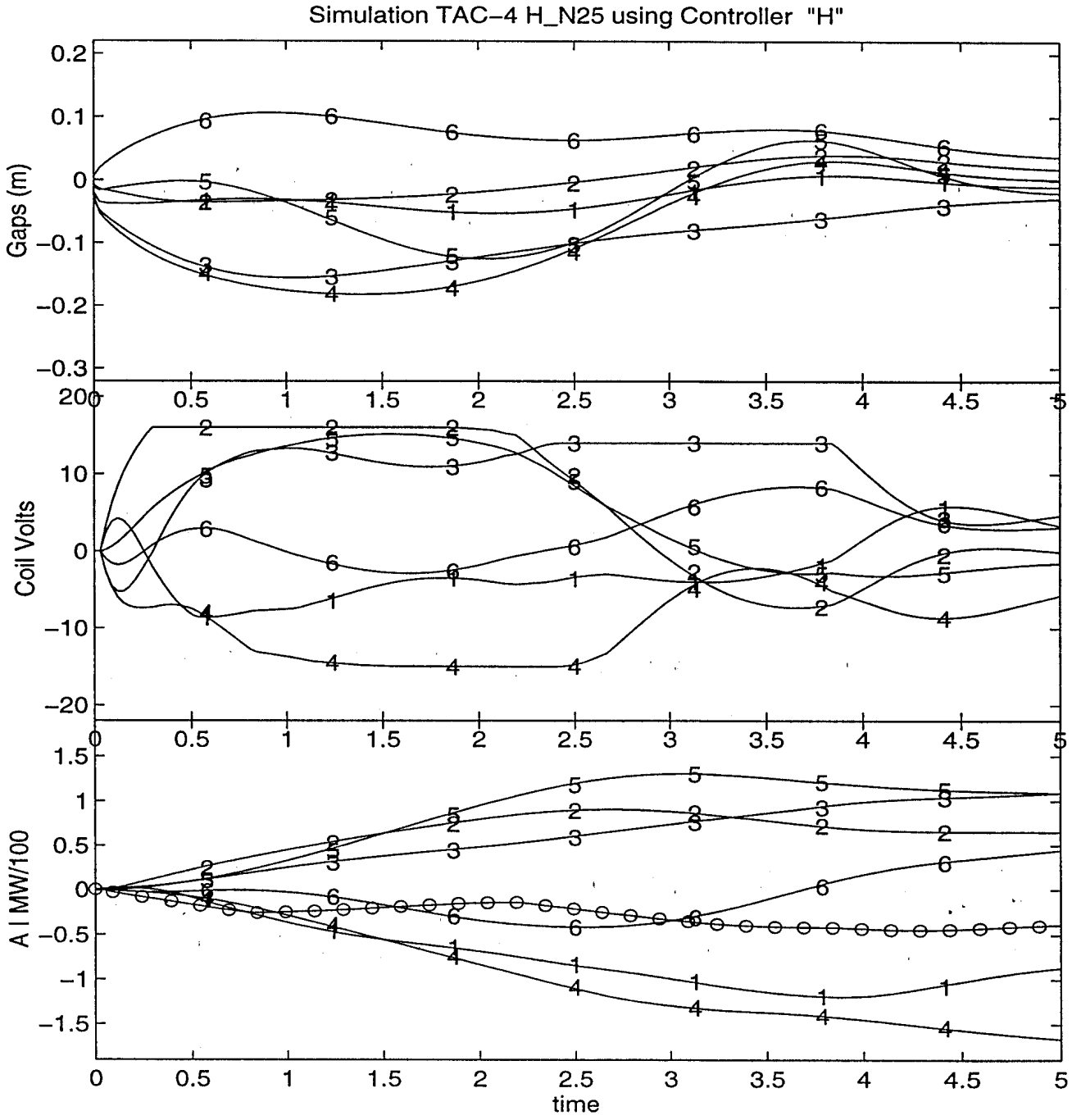

Maximum Gap = 0.05 0.04 0.16 0.18 0.13 0.11
Average Vsq = 22.1 119.4 121.8 109.3 77.6 16.8
Maximum Power for Each Coil = 96.0 122.9 180.8 117.9 101.4 50.3
Maximum Total Power = 44.59 MW
Currents in PF2,3 = –11 –7.8 MA
Currents in PF4,5 = –13.5 –6.8 MA
Currents in PF6,7 = 6 6 MA
Plasma Current = 24 MA

H_N25 : 15–Jun–96

Fig. 5b *Disturbance of $\Delta\beta$ = -0.25 with the saturation controller.*

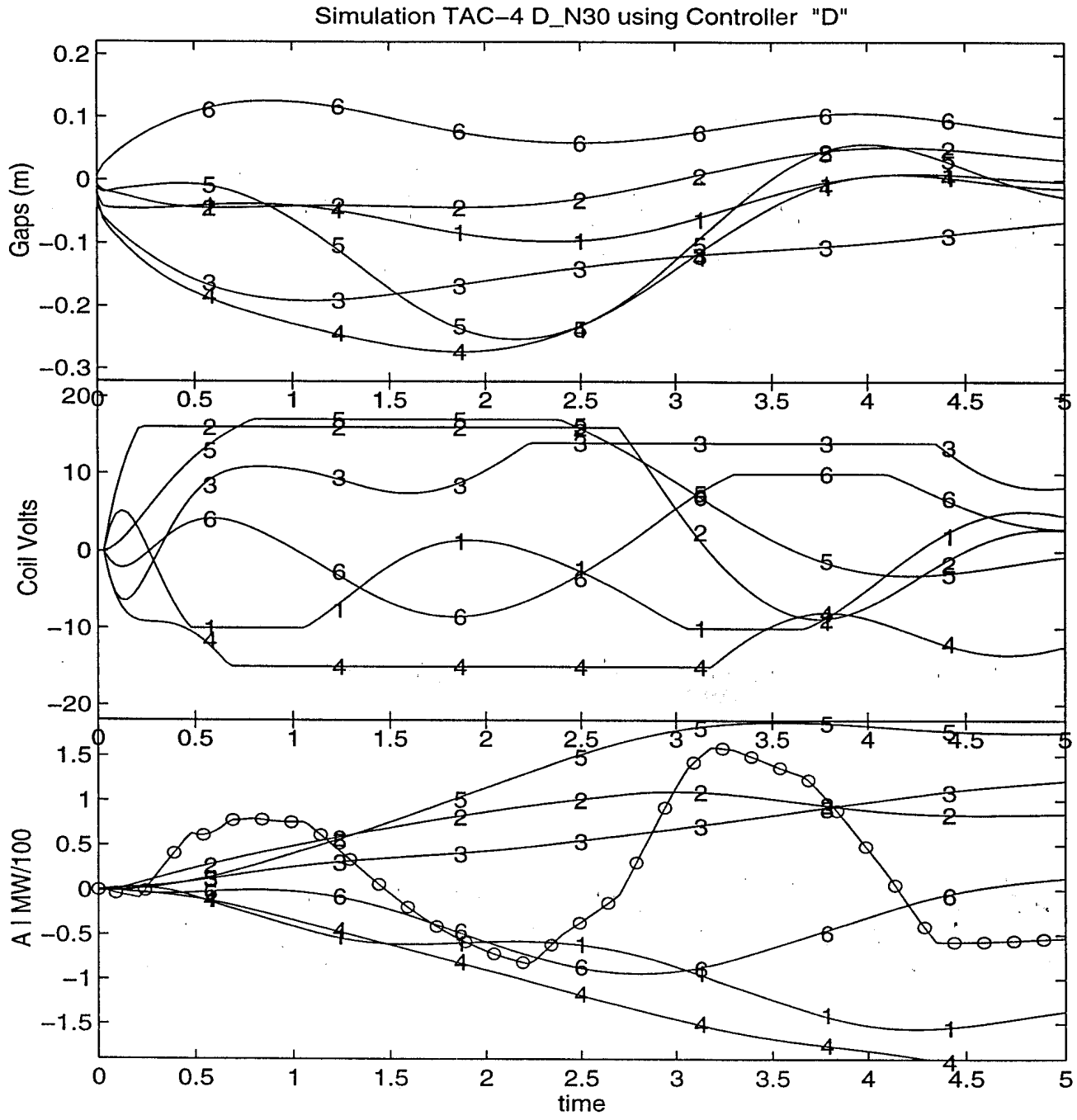

Maximum Gap = 0.10 0.05 0.19 0.27 0.25 0.13
Average Vsq = 41.1 146.6 128.2 168.4 133.6 39.4
Maximum Power for Each Coil = 123.4 123.3 182.2 125.2 126.2 57.5
Maximum Total Power = 159.4 MW
Currents in PF2,3 = –11 –7.8 MA
Currents in PF4,5 = –13.5 –6.8 MA
Currents in PF6,7 = 6 6 MA
Plasma Current = 24 MA

D_N30 : 15–Jun–96

Fig. 6a *Disturbance of $\Delta\beta$ = -0.3 with the discrete-time controller.*

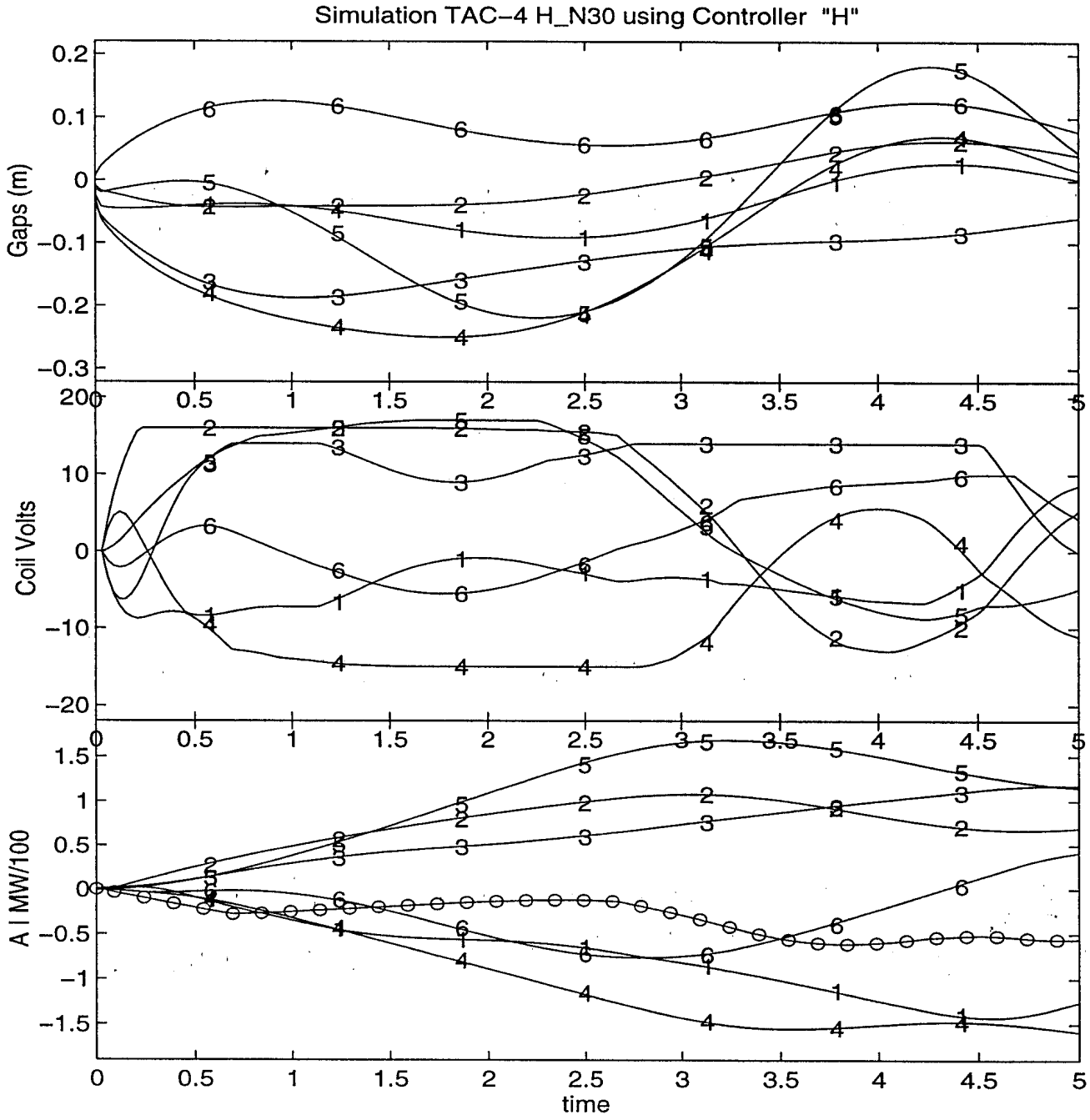

Maximum Gap = 0.09 0.06 0.19 0.25 0.22 0.13
Average Vsq = 24.7 162.0 139.5 123.2 129.2 31.7
Maximum Power for Each Coil = 105.4 123.1 186.2 121.7 123.6 62.4
Maximum Total Power = 61.2 MW
Currents in PF2,3 = –11 –7.8 MA
Currents in PF4,5 = –13.5 –6.8 MA
Currents in PF6,7 = 6 6 MA
Plasma Current = 24 MA

H_N30 : 15–Jun–96

Fig. 6b Disturbance of $\Delta\beta$ = -0.3 with the saturation controller.

EIDGENÖSSISCHE TECHNISCHE HOCHSCHULE LAUSANNE
POLITECNICO FEDERALE DI LOSANNA
SWISS FEDERAL INSTITUTE OF TECHNOLOGY LAUSANNE

CENTRE DE RECHERCHES EN PHYSIQUE DES PLASMAS
Association EURATOM - Confédération Suisse

ÉCOLE POLYTECHNIQUE
FÉDÉRALE DE LAUSANNE

ITER task D255

Final Report

Work Envelope F

Nonlinear Simulations without Feedback

D. J. WARD, J. B. LISTER
(CRPP-EPFL)

using linear model data provided by
CREATE Consortium, Naples, Italy

24 juillet, 1996

1. INTRODUCTION

This report contains the results of the open loop (without feedback) simulations of disturbances for ITER performed with the Tokamak Simulation Code (TSC). Two types of perturbations are considered. First, a one second, open loop, square pulse is applied to each of the 8 PF coils separately. The evolution is followed for an additional one second. Secondly, perturbations in li and βp are examined in open loop. The results are compared in detail to the linear model of the CREATE group in order to access the validity of their model compared to the full simulation in TSC.

2. THE CALCULATION

The Tokamak Simulation Code (TSC) [1] is a nonlinear plasma simulation code that models an axisymmetric tokamak plasma and the associated control systems. The code simulations the time evolution of a free boundary plasma by solving the dynamic MHD equations on a rectangular computational grid. These MHD equations are coupled through the boundary conditions to circuit equations, which describe the poloidal field coil circuits. The code includes calculations to model transport, plasma heating, and control systems.

2.1 Equilibrium

An ITER equilibrium was created with the TSC code for the TAC-8 End-of-Burn (EOB) configuration. The equilibrium pressure profile is described by

$$P(\Psi,t) = P_0(t)((\Psi_{lim} - \Psi) / (\Psi_{lim} - \Psi_{min}))^{1.5} \qquad (1)$$

Here, Ψ_{lim} is the value of the poloidal flux at the plasma edge (i.e., separatrix or limiter), and Ψ_{min} is the minimum value of Ψ (at the magnetic axis). The density profile takes the form

$$\rho(\Psi,t) = \rho_0(t)[1 - ((\Psi - \Psi_{min})/(\Psi_{lim} - \Psi_{min}))^4]^{1.5} \qquad (2)$$

The current density profile is determined through the MHD transport calculations, based upon the form of the toroidal field function $g(\Psi)$ and its evolution. The initial toroidal field is given by $B_T = g(\Psi)\nabla\phi$, where

$$g^2 = g0^2 - 2\{g1((\Psi_{lim} - \Psi)/(\Psi_{lim} - \Psi_{min}))^{1.25} \quad (3)$$
$$+ 4g2((\Psi_{lim} - \Psi)/(\Psi_{lim} - \Psi_{min}))^{1.25}\,[1 - ((\Psi_{lim} - \Psi)/(\Psi_{lim} - \Psi_{min}))]\}$$

Here, $g1$ and $g2$ are determined so that $q(0)$=0.80 and Ip = 21.0MA. This simulation is run out to t=500sec. to allow the current profile to relax. Details of the TSC calculation can be found in Refs. [1] and [2].

The equilibrium parameters are listed in Table 1.

Equilbrium Parameters	TSC
Major radius R	8.17m
Minor radius a	2.76m
Plasma current Ip	20.98 MA
Magnetic axis (Rmag,Zmag)	8.415, 1.469
Beta poloidal βp	0.893
Internal inductance li	0.864
X-point (X,Z)	7.306,-4.126
PF1 coil current	-153.7 MA
PF2 coil current	-8.23 MA
PF3 coil current	-7.098 MA
PF4 coil current	-13.198 MA
PF5 coil current	-6.041 MA
PF6 coil current	8.010 MA
PF7 coil current	2.865 MA
PF8 coil current	0.0 MA
gap #1 reference point; value	5.253,-4.962; 0.381
gap #2 reference point; value	8.599,-5.401; 0.267
gap #3 reference point; value	11.22, 1.6295; 0.301
gap #4 reference point; value	9.867, 4.608; 0.180
gap #5 reference point; value	6.637, 6.045; 0.450
gap #6 reference point; value	5.156, 0.911; 0.249

Table 1: Equilibrium Parameters of the TAC-8 EOB equilibrium as calculated by TSC.

2.2 Conducting Structure

The structure has been defined according to the latest TAC-8 specifications [3]. The toroidal resistances of the various poloidal structure elements are given by:

- vacuum vessel: $R_{VV} = 10.4\mu\Omega$
- blanket structure: $R_{BP} = 7.4\mu\Omega$
- first wall: $R_{FW} = 100\mu\Omega$
- total structure resistance: $R_{TOT} = 4.3\mu\Omega$
- PF coils: $R_{PF} = 0$
- divertor fins: $R = infinite$

The conducting structure is modelled using the TSC wire model. The first wall is modelled as a set of 72 wires, and the back plate structure is represented by a set of 82 wires. The vacuum vessel is represented by an inner set of 116 wires and an outer set of 128 wires (each with $20.8\mu\Omega$ resistance).

2.3 The Disturbances

The disturbances studied in this report fall into two categories: square-pulse injection onto each of the PF coils in turn, and disturbances in the pressure and current profiles corresponding to drops in in li and βp.

The first set of perturbations are one second, square pulse injections into each of the 8 PF coils. The magnitude of the voltage of the square pulse was chosen to result in a similar perturbation to the plasma for each case. The voltages applied to each of the PF coils are (V1,. . .,V8) = (1V, 1V, 1.5V, 2.5V, 2.5V, 3V, 2.5V, 6V). The simulation is continued in open loop for an additional one second to follow the evolution. The simulations of these perturbations are compared in detail to the CREATE linear model.

We also examine the open loop response of a drop in βp of 0.2, a drop of li of 0.1, and a combination drop of βp and li. These perturbations are evolved in open loop, and also compared in detail to the CREATE model.

The drop in βp is modelled [2] in TSC by enhancing the anomalous thermal diffusion coefficient over a short time (4 ms) and then returning it to the nominal values.

The drop in li is modelled using a hyperresistivity (or current viscosity) term in the resistive diffusion equation. It has been shown [4] that such a term models the effects of 3-D MHD fluctuations on the mean-field of a plasma. It is included in Ohm's law, and satisfies the following assumptions: (1) The exact magnetic field energy and helicity are closely approximated by the energy and helicity of the mean field; (2) the fluctuating field can cause differential transport of both the field energy and the field helicity; and (3) the fluctuating field can lead to enhanced dissipation of field energy but not field helicity. These assumptions are expected to be satisfied by the real fluctuating field that leads to such an li-drop disturbance in an experiment.

Modelling of the βp and li drops in this way, through the enhancement of anomalous diffusion terms in a dynamic MHD calculation as described above, allow one to keep the underlying physics in the calculation, thus making the MHD transport time-scale simulations as realistic as possible.

3. SIMULATION RESULTS

3.1 Square pulse injection

We simulate the evolution of the one second square pulse injection, and let the system evolve for another second after the pulse. The results are shown in Figures 1-8. The TSC results are the solid curves and the dot-dash (.-) curves are the results from the linear CREATE model. The results show that the evolution of the PF coil currents agree quite well between the linear model and TSC. However, the response of the plasma to the square pulse differs with the TSC results showing a 30%-40% smaller displacement in the position and gaps separations with time. The shape of the gap contours evolve in time in a very similar fashion for the linear and TSC results (given the difference in magnitude just mentioned), with the exception of the response from PF1.

Figure 9 shows the separatrix contours immediately before the perturbation (dashed) and 1 second after the square-pulse injection on PF2 for the TSC results (solid) and for the CREATE linear model (dash-dot).

3.2 βp and li disturbances

Figure 10 shows the results of the li drop (Δli =-.1) disturbance. The evolution of the gaps, PF currents, and gap contours are shown. Also shown is the time evolution of Xmag(*10), Zmag, li, and βp. The gaps show a somewhat different instaneous change, but then evolve in very much the same way later (the curves are parallel). At 0.5s the evolution of the gaps contour is in very good agreement between the TSC and CREATE linear models.

Figure 11 shows the results of the βp drop disturbance ($\Delta\ \beta p$=-.2). Here the evolution of the gaps contour is not in as good agreement as the li drop. The TSC evolution shows a larger displacement upwards near the top of the plasma (near gap#5). Figure 12 shows the evolution after this disturbance out to 2 seconds.

Figure 13 shows the results for the combination li drop and βp drop disturbance. Here the agreement is not bad after 0.40 seconds despite the fact that the magnitude of the li and βp drops are not identical between the two models.

Figure 14 shows the separatrix contours 0.40 seconds after the βp drop disturbance. The contour just prior to the disturbance is also shown (dashed). The TSC contour is solid, while the dash-dot contour is from the linear model. Figure 15 shows the same contours 0.40 seconds after the combination li drop and βp drop.

4. CONCLUSIONS

The comparisons between the full nonlinear TSC simulation and the CREATE linear model show reasonable agreement. The displacements resulting from a square-wave injection are 30%-40% larger in the linear model than from the TSC code.

The open loop evolution following the li drop and βp drop drops show reasonable agreement between these two models, despite significant differences in the way the perturbations are induced and the underlying physics that is treated.

REFERENCES

[1] S. C. Jardin, N. Pomphrey, and J. DeLucia, ``Dynamic Modelling of Transport and Position Control of Tokamaks,'' J. Comput. Phys., **66** (1986) 481-507.

[2] S. C. Jardin, et al., ``Modelling of Post-Disruptive Plasma Loss in the Princeton Beta Experiment,'' Nucl. Fusion, **27** (1987) 569-578.

[3] Y. Gribov, Memo to the Home Team Members, March 8, 1996.

[4] A. H. Boozer, J. Plasma Phys., **35** (1986) 133.

FIGURE CAPTIONS

Fig. 1 Comparison of time evolution of six nominal gaps and eight PF coil currents, and the gaps contour evolution of PF currents at 0.5s, 1.0s, and 1.9s following a one second square-pulse injection into PF 1.

Fig. 2 Comparison of time evolution of six nominal gaps and eight PF coil currents, and the gaps contour evolution of PF currents at 0.5s, 1.0s, and 1.9s following a one second square-pulse injection into PF 2. (linear = -.)

Fig. 3 Comparison of time evolution of six nominal gaps and eight PF coil currents, and the gaps contour evolution of PF currents at 0.5s, 1.0s, and 1.9s following a one second square-pulse injection into PF 3. (linear = -.)

Fig. 4 Comparison of time evolution of six nominal gaps and eight PF coil currents, and the gaps contour evolution of PF currents at 0.5s, 1.0s, and 1.9s following a one second square-pulse injection into PF 4. (linear = -.)

Fig. 5 Comparison of time evolution of six nominal gaps and eight PF coil currents, and the gaps contour evolution of PF currents at 0.5s, 1.0s, and 1.9s following a one second square-pulse injection into PF 5. (linear = -.)

Fig. 6 Comparison of time evolution of six nominal gaps and eight PF coil currents, and the gaps contour evolution of PF currents at 0.5s, 1.0s, and 1.9s following a one second square-pulse injection into PF 6. (linear = -.)

Fig. 7 Comparison of time evolution of six nominal gaps and eight PF coil currents, and the gaps contour evolution of PF currents at 0.5s, 1.0s, and 1.9s following a one second square-pulse injection into PF 7. (linear = -.)

Fig. 8 Comparison of time evolution of six nominal gaps and eight PF coil currents, and the gaps contour evolution of PF currents at 0.5s, 1.0s, and 1.9s following a one second square-pulse injection into PF 8. (linear = -.)

Fig. 9 Separatrix contours 1 second after the square pulse injection on PF2. Dashed contour is before perturbation, the solid contour is the TSC result, and the dashed-dot is the linear model.

Fig. 10 Comparison of time evolution of six nominal gaps and eight PF coil currents, and the gaps contour evolution of PF currents at 0.1s and 0.5s following an li drop of 0.1. (linear = -.)

Fig. 11 Comparison of time evolution of six nominal gaps and eight PF coil currents, and the gaps contour evolution of PF currents at 0.1s and 0.5s following an βp drop of 0.2. (linear = -.)

Fig. 12 Comparison of time evolution of six nominal gaps and eight PF coil currents, and the gaps contour evolution of PF currents at 1.0s and 2.0s following an βp drop of 0.2. (linear = -.)

Fig. 13 Comparison of time evolution of six nominal gaps and eight PF coil currents, and the gaps contour evolution of PF currents at 0.1s and 0.5s following a combination βp drop of 0.2 and li drop of 0.1. (linear = -.)

Fig. 14 Separatrix contours 0.4 s after the li drop disturbance. Dashed contour is before perturbation, the solid contour is the TSC result, and the dashed-dot is the linear model.

Fig. 15 Separatrix contours 0.4 s after the βp drop disturbance. Dashed contour is before perturbation, the solid contour is the TSC result, and the dashed-dot is the linear model.

Fig. 1 Comparison of time evolution of six nominal gaps and eight PF coil currents, and the gaps contour evolution of PF currents at 0.5s, 1.0s, and 1.9s following a one second square-pulse injection into PF 1. (linear = -.)

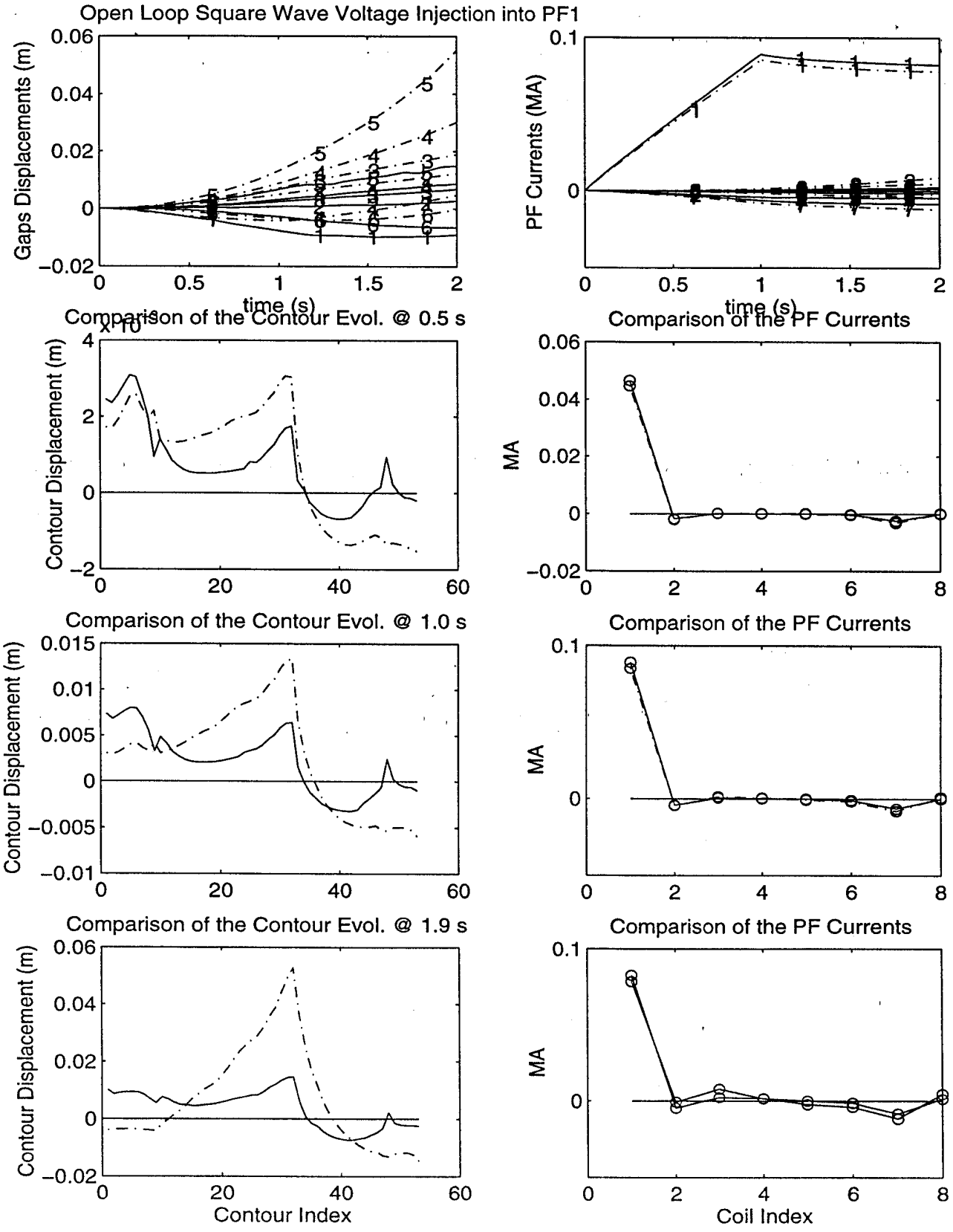

Fig. 2 Comparison of time evolution of six nominal gaps and eight PF coil currents, and the gaps contour evolution of PF currents at 0.5s, 1.0s, and 1.9s following a one second square-pulse injection into PF 2. (linear = -.)

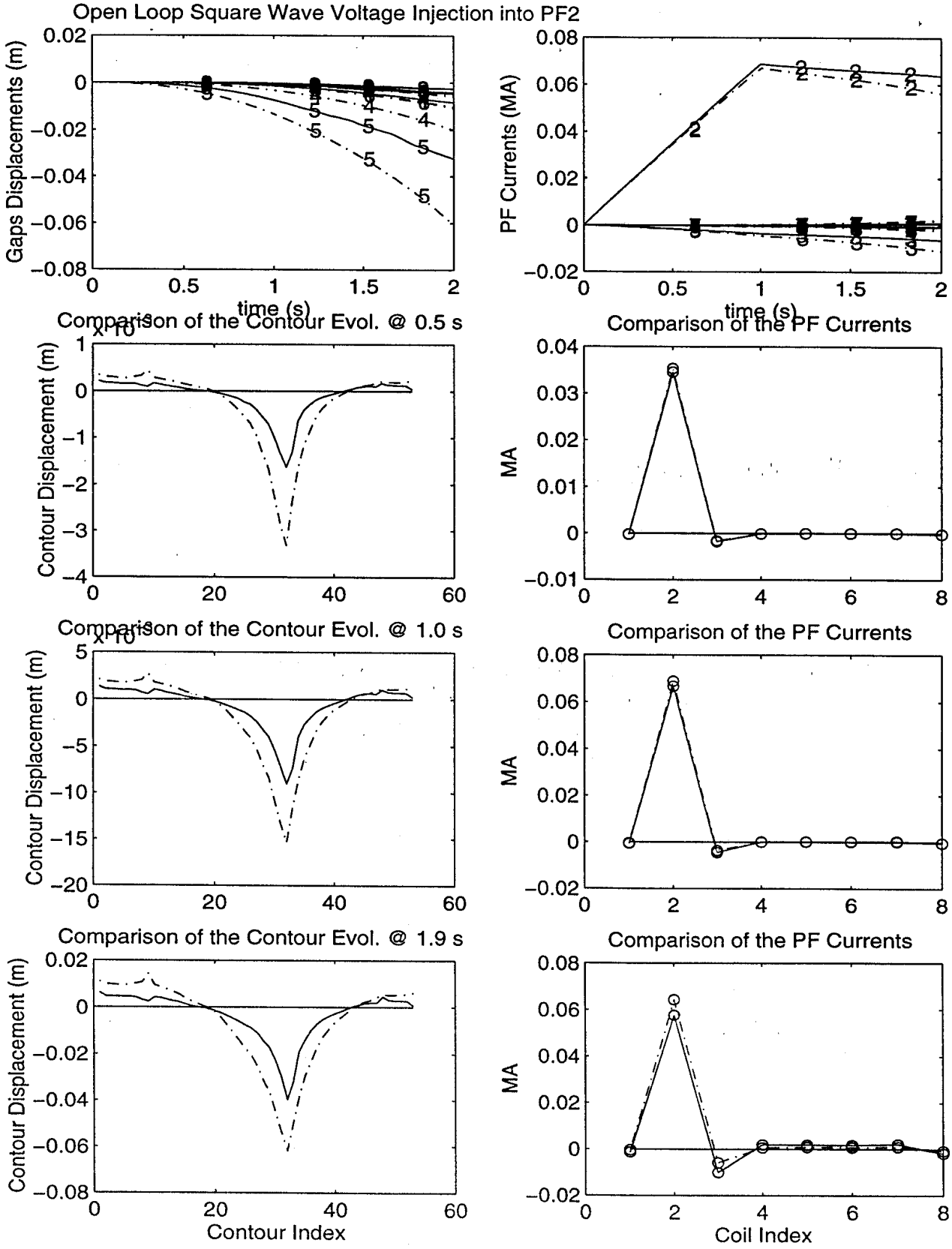

Fig. 3 Comparison of time evolution of six nominal gaps and eight PF coil currents, and the gaps contour evolution of PF currents at 0.5s, 1.0s, and 1.9s following a one second square-pulse injection into PF 3. (linear = -.)

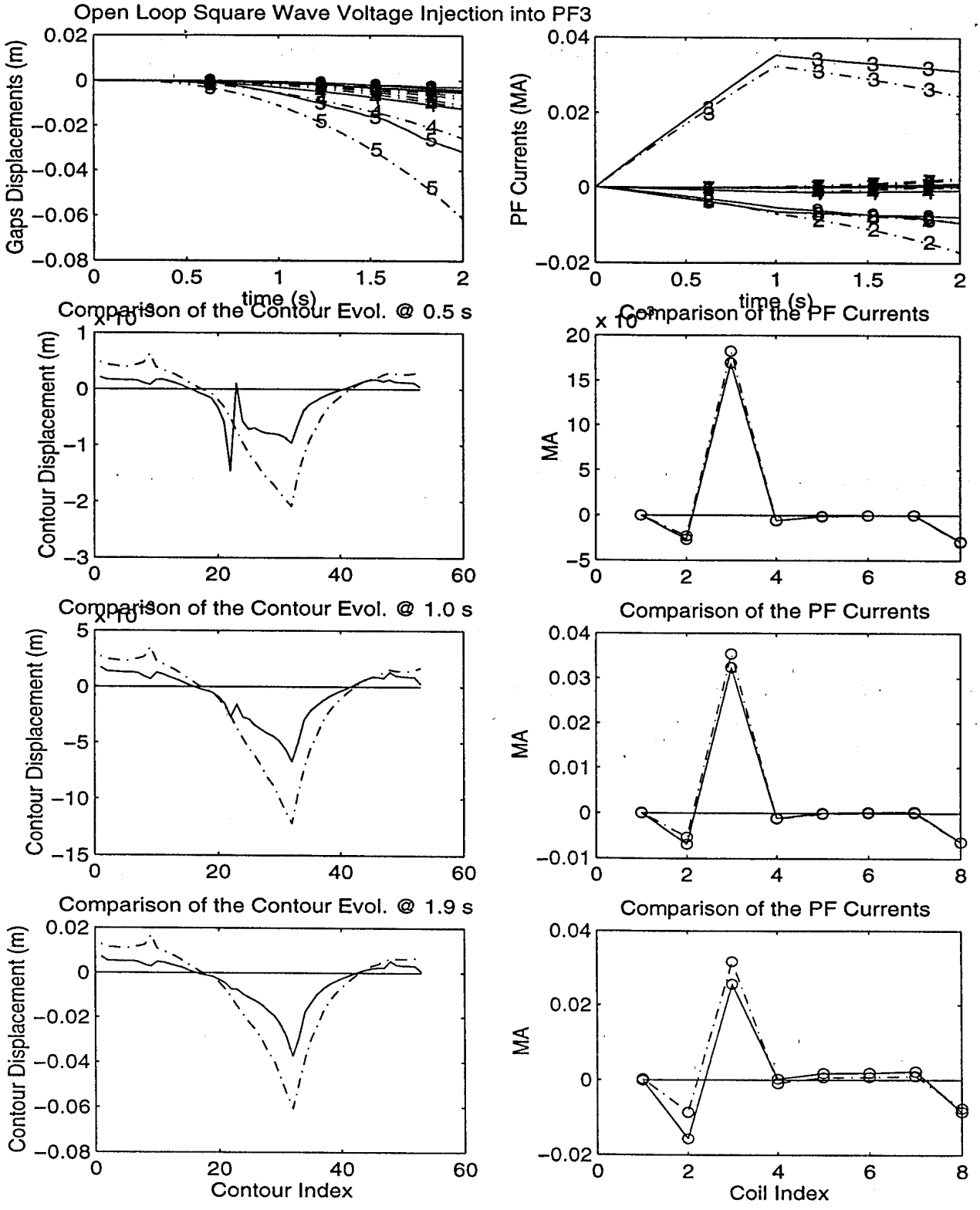

Fig. 4 Comparison of time evolution of six nominal gaps and eight PF coil currents, and the gaps contour evolution of PF currents at 0.5s, 1.0s, and 1.9s following a one second square-pulse injection into PF 4. (linear = -.)

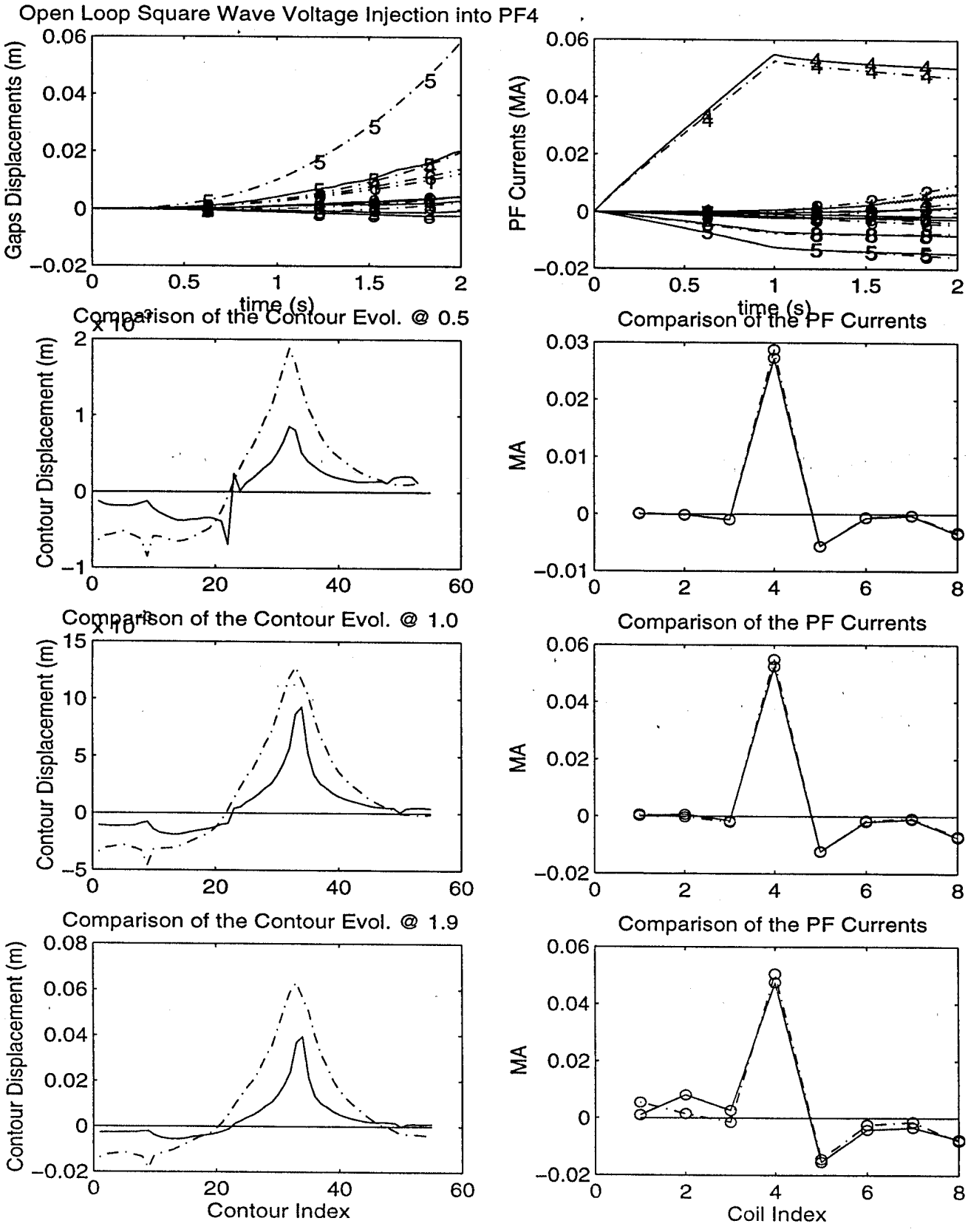

Fig. 5 Comparison of time evolution of six nominal gaps and eight PF coil currents, and the gaps contour evolution of PF currents at 0.5s, 1.0s, and 1.9s following a one second square-pulse injection into PF 5. (linear = -.)

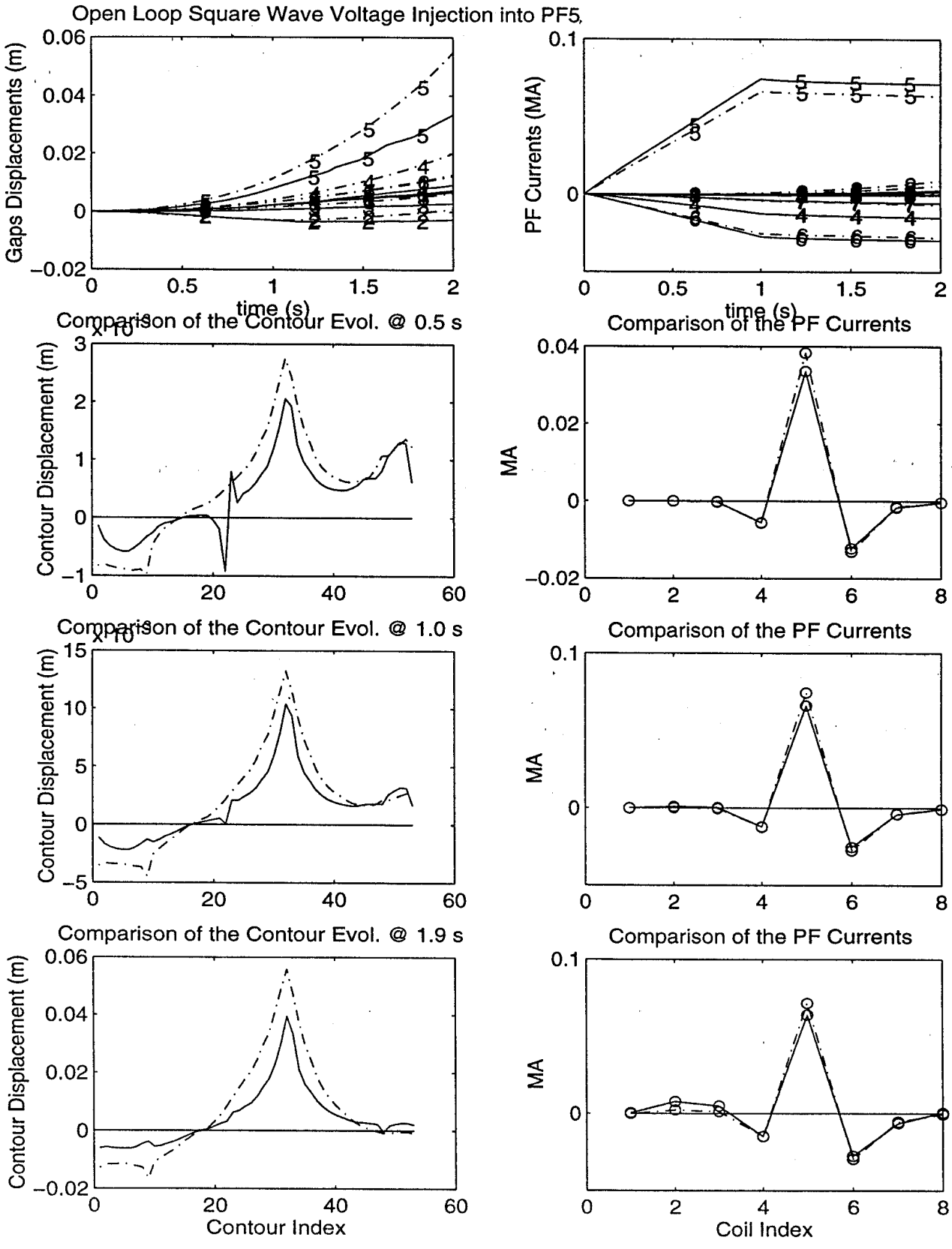

Fig. 6 Comparison of time evolution of six nominal gaps and eight PF coil currents, and the gaps contour evolution of PF currents at 0.5s, 1.0s, and 1.9s following a one second square-pulse injection into PF 6. (linear = -.)

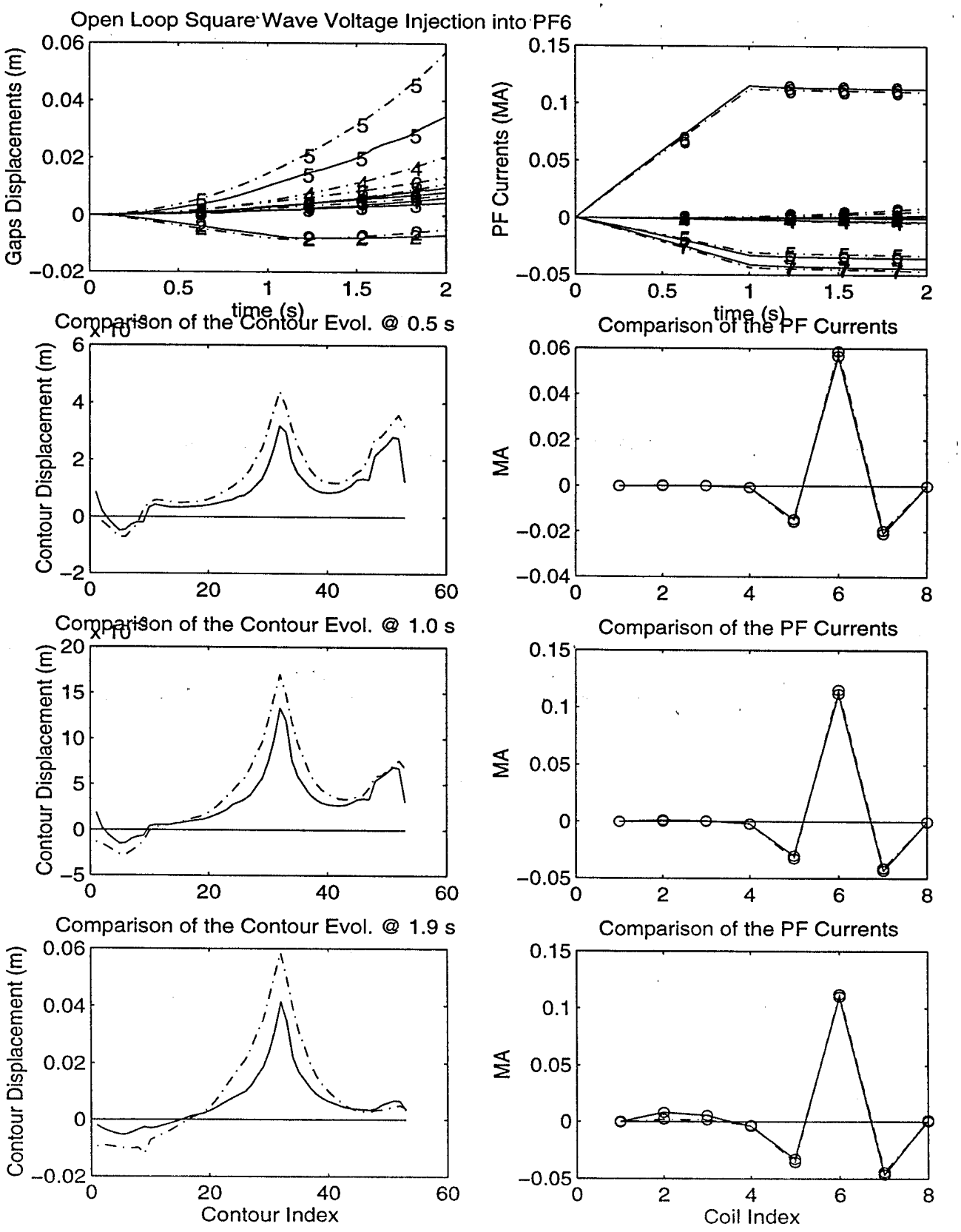

Fig. 7 Comparison of time evolution of six nominal gaps and eight PF coil currents, and the gaps contour evolution of PF currents at 0.5s, 1.0s, and 1.9s following a one second square-pulse injection into PF 7. (linear = -.)

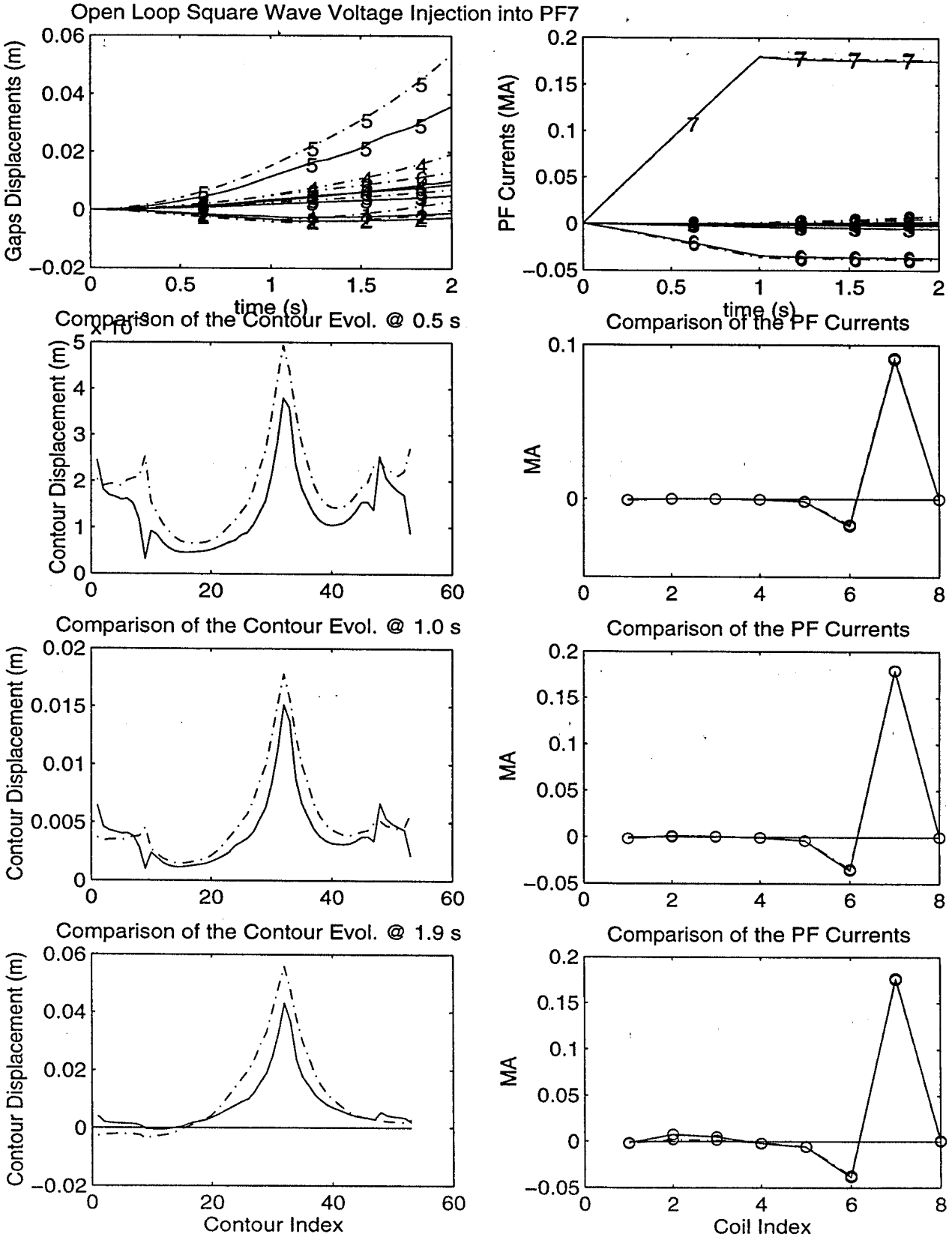

Fig. 8 Comparison of time evolution of six nominal gaps and eight PF coil currents, and the gaps contour evolution of PF currents at 0.5s, 1.0s, and 1.9s following a one second square-pulse injection into PF 8. (linear = -.)

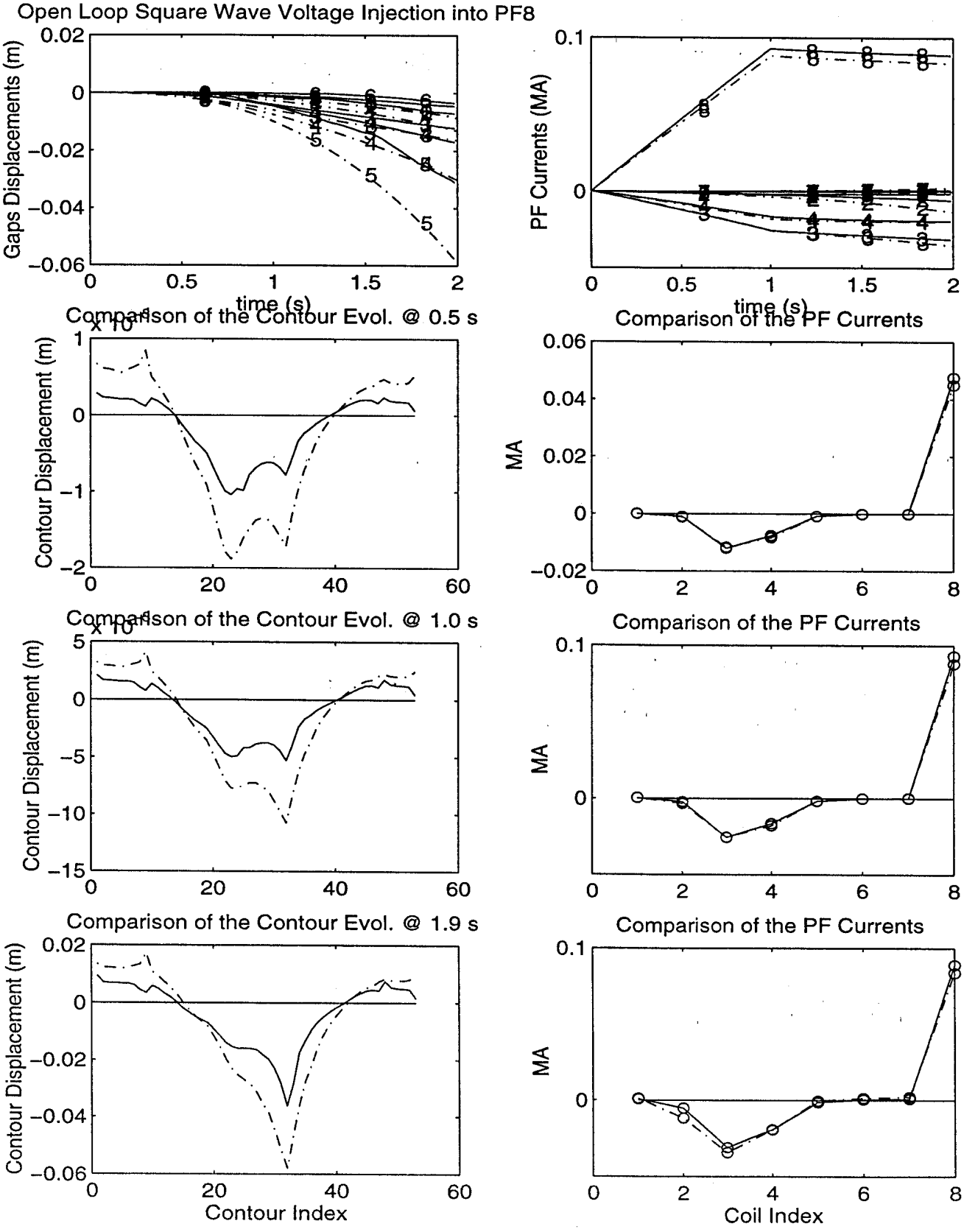

Fig. 9 Separatrix contours 1 second after the square pulse injection on PF2. Dashed contour is before perturbation, the solid contour is the TSC result, and the dashed-dot is the linear model.

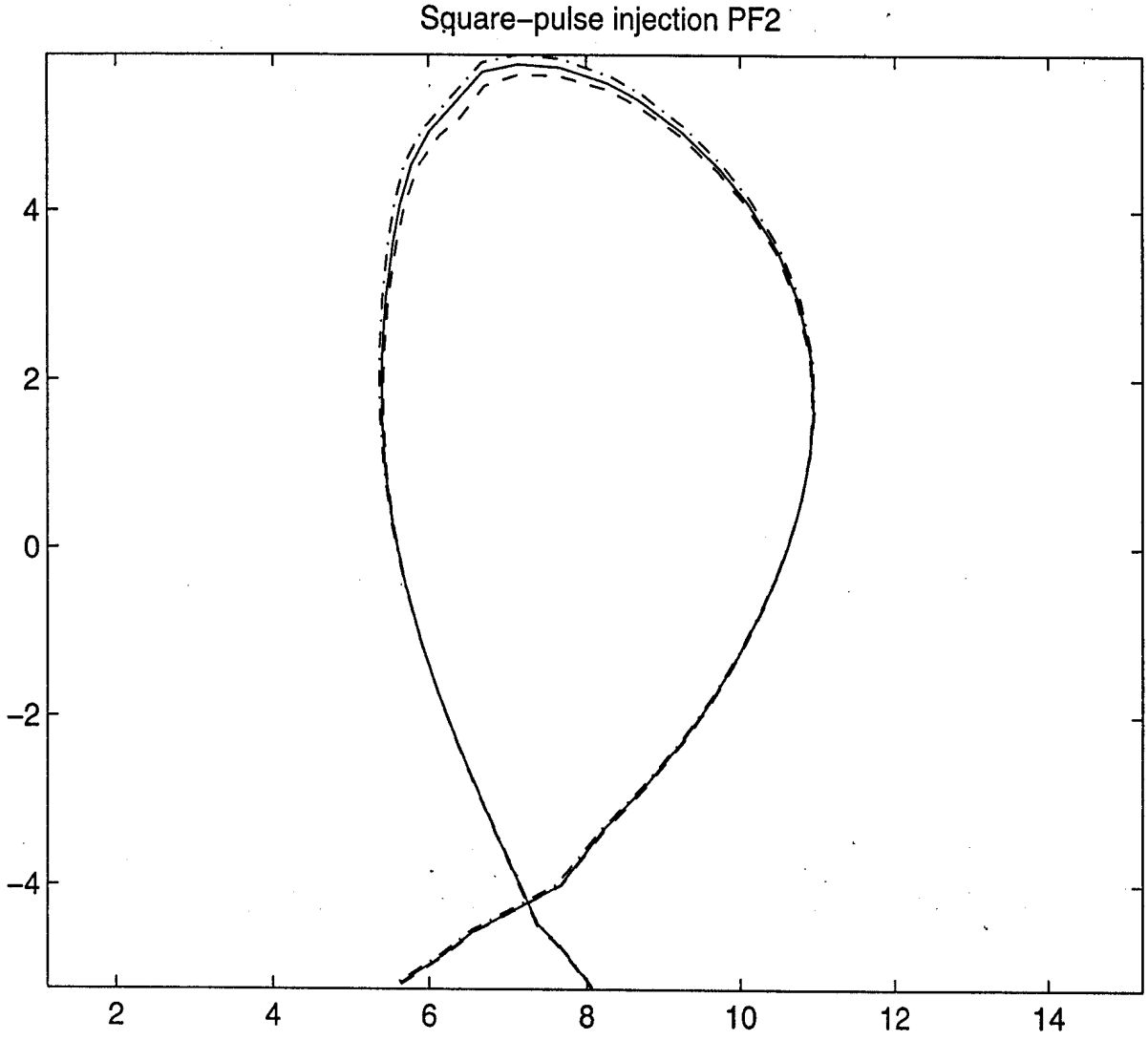

Fig. 10 Comparison of time evolution of six nominal gaps and eight PF coil currents, and the gaps contour evolution of PF currents at 0.1s and 0.5s following an *li* drop of 0.1. (linear = -.)

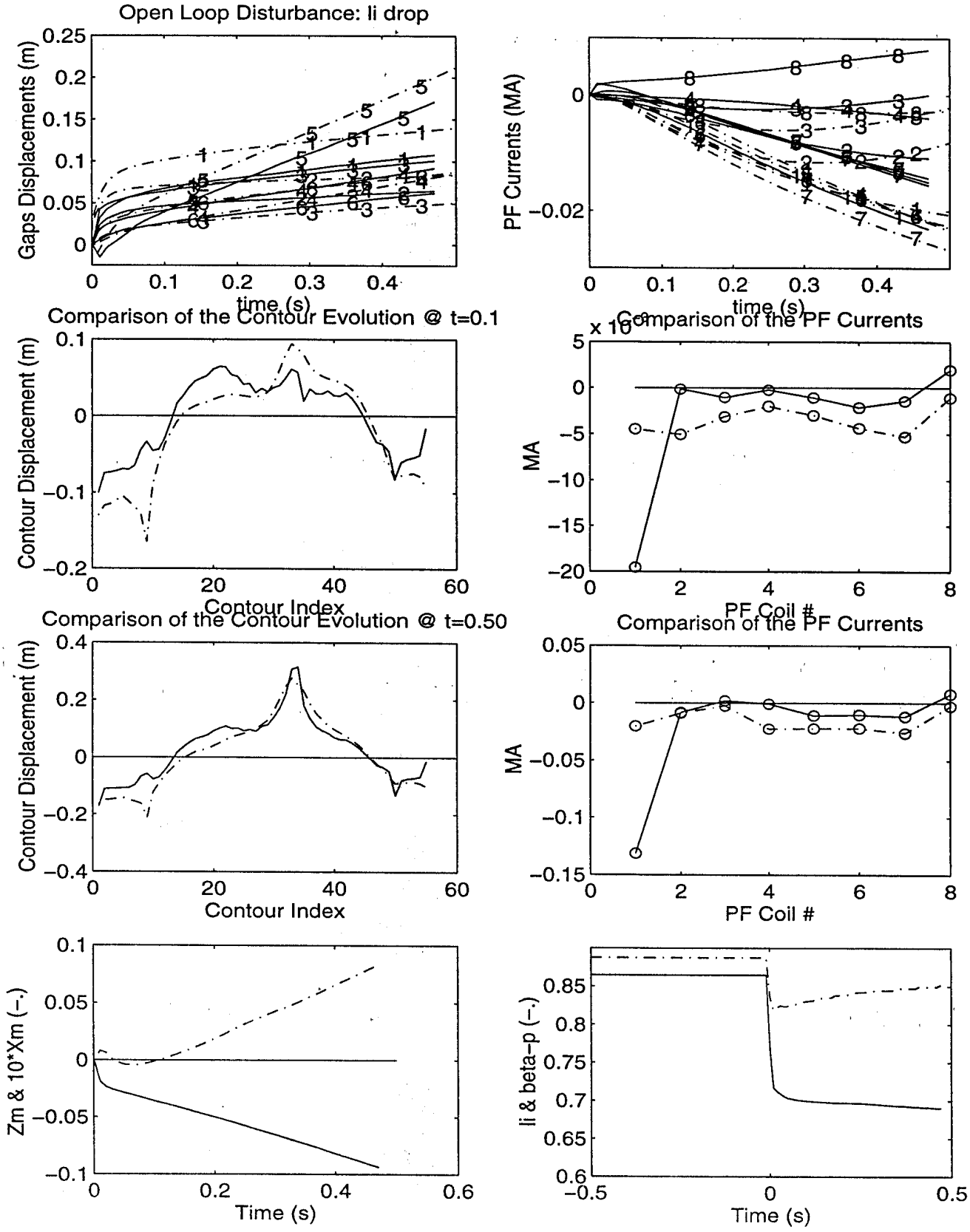

Fig. 11 Comparison of time evolution of six nominal gaps and eight PF coil currents, and the gaps contour evolution of PF currents at 0.1s and 0.5s following an βp drop of 0.2. (linear = -.)

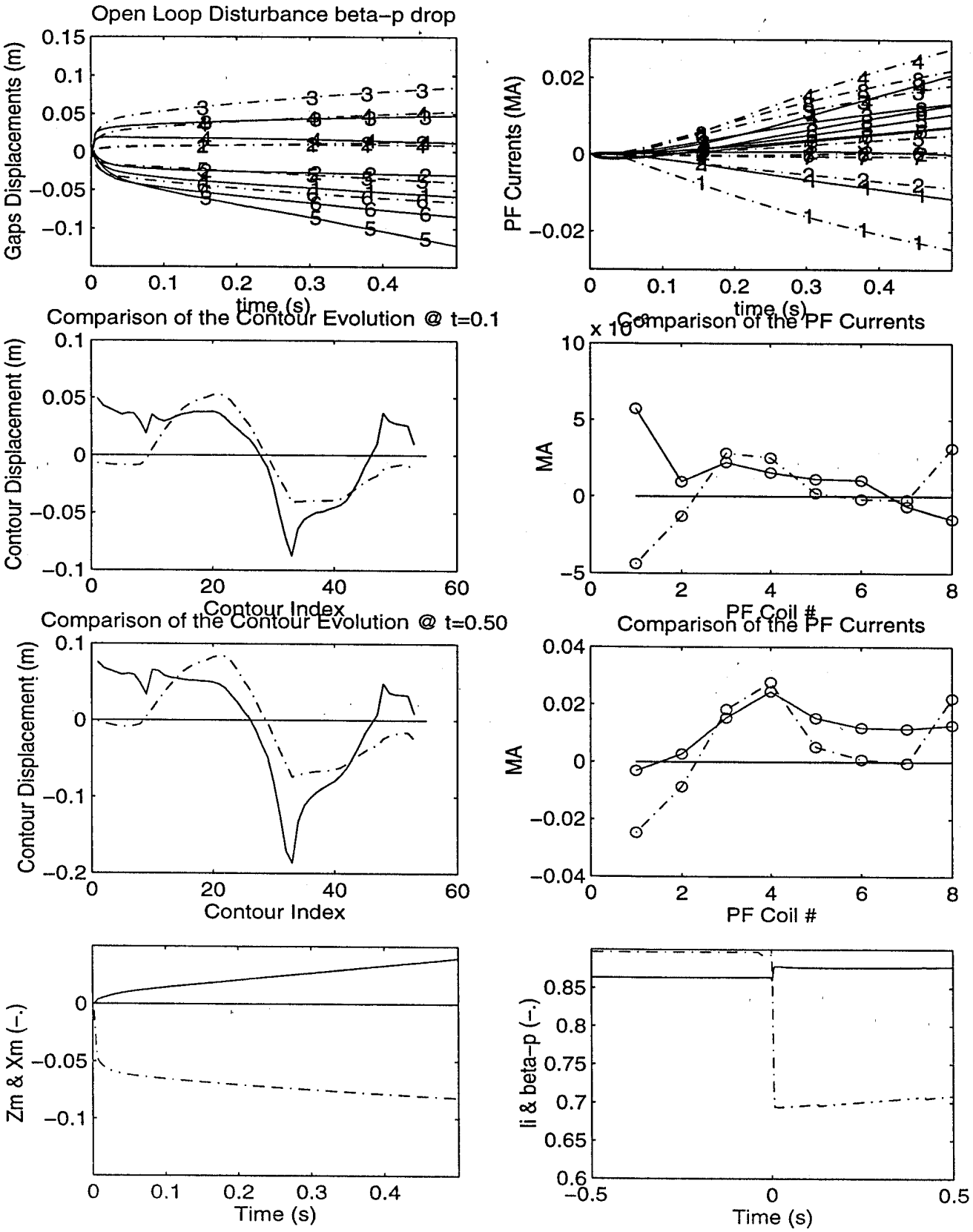

Fig. 12 Comparison of time evolution of six nominal gaps and eight PF coil currents, and the gaps contour evolution of PF currents at 1.0s and 2.0s following an βp drop of 0.2. (linear = -.)

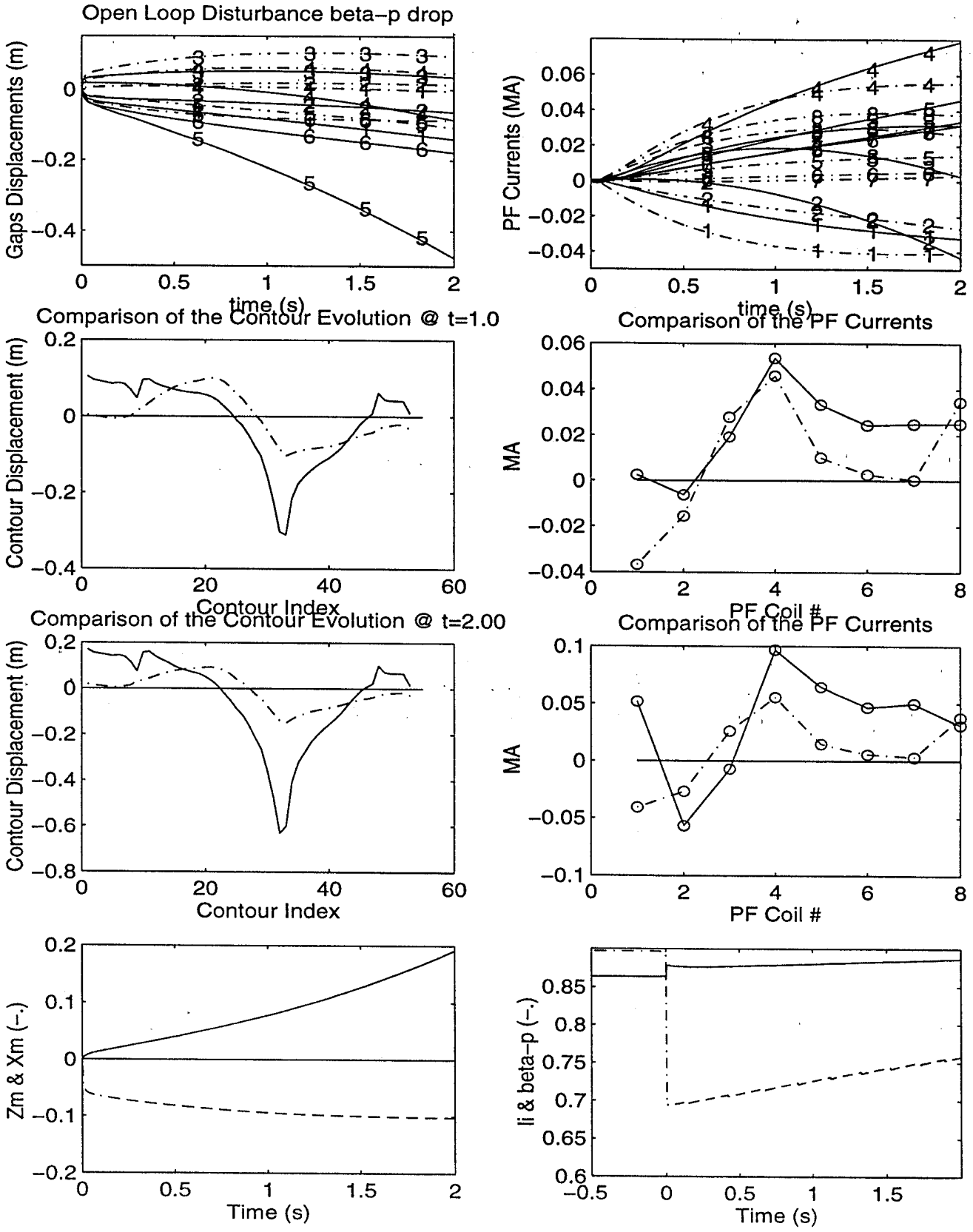

Fig. 13 Comparison of time evolution of six nominal gaps and eight PF coil currents, and the gaps contour evolution of PF currents at 0.1s and 0.5s following a combination βp drop of 0.2 and li drop of 0.1. (linear = -.)

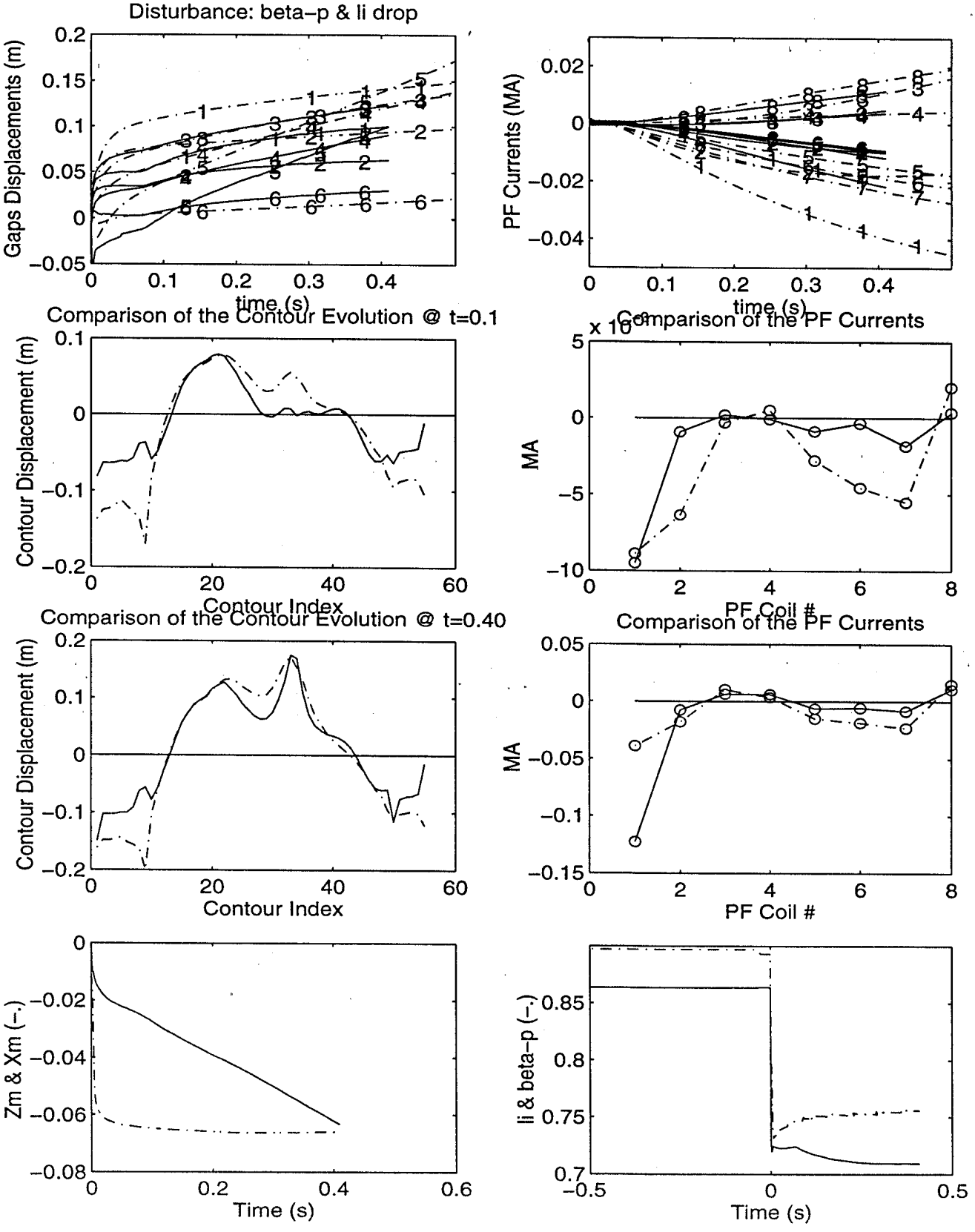

Fig. 14 Separatrix contours 0.4 s after the *li* drop disturbance. Dashed contour is before perturbation, the solid contour is the TSC result, and the dashed-dot is the linear model.

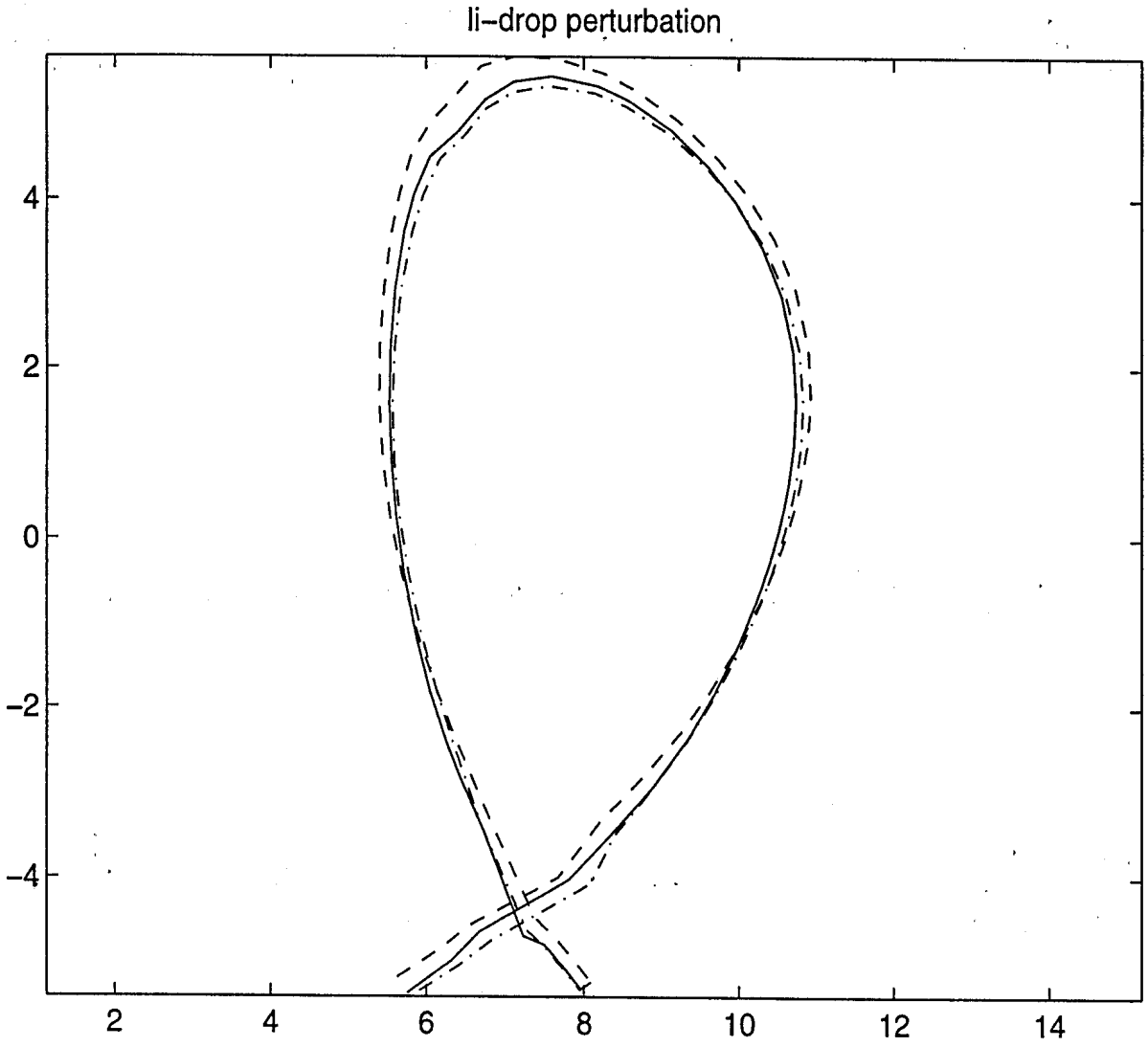

Fig. 15 Separatrix contours 0.4 s after the βp drop disturbance. Dashed contour is before perturbation, the solid contour is the TSC result, and the dashed-dot is the linear model.

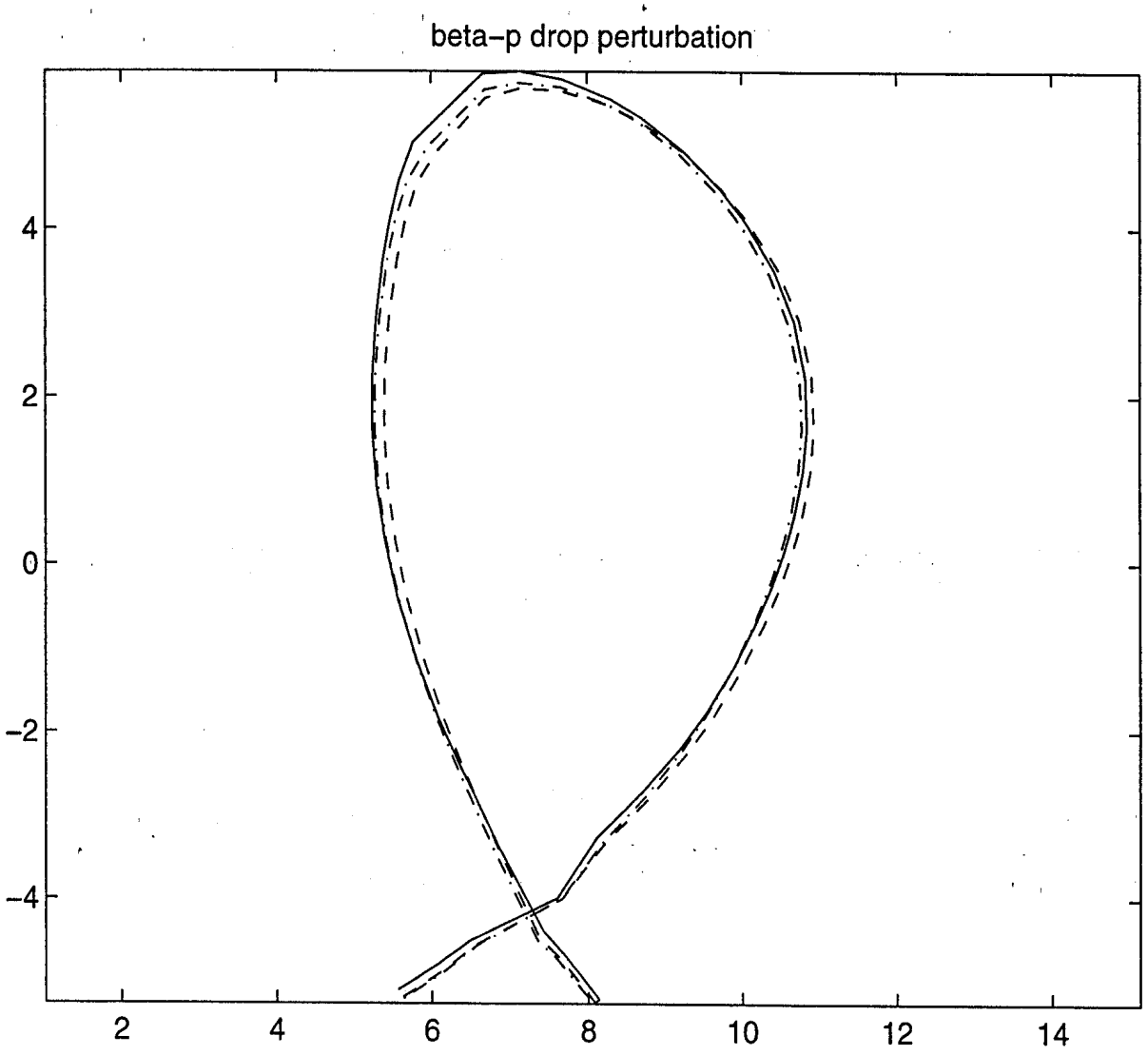

EIDGENÖSSISCHE TECHNISCHE HOCHSCHULE LAUSANNE
POLITECNICO FEDERALE DI LOSANNA
SWISS FEDERAL INSTITUTE OF TECHNOLOGY LAUSANNE

CENTRE DE RECHERCHES EN PHYSIQUE DES PLASMAS
Association EURATOM - Confédération Suisse

ÉCOLE POLYTECHNIQUE
FÉDÉRALE DE LAUSANNE

Final Report

ITER Design Task D324-1 Phase I

Work Envelope A

Model of Errors on the Estimators of the Controlled Parameters

J.B. LISTER
(CRPP-EPFL)

With Contribution from: O. Gruber (A-UG), J-M. Moret (TCV), A.W. Morris(COMPASS-D), D.J. Campbell (JET), E. Joffrin (TORE-SUPRA)

19 July, 1996

E_A_TC_1.DOC

1. PREAMBLE

The aim of this modest study is to provide a realistic model of the diagnostic measurement errors in order to perform realistic simulations using both linear and non-linear plasma models.

The current status of this work is that a useable definition of the errors which can be assessed by the experiments has been made after consultation. A questionnaire has been made, annexed, which is currently circulating (April 1996). It was intended that during May and June a second iteration should be circulated based on the assessment difficulties of this first current iteration.

This Intermediate Report it intended to elicit a reaction to establish the noise to be used in modelling during 1996-1997 for the D324-1 work. As of July 1996, only the Compass-D tokamak has supplied data for this study. It is hoped that the results will be available during the autumn of 1996.

Desired contributors to the questionnaire: O. Gruber (A-UG), J-M. Moret(TCV), A.W. Morris (COMPASS-D), D.J. Campbell (JET), E. Joffrin (TORE-SUPRA)

2. ERROR SOURCES

Different sources of errors in the observers are to be considered :

1. Constant systematic errors (e.g. calibration, positioning)
2. Variable systematic errors (e.g. neutron activation, Integrators, thermal variations of (1))
3. Noise (e.g. electronic, electrical pick-up)
4. Time delays (e.g. algorithmic calculation cycle time)
5. Filtering (e.g. electronic filtering, sensor shielding)
6. Digital treatment noise
7. Shielding (e.g. 2-D Passive structures)
8. Shielding (e.g. 3-D Passive structures)

9. Distortion of the observer mapping

10. Non axi-symmetric plasma signal

11. Power Supply switching noise

3. ASSESSMENT OF THE ERRORS IN THE CONTROL LOOP

The individual sources of errors are now discussed in turn.

1) Constant systematic errors

These errors are considered to be separable from the dynamical control problem which is the most crucial part of the control in so far as the requirements of the power supplies are concerned. Spatial errors can be considered to be a change in the reference of the diagnostic, and map simply to a resulting error in the shape. We assume that there will be a higher control level with strong integral gain, which will optimise operational parameters such as first wall heat-load in such a way as to annul any constant systematic errors. However, during the commissioning of the poloidal systems, it will be essential to carry out systematic work to reduce these errors to the minimum. An example of such work was carried out by Moret on TCV and Walker on DIII-D. In the work by Moret, modifications to the calibration constants and spatial locations of both current carrying coils and sensors were treated as free variables. A cost function was established to minimise the differences between the calculated responses and the measured responses to DC currents, weighting the required modifications. Using this technique an improvement to consistency between currents and sensors was obtained.

Pending Phase II - Insert the TCV results and the general questionnaire results

As a result of this work, we consider that ITER should not do worse than the current tokamaks, provided adequate effort is put into such an auto-consistency procedure.

We therefore consider that:

- previous estimates of the systematic errors may have been over-estimated
- this class of errors is always recovered by a higher control layer than the magnetic control during normal tokamak operation.

2) Variable systematic errors

Progressive degradation of sensors and their calibration will occur over many discharges and will have to be recovered by repetition of the auto-consistency checks. This problem is a little more difficult to quantify. However, we feel that the timescales of the evolution of these systematic errors is many times longer than the dynamics of the poloidal field control and many times longer than the timescales of the operational control layer. "De-calibration" during a single ITER discharge will occur over many 100s of seconds, long compared with the characteristic timescales of the control dynamics. If adequate attention is brought to bear on this point, then modelling of the variation of the machine geometry as a function of OH magnetisation and structure temperature would allow first order corrections to be made. Finally, these errors are also recovered by a higher control layer than the magnetic control.

3) Noise

We consider that the degree of random non-plasma noise on the magnetics diagnostics will be negligible in ITER due to the long characteristic timescale of the control. On existing devices, this source of noise is already negligible.

Typical results of RMS variation of the acquired signals from data received from the questionnaire are :

Pending Phase II, tabulated data such as :

	Local Bpol	*Poloidal Flux*
No Supplies working	*NNNN*	*NNNN*
With Plasma during Flat-top	*NNNN*	*NNNN*

Electrical pickup, cross-talk between sensors and field components which they are not designed to detect, will be a less severe problem on ITER than on existing devices. Firstly, this is due to the large size of the device compared with the characteristic lengths of the bus-bar separations and secondly, due to the long time-constants. We do not, therefore, consider that the level of noise from electrical pickup will be significant, compared with plasma-related noise (which is signal, in terms of the sensors).

This assumption must be verified during the commissioning of the magnetics diagnostics when the sensor itself could be shorted during supply tests.

4) Time delays

Strict time delays are generated by a) the time between a sensor signal sampling and the production of an actuator command (control system calculation delay or latency), b) the time between successive sensor samplings (time discretisation) and c) a time delay in the response of the power supplies. The significance of the cumulative delay on the control loop is likely to be negligible, given the long dynamic timescales. The state of the art (TCV Digital Plasma Control System) allows a cycle-time of 70 μsec and a latency between sampling and actuator demand input of <70 μsec. This performance corresponds to the time necessary for treating 192 analog sensor inputs and 64 internal states using standard control methods and an effective calculation speed of 800 MFLOPS. (Confirmation during 1996). A full equilibrium reconstruction is not yet performed. Allowing ITER to implement more complex algorithms, including real-time inverse equilibria, a calculation delay of 5 milliseconds would seem to be extremely conservative for the magnetics control loop.

The second source of time delay is in the actuators themselves, which must also be modelled, but is not part of the sensor behaviour. A complete thyristor model is probably not necessary for the evaluation of the magnetics control loop, due to the relative speed of the supplies relative to the timescale of the control loop. ITER will have 1.6 msec firing intervals (assuming a 50 Hz suppply) and 1 second^{-1} growth rates. This ratio compares very favourably with TCV which has 0.8 msec firing intervals (100Hz) and 1000 second^{-1} growth rates.

In order to model these two effects before a true power supply model is included in the control loop, we propose a conservative cumulative delay of 5 milliseconds.

5) Filtering

We assume that the effects of electronic filtering and shielding of the sensors be modelled by a one-pole filter with a time-constant of 0.5 milliseconds. This would appear to be conservative. In fact, the time discretisation of the control loop will require careful anti-aliasing filtering which should also be modelled.

6) Digital Treatment Noise

The A to D conversion and the D to A reconstruction of the output data are subject to noise. In order to simulate this, we propose that the input signals be subject to broadband noise of a range +-0.1% FSR, corresponding to 2 LSB of a 12-bit digitiser (taken as a reference value with which current experiments are familiar, in spite of the ITER choice of 16-bit digitisation). The mapping from the input signals to the control variables must be specified in order to implement this. For simplicity, we propose the following formulae to include input and output noise on the gaps or other distances or the plasma current; a factor of 3 is included for the conditioning of the mapping :

- Gap_Dig_Noise = Random(-0.001 : 0.001) * (Ipmax * Gap-Range/Ip)
- Ip_Dig_Noise = Random(-0.001 : 0.001) * Ipmax

This noise is to be applied at each sampling.

7) 2-D Shielding

Shielding by 2-D passive structures is part of the electromagnetic model of ITER and is therefore not to be considered as part of a sensor response, which is assumed to be prompt with respect to its locally measured quantities. This presupposes that the algorithms used to reconstruct the controlled variables include a 2-D model of these structures without making assumptions about the spatial distribution of the shell currents. Such a methodology is current in many inverse equilibrium codes and this assumption is therefore considered to be reasonable.

8) 3-D Shielding

Shielding by 3-D passive structures has no effect on the 2-D sensors, such as complete flux loops, one of the reasons to continually insist on as many toroidally complete loops as feasible. The consistency of the 2-D equivalent model on the sensors is totally knowable from the commissioning measurements of the ITER structure. The effect of 3-D passive structures on 3-D sensors is the greatest uncertainty in the model of the sensors. We cannot a-priori differentiate between model errors and the presence of 3-D shielding effects. We are therefore forced to assume that :

- the 2-D model is correct, once adjusted to the continuous flux measurements
- the construction of the local sensor contains no filter time constants

Having made these assumptions, the difference between the modelled and measured responses of the sensors can be attributed to 3-D shielding and a model of the shielding time constant(s) is obtained immediately. We make the assumption that the effect should be modelled as a 1- or 2-pole filter with the characteristic timescale of the slowest 3-D shielding modes for that sensor. An estimate of this effect will be required from the ITER diagnostics group.

9) Distortion of the observer mapping

The mapping M between physical sensors (s) and the controlled variables (v) such that $v = M(s)$ is considered to be approximate, defined by an approximate mapping technique such as FP or ANN or local linearisation. In this case, the error in the mapping εM is a source of error which is injected into the feedback loop, via: $\delta v = M\,\delta s + d\varepsilon M/ds\,\delta s$. Since this error is not a random "noise" error but effectively a transfer function modification to the observer, its effect on the loop stability could be more than simple noise.

This effect is difficult to estimate, since it depends upon the chosen mapping. We should therefore impose a limit on the local variation of εM with respect to s when choosing or designing the mapping. If we assume that the mapping M is the result of an equilibrium code the problem does not go away. Care must be taken over this, but no modelling is proposed.

This element of the noise is precisely that which is under study by CREATE in the context of the D324-1 Task. When this work is completed, modelling will be possible.

10) Non axi-symmetric plasma signal

2-D sensors perform toroidal integration of the non-axisymmetric plasma signal from coherent plasma modes or from turbulence. These sensors therefore do not contain this error. However local sensors, such as the local poloidal magnetic field, pick up this signal as an error and we consider this to be by far the greatest source of noise in the feedback loop. The largest component is n=1 signal which will be cancelled out by careful design of the poloidal field detection system. The amplitude of this error is difficult to estimate and we are in the process of compiling some data according to the questionnaire annexed.

11) Power supply noise

Power supply switching noise falls into two classes. Firstly, it provides a noise level on the actuator signals (applied coil voltages) which is a dominant external noise source in present day experiments. This noise continuously excites the closed loop system which must continuously recover from the errors produced by this noise. In ITER, the frequency of this noise will be so far from the closed loop characteristic times, that it will not be as significant as it is today. This effect can be crudely modelled by inserting a sawtooth with the switching frequency into the actuator inputs, to confirm this supposition. Such a test should be performed. Secondly, the switching noise will more likely be picked up extraneously on sensor signal cabling, due to its higher frequency, but again, the frequency separation should allow filtering of the switching frequency before the digital control loop. This point must be considered.

SUMMARY

We consider that the magnetic diagnostic measurements be subject to the following "errors" with respect to perfect knowledge of the control variables:

- a time delay of 5 msec between signal and actuator
- a single pole filter time constant of 0.5 msec for shielding
- anti-aliasing filtering, to be defined
- a 0.1% FSR digital sampling noise
- an RMS noise injection of *NN*% of the individual poloidal field contributions to the control variable estimator (*TBD*!)

We suggest that in addition to these nominal models, at least 1 full simulation be carried out with values 3 times these, to test that the conclusions are not overly sensitive to these assumptions.

ANNEXE The questionnaire currently circulating among the EUHT experiments

EUHT Task D324-1 : Noise Sources and Levels in Existing Tokamaks

- All values are in Volts unless otherwise stated. Noise is in RMS.
- Full scale corresponds to normal plasma full scale.
- The 3dB point is the 3 dB roll-off frequency for the different quantities, after signal processing
- Poloidal Fluxes are flux difference with respect to a reference flux.
- A figure should be given for the outer-midplane B's and the inner-outer flux difference. Figures showing the poloidal distributions should be added if available.
- The Blind Coil corresponds to a complete signal processing chain from a shorted flux or field probe, for devices which have at least one non-working probe.

A. Raw Noise in the absence of Plasma and coil currents

	Full-Scale	Noise Level	3 dB Point
B-Poloidal			
d/dt B-Poloidal			
Poloidal Flux			
d/dt Poloidal Flux			
Coil Currents			
d/dt Coil Currents			
Blind Coil			

B. Signal Variation in the presence of a single Poloidal Current in an effectively steady state

	Full-Scale	Noise Level	3 dB Point
B-Poloidal			
d/dt B-Poloidal			
Poloidal Flux			
d/dt Poloidal Flux			
Coil Currents			
d/dt Coil Currents			
Blind Coil			

C. Signal in the presence of Plasma in as "steady state" as possible to give a lower limit. If possible please show 2 values for OH / strongly-heated discharges.

	Full-Scale	Noise Level	3 dB Point
B-Poloidal n=0			
B-Poloidal n=1			
B-Poloidal n>=2			
d/dt B-Poloidal n=0			
d/dt B-Poloidal n=1			
d/dt B-Poloidal n>=2			
Poloidal Flux			
d/dt Poloidal Flux			
Coil Currents			
d/dt Coil Currents			
Blind Coil			

D. Calibration Precision (percentage)

	Percentage	
B-Poloidal		
d/dt B-Poloidal		
Poloidal Flux		
d/dt Poloidal Flux		
Coil Currents		
d/dt Coil Currents		
B-Poloidal major radius		
B-poloidal tilt		
B-poloidal azimuthal angle		

E. Observer Noise (percentage Full Scale)

This is delicate since it is not possible to measure "noise". However, in the steady state, we could estimate the RMS on some control parameters and use this as an upper limit on noise, assuming a perfect controller. Very artificial but.... Any other ideas ?

Up-down flux differences, if used, should quote an effective calibration (weber per amp-metre).

These values correspond to noise level at the reference subtraction point in the feedback loop.

	Percentage Full Scale
Ip	
zIp	
RIp	
Gapin (or similar)	
Up-down Flux Difference	
other...	

EIDGENÖSSISCHE TECHNISCHE HOCHSCHULE LAUSANNE
POLITECNICO FEDERALE DI LOSANNA
SWISS FEDERAL INSTITUTE OF TECHNOLOGY LAUSANNE

CENTRE DE RECHERCHES EN PHYSIQUE DES PLASMAS
Association EURATOM - Confédération Suisse

ÉCOLE POLYTECHNIQUE
FÉDÉRALE DE LAUSANNE

Final Report

ITER Design Task D324-1 Phase I

Work Envelope P

Protective and Corrective Strategy Control Modes

J.B. LISTER
(CRPP-EPFL)

In collaboration with Y. Gribov, A. Portone (Naka JCT)

19 July, 1996

E_P_1.DOC

1. PREAMBLE

This report is an Intermediate report (end of Phase I) on work performed as part of the D324-1 ITER Design Task. It intends to set out the methodology for handling abnormal conditions during ITER operation. This approach, if and when agreed/modified can be used to document fully the abnormal conditions which must be handled for ITER operation.

2. INTRODUCTION

The PF and Plasma Control Systems must provide reliability of commissioning, testing, non-burning plasma operation and burning plasma operation. In addition, the sum of all the control systems must provide maximum safety of an extremely complex plant. These 2 requirements can be conflicting, such as the acceptance of risk, contrary to the 2nd requirement, and complete safety, contrary to the aim of full and regular performance. Although this type of conflict is relatively new to the Tokamak field, it is current in many fields with both significant operational and safety aspects. We shall try to base the proposed strategy on 3 such conventional systems which at first sight appear to have some similarities with our requirements, and appear to yield intuitive analogies, namely:

- - Aircraft
- - Nuclear Fission Plants
- - Road Traffic

In order to fulfill the ITER objectives, the PF system will have to have a flexible approach to the presence of abnormal conditions for the following four main reasons:

- Firstly, the long pulse length of 1000 seconds will allow recovery from some abnormal conditions via operator or automated intervention
- Secondly, the complexity of the plant and the requirement to demonstrate reliable operation will preclude the primitive "shutdown" approach currently prevalent in the presence of abnormal conditions
- Thirdly, the superconducting PF magnets will be less tolerant to uncontrolled events than conventional magnets

- Fourthly, the minimisation of the total ITER cost leads to a reduction in the margin in all systems, such as coil currents, voltages and total available power.

For these reasons, in the event of the detection of abnormal operating conditions, the control systems will be allowed to perform actions which are loosely grouped into three categories:

- Corrective Actions, allowing normal operation to be resumed once the abnormal condition has been cleared
- Termination Actions, allowing the pulse to terminate, or at least considerably reduce the magnetic and kinetic plasma energy, under full, or at least adequate diagnostics and full or at least adequate PF control
- Protective Actions, designed to avoid the most serious risks to the ITER device.

Examples of abnormal conditions which will be considered as candidates for Corrective Actions include:

- Saturation of the current in a PF coil
- Overheating of plasma-facing components
- Loss of voltage on a PF coil, possibly recoverable
- Loss of control of an inessential PF coil, such as PF8
- Excessive instantaneous AC losses
- Loss of quality of the diagnostic information, possibly recoverable
- Loss of communication with important but inessential devices

Examples of Corrective Actions include:

- Reduction of plasma bp (to modify the PF current requirements)
- Modification to the plasma-wall spacing (to reduce the required precision and voltage control margin)
- Reduction of the control precision (to accept reduced voltage limits)
- Reduction of plasma current (to reduce magnetic energy).

Examples of abnormal conditions which will be considered as candidates for Termination Actions or Fast Controller Shutdown include:

- Request by an external system, such as PF power supplies for its own reasons
- Serious loss of voltage on a PF coil, not recoverable
- Loss of control of an important PF coil
- Excessive accumulated AC losses
- Loss of essential diagnostic information, not recoverable
- Unrecoverable loss of communication with important devices.

Examples of actions which may correspond to Termination Actions include:

- Reduce the burn as fast as possible, in a controlled manner (to reduce bp)
- Change to a robust and simple control variable set (to require fewer diagnostics)
- Execute the fastest current ramp-down according to the actual state (to reduce the magnetic energy)
- Execute the fastest elongation reduction, according to the actual state (to minimise the VDE probability)
- Program the additional heating (to minimise the disruption probability).

Examples of abnormal conditions which will be considered as candidates for Protective Actions include:

- Request by an external system, such as PF power supplies for its own reasons
- Decisions by the Scenario Controller
- Automatic detection of an excessive force on the PF coil system
- Loss of voltage on essential PF coils, predicted to lose vertical control
- Loss of control of essential PF coils
- Unrecoverable loss of essential diagnostic information
- Loss of communication with essential devices.

Examples of actions which may correspond to Protective Actions include:

- PF voltages set to zero (constant flux, to minimise induced voltages)
- PF voltages set to control constant PF current (to minimise induced currents)
- PF voltages set to preprogrammed values (to reduce forces on the vessel according to modelling)
- Additional heating shutdown (to avoid wall damage, executed by the Scenario Controller)
- Injection of a killer-pellet (to limit the VDE excursions, executed by the Scenario Controller)

Of the three categories of abnormal condition actions, Termination Actions and Protective Actions will be absolutely defined according to the initial state. They are irreversible and must be adequately studied and simulated before beginning ITER operation. They can be subsequently perfected during operation. The Corrective Action strategies are more dependent on the specific problems which might appear during operation and will evolve as ITER gains operational experience.

In the following sections, we propose a structure which can handle these conditions in a simple and relatively transparent way.

3. OUTLINE OF THE PROPOSED 4-MODE CONTROL STRUCTURE

Firstly, we must define our terminology. We are considering the highest level of control, at which the manner of operating the machine is chosen. It is the level at which all other decisions are over-ridden. As such, it commands the real control layers which contain the different feedback loops. In order to avoid confusion with the word State, which has very precise connotations, the word Mode is chosen. However, by analogy with the State-Transition diagrams, we will be proposing Mode-Transition diagrams. The word Mode is therefore retained as signifying the mode in which the control itself operates.

Although this document specifically addresses the questions of Poloidal Field control, there appears no reason why this proposed layout should not be adopted for other ITER control systems.

It is proposed to use 4 Control Modes for the PF and Plasma Control Systems. It is assumed that each Control Mode has **complete** information of the ITER plant.

The 4 Control Modes illustrated in Fig. 1 comprise:

1 - Normal Control Mode

2 - Corrective Action Control Mode

3 - Controlled Termination Control Mode

4 - Protective Action Control Mode

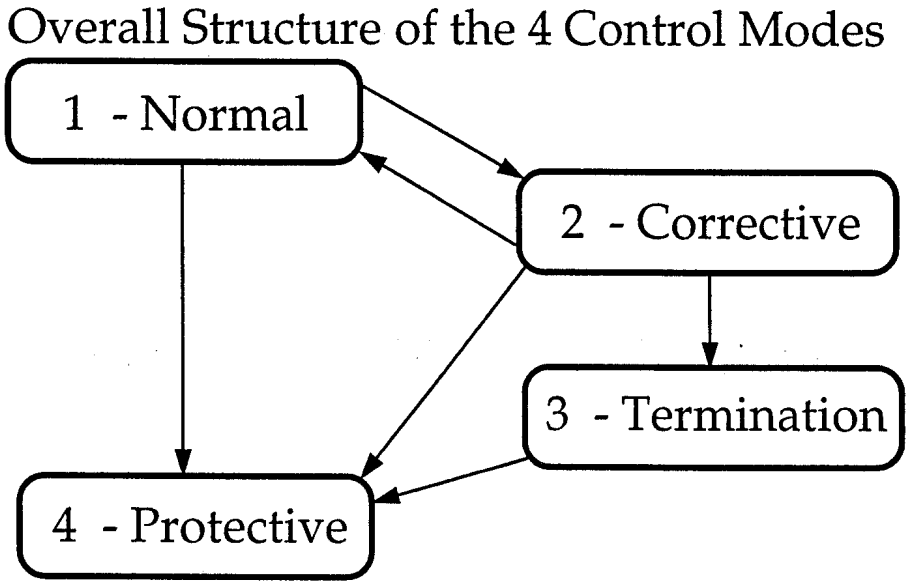

Fig. 1 Overall Structure of the 4 Control Modes

The differentiation between these proposed Control Modes is as follows:

- # 1 Normal Control Mode. This is the Control Mode which should normally be in operation. It is the default Control Mode and does not need any additional information in order to be defined, except for the sum of the necessary conditions in which it can remain valid.

- # 2 Corrective Control Mode. This Control Mode is used in the case of real or apparent malfunctioning of the plant, in cases in which the plant should be able to continue functioning without significantly increased danger to the plant itself, perhaps at reduced performance. It is entered by satisfying conditions defined in the Normal Control Mode. It will contain a set of actions to be carried out when entered, as well as a continuing strategy to be applied. It can exit either:

- back to the Normal Control Mode if the plant state allows this, or
- to the Termination Control Mode, or
- to the Protective Control Mode, as required.

- # 3 Termination Control Mode. Although this Control Mode could be considered to be part of the Corrective Control Mode, its likely frequency of use and its clear significance suggest that it be considered as a separately identified Control Mode. It can only be entered from the Corrective Action Control Mode which identifies the perceived problems as non-recoverable.

- # 4 Protective Control Mode. This Control Mode corresponds to the abandoning of the current discharge with no chance of returning, as a consquence of real or apparent conditions which are determined to present an inacceptable and unavoidable near-term risk to the plant. It is entered from the Normal Control Mode, the Termination Control Mode or from the Protective Control Mode, on satisfying a set of conditions, specified differently for these Control Modes.

Of course, we could always introduce a 5th or 6th Control Mode, but we consider that such additions should be added to one of the 4 proposed Control Modes, as they are presented here, as options or as part of the strategy. Since we will be dealing with the safety and reliability of the ITER plant, clarity and unambiguity will be essential.

4. DISCUSSION OF THE CONTEXT

Here we shall insert detailed discussion of the relevant analogies during Phase II of this work.

5. REQUIREMENTS

Figure 2 represents the relationships between the Control Modes in a more complete but informationally confused way. From this figure, this Control Mode Structure requires the following list of definitions:

S-1. Continuous Control Strategy for Control Mode # 1

S-2. Continuous Control Strategy for Control Mode # 2

S-3. Continuous Control Strategy for Control Mode # 3

S-4. Continuous Control Strategy for Control Mode # 4

C-1-2. Conditions which provoke a Transition from Mode # 1 to Mode # 2

C-2-1. Conditions which provoke a Transition from Mode # 2 to Mode # 1

C-1-4. Conditions which provoke a Transition from Mode # 1 to Mode # 4

C-2-3. Conditions which provoke a Transition from Mode # 2 to Mode # 3

C-2-4. Conditions which provoke a Transition from Mode # 2 to Mode # 4

C-3-4. Conditions which provoke a Transition from Mode # 3 to Mode # 4

A-1-2. Actions to be performed on the Transition from Mode # 1 to Mode # 2

A-2-1. Actions to be performed on the Transition from Mode # 2 to Mode # 1

A-1-4. Actions to be performed on the Transition from Mode # 1 to Mode # 4

A-2-3. Actions to be performed on the Transition from Mode # 2 to Mode # 3

A-2-4. Actions to be performed on the Transition from Mode # 2 to Mode # 4

A-3-4. Actions to be performed on the Transition from Mode # 3 to Mode # 4

For simplicity, we shall try to re-use the same sets of actions/conditions where possible, and we shall list these sub-actions and sub-conditions as A-n, C-n. Each of the above definitions of the action and condition requirements will simply be a list of simple sub-definitions. In the case of the actions, the list is an AND list, whereas in the case of the conditions, the list is an OR list. Our intention is to complete these lists as our understanding of ITER increases during the EDA. This simplified structure is also chosen since it can be very directly implemented in a very simple and clear fashion, allowing regular updating under the stringent requirements of software quality control.

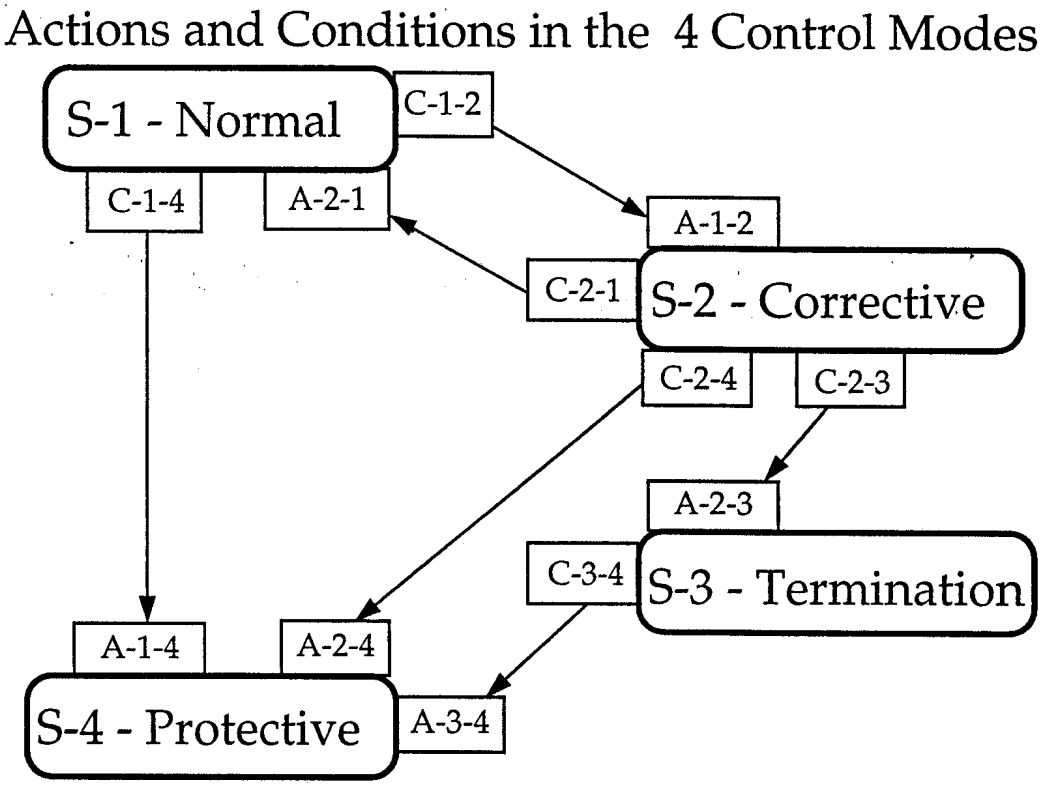

Fig. 2 Relationships between the Actions, Strategies and Transitions

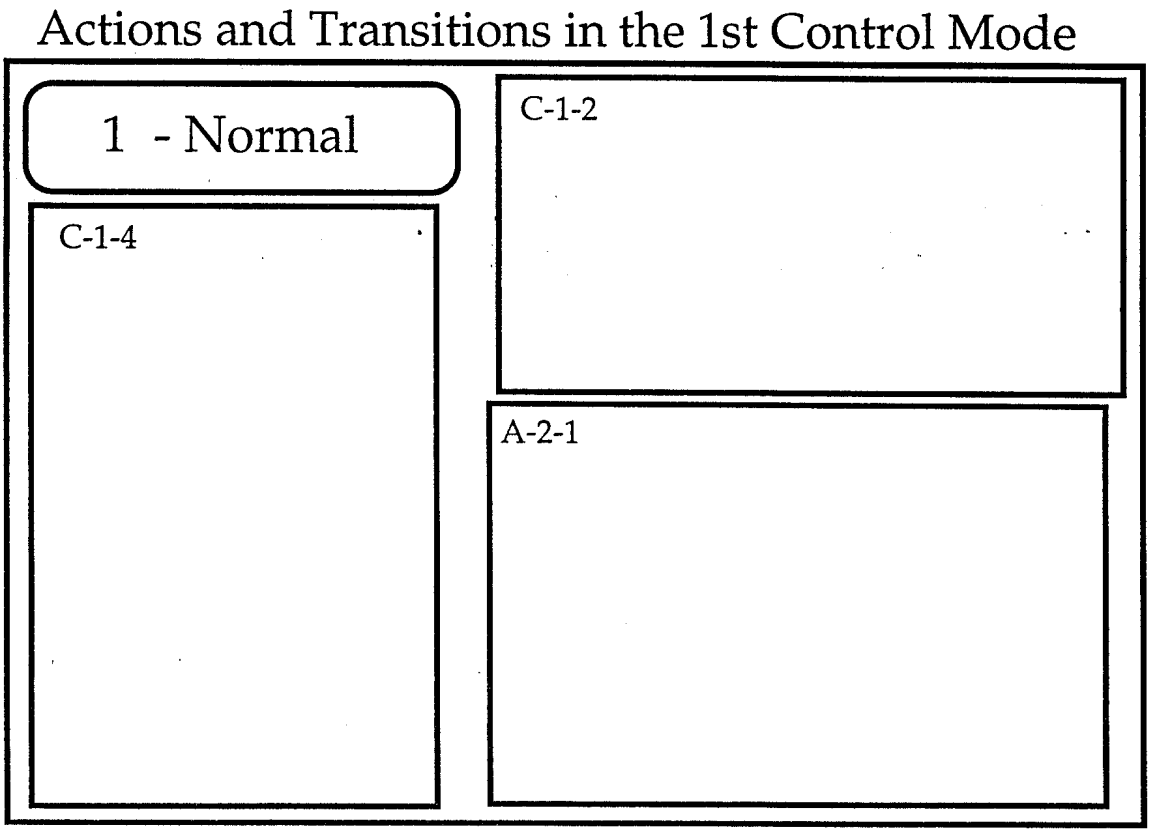

Fig. 3 - Full list of Actions and Conditions in the 1st of the 4 Control Modes

Actions and Transitions in the 2nd Control Mode

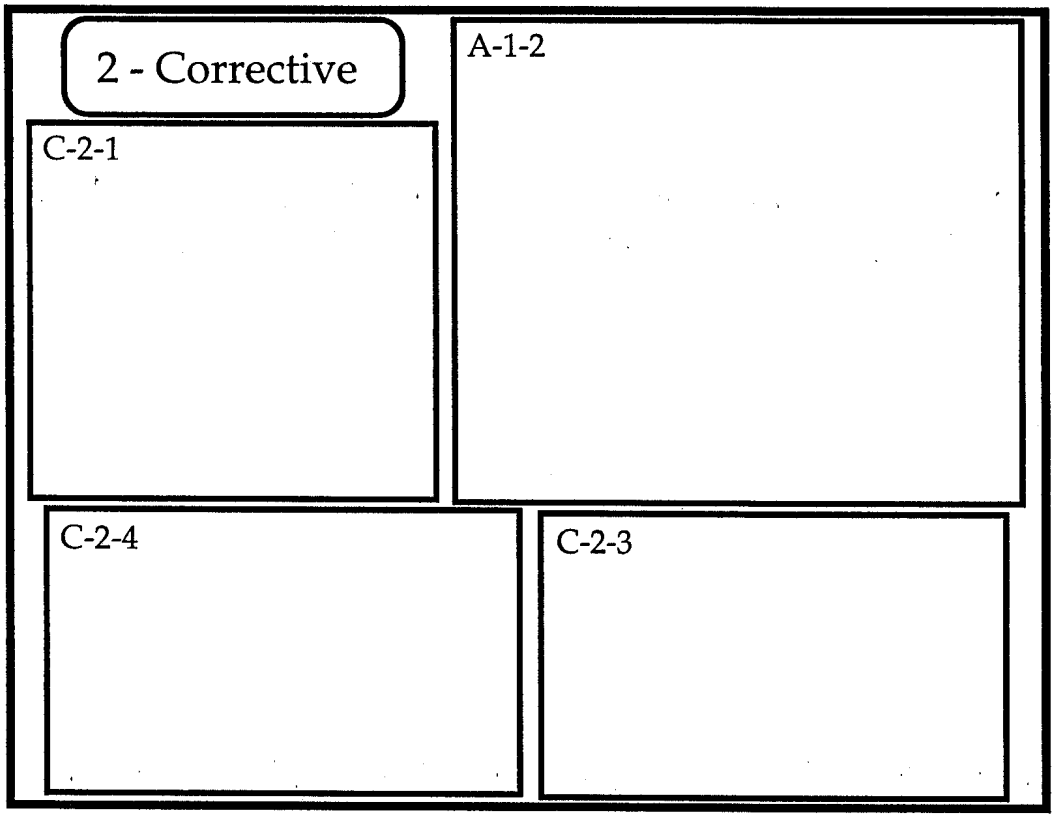

Fig. 4 - Full list of Actions and Conditions in the 2nd of the 4 Control Modes

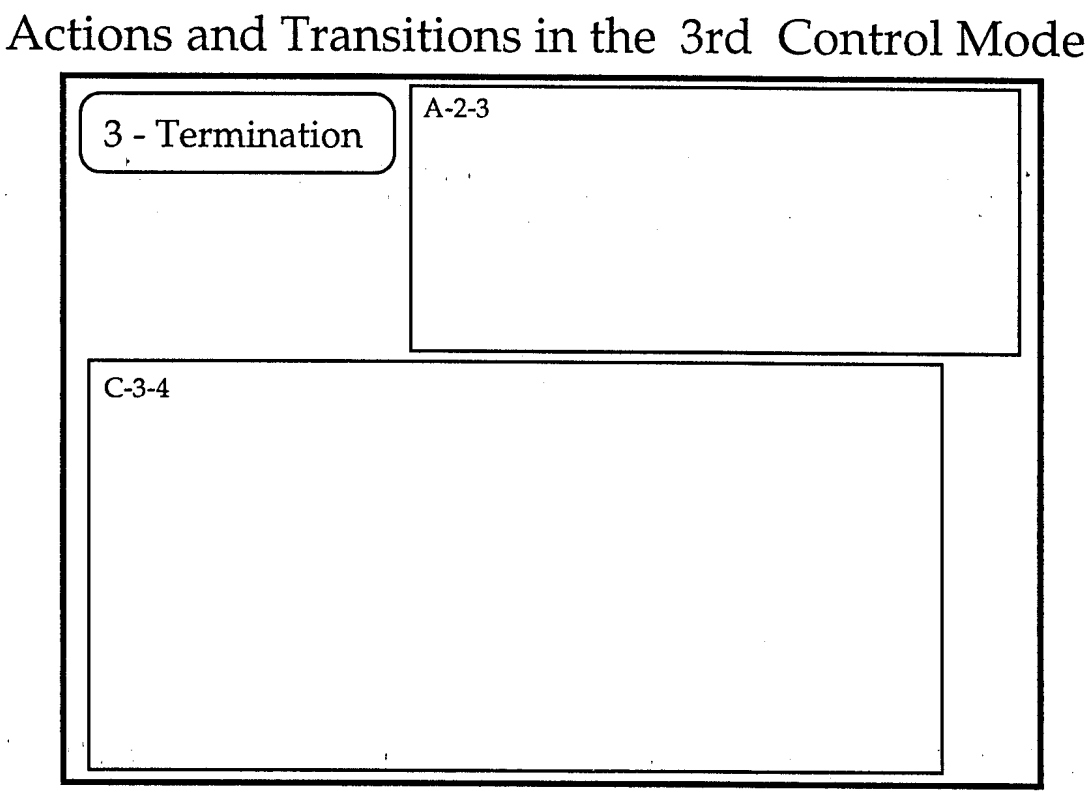

Fig. 5 - Full list of Actions and Conditions in the 3rd of the 4 Control Modes

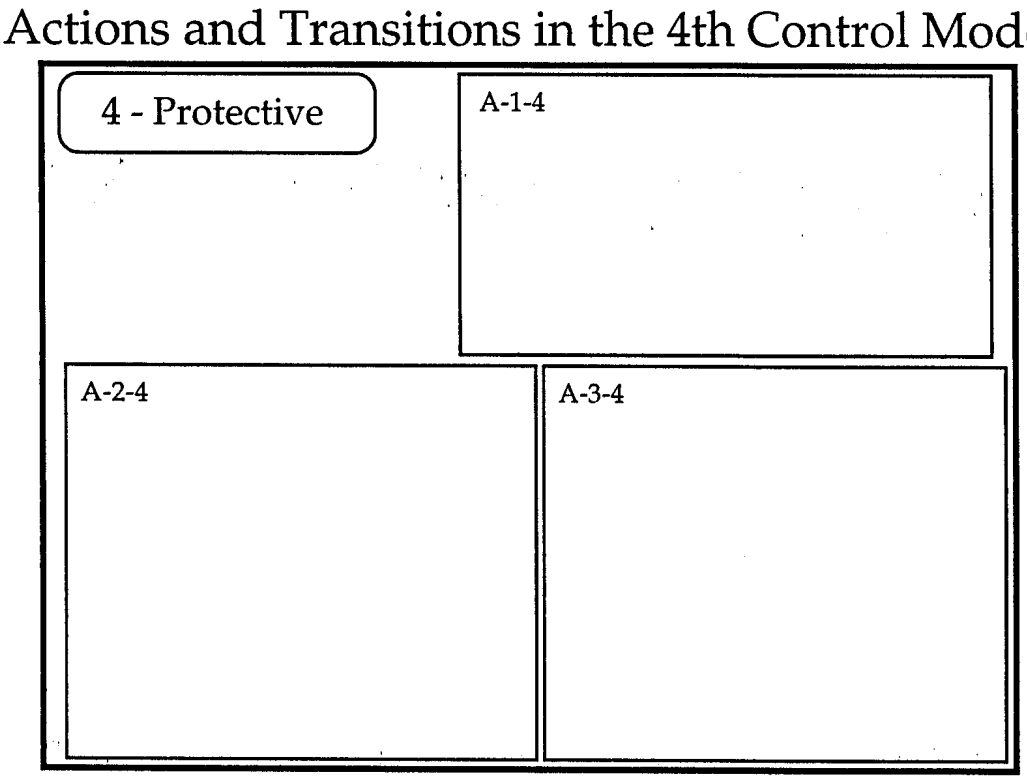

Fig. 6 - Full list of Actions and Conditions in the 4th of the 4 Control Modes

4. DEFINITIONS

Preliminary definitions of the Strategies

1) Normal Control Mode

- Provides optimal control of ITER, using all available information.
- Normal operation strategies are not part of the present discussion.

2) Corrective Control Mode

- Provides control of ITER during abnormal conditions which have not been signalled as pre-fatal.
- ITER is moved towards, and should reach, a safer operating condition from which any subsequent required protective action would cause less damage to the plant.
- Normal control should be resumed if the abormal condition can be removed or recovered.

- Fast shutdown (Termination Control Mode) should be launched if the abnormality will not be recovered and before continuation of the corrective action would lead inevitably to demand for the Protective Action Control Mode.

3) Termination Control Mode

- This Control Mode is entered from the Corrective Action Mode when it is decided that normal conditions will not be recovered, or if predefined fault conditions satisfy this transition request automatically, e.g. Shutdown requests from certain essential sub-systems. During Termination, control of the Plasma and PF systems is maintained in order to cause as little damage as possible, and to resume operation with minimum delay following the Termination.

4) Protective Control Mode

- Provides control of ITER when the control of the plasma has been declared impossible, or if a serious event, e.g. disruption, is declared as imminent.

Preliminary definitions of the Conditions (OR) { Illustrative, completed for Phase II}

a) C-1-2. Conditions which provoke a Transition from Mode # 1 to Mode # 2

- AC Losses Inventory is becoming too high
- First Wall Loading is becoming too high

b) C-2-1. Conditions which provoke a Transition from Mode # 2 to Mode # 1

- Absence of all C-1-2 Conditions

c) C-1-4. Conditions which provoke a Transition from Mode # 1 to Mode # 4

- Un-recoverable VDE

d) C-2-3. Conditions which provoke a Transition from Mode # 2 to Mode # 3

- AC Losses are too high to continue the normal pulse
- First Wall Loading is too high

e) C-2-4. Conditions which provoke a Transition from Mode # 2 to Mode # 4

- Un-recoverable VDE

f) C-3-4. Conditions which provoke a Transition from Mode # 3 to Mode # 4

- Un-recoverable VDE

Preliminary definitions of the sub-conditions { Illustrative, completed for Phase II}

C-1 Unrecoverable VDE

C-2 Accumulated AC Losses too high

C-3 Fast Shutdown Request from the Scenario Supervisor

C-4

C-5

Preliminary definition of the Actions (AND) { Illustrative, completed for Phase II}

a) A-1-2. Actions to be performed on the Transition from Mode # 1 to Mode # 2

- Increase distance to operational boundary
- Reduce Plasma Energy
- Reduce the performance of the PFCS feedback loops

b) A-2-1. Actions to be performed on the Transition from Mode # 2 to Mode # 1

- Recover the demand signals from the Scenario Supervisor

c) A-2-3. Actions to be performed on the Transition from Mode # 2 to Mode # 3

- Enter the Fast Shutdown Operation

d) A-2-4. Actions to be performed on the Transition from Mode # 2 to Mode # 4

- Killer Pellet Injection
- Feedforward programming of the PF coil voltages
- Additional Heating shutdown

e) A-3-4. Actions to be performed on the Transition from Mode # 3 to Mode # 4

- Killer Pellet Injection
- Feedforward programming of the PF coil voltages
- Additional Heating shutdown

Preliminary definition of the sub-actions { Illustrative, completed for Phase II}

A-1 Killer Pellet Injection

A-2 PF Feedforward Programming

A-3 Additional Heating Shutdown

A-4

A-5

SUMMARY

These ideas are for discussion purposes and propose a structure into which all abnormal conditions can be slotted as the understanding of ITER operation progresses. The particular conditions and actions illustrate how particularly simple cases of abnormal operation can be categorised and handled.